Lake water quality modelling to assess management options for Lake Hayes

April 2019

ERI report: 129

Prepared for Otago Regional Council

By Chris G. McBride, Kohji Muraoka and Mathew G. Allan

Environmental Research Institute, The University of Waikato, Pvt Bag 3105, Hamilton, New Zealand

THE UNIVERSITY OF WAIKATO
Te Whare Wānanga o Waikato

Environmental Research Institute
Te Pūtahi Rangahau Taiao
THE UNIVERSITY OF WAIKATO

Citation

McBride CG, Muraoka K, and Allan MG (2019). Lake water quality modelling to assess management options for Lake Hayes. Client report prepared for Otago Regional Council. *Environmental Research Institute Report No. 129*, The University of Waikato, Hamilton. 72 pp.

Availability

Data providers

Otago Regional Council

NIWA

NZ MetService

Cover image

'Lake Hayes in Winter' (reproduced with permission from www.momentaddictphotography.com)

Acknowledgements

We acknowledge Otago Regional Council for funding this project, and for their collaboration, field work, collection and sharing of data as the project evolved. This work was partially supported by MBIE contract Enhancing the Health and Resilience of New Zealand Lakes (UOW1503). Lake models DYRESM-CAEDYM were developed at The University of Western Australia.

Reviewed by:

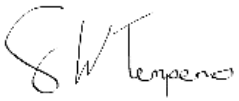

Grant Tempero

Research Officer

University of Waikato

Approved for release by:

John Tyrrell

Business Manager

University of Waikato

Executive Summary

Lake Hayes is an important ecological, historical and cultural asset to the Otago Region. The lake and its catchment have been substantially altered from their natural condition, including conversion of the catchment from forest to pasture, invasion of the lake by non-native macrophytes, blooms of cyanobacteria (blue-green algae) and lake Trophic Level Index has increased over recent years (Figure A). Since 2010 the lake has been characterised by very poor water quality and pronounced summer algal blooms. This has attracted public attention and provided impetus from community and stakeholders to assess available management options for restoring water quality in the lake.

This report examines the drivers of poor water quality and associated algal blooms in the lake, and assesses various management options that have been either specifically proposed for Hayes, or have proven effective for other lakes in New Zealand and globally. Here we report on monitoring undertaken by Otago Regional Council in the catchment (surface inflows) and in the lake. Primarily, we apply state-of-the-art computer models to simulate physical, chemical, and biological processes within the lake. These simulations are then used to evaluate a range of management scenarios to provide guidance on the likely effects of management options.

Catchment and lake monitoring data were synthesised for the period 1983 to 2017. Long-term monitoring showed strong evidence for substantial internal nutrient loading to the lake (i.e., recycling of nitrogen (N) and phosphorus (P) from bottom sediments during lake stratification over warmer months). Also evident were changes in the magnitude of internal loading over the c. 35 years of monitoring data including a possible reduction over recent years, however, inconsistent timing and measurement depth makes analysing for trends difficult. Similarly, calculation of long-term changes in lake Trophic Level Index (TLI) was confounded somewhat by intermittent sampling, but nonetheless showed a notable increase in the mid-2000s followed by a steady decline in TLI since, indicating slowly improving water quality over the present decade (Figure A).

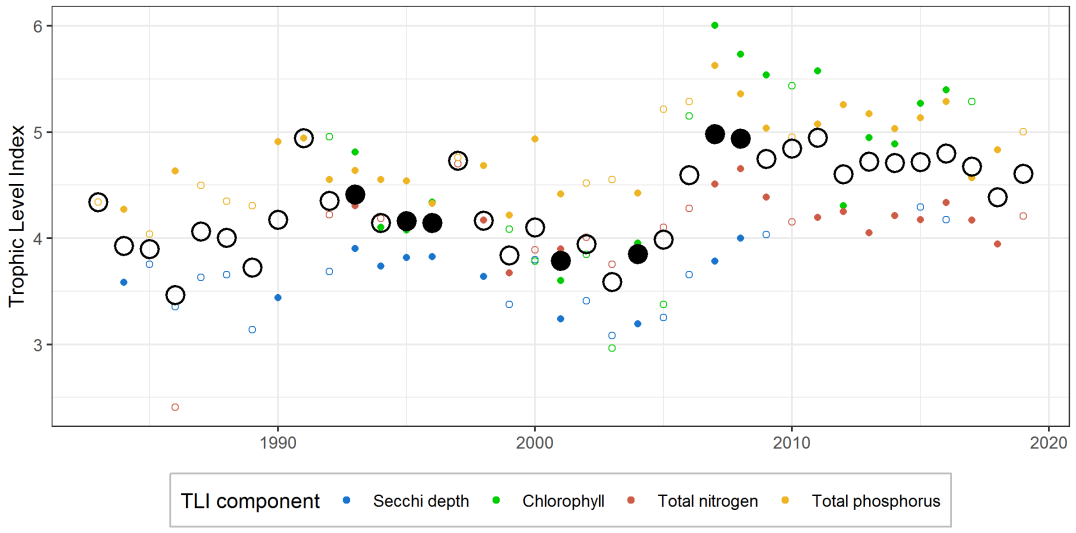

Figure A. Annual Trophic Level Index (TLI) for Lake Hayes by hydrological year (previous July to present June). Each coloured circle is the mean of seasonal means, for one TLI variable with the relevant TLI equation applied (Burns et al. 1999). Large black circles are the annual TLI (average of four components). Solid circles denote years for which at least one measurement was available for all four seasons (solid black circles denote that all four component variables of the TLI were sampled each season). Open circles denote that measurements were missing for at least one season.

Following initial analyses of observational data, the period 2007 – 2017 was selected for management scenario modelling (i.e., to better reflect the present state of the lake), and a process-based physical-biogeochemical model (DYRESM-CAEDYM) was configured for Lake Hayes. A review of historical phytoplankton analyses was undertaken, and on this basis, a synthetic approximation of seasonal phytoplankton succession (changes in community composition over annual cycles) was constructed with which to calibrate the phytoplankton components of the lake model.

The model was able to reproduce physical and chemical in-lake dynamics with acceptable accuracy relative to previous applications of DYRESM-CAEDYM. The established model can therefore be considered the most advanced tool available with which to assess potential management options for Lake Hayes. Four broad categories of model scenarios were undertaken using model simulations, with results as follows:

1. **Nutrient load reduction:** Reduction of nutrient loads from the immediate catchment resulted (expectedly) in improved overall water quality, with reductions in lake TLI resulting from catchment loading reductions of just 10 and 25%**.** A further scenario of 50% reduction, which can be considered as a sensitivity test rather than an achievable management option, produced a dramatic improvement in water quality.

2. **Arrow River diversion**: Diversion of Arrow River irrigation water into Lake Hayes had a positive effect on overall water quality. Synergistic effects were observed such that diversion of Arrow River water in combination with a 10% catchment load reduction gave a similar magnitude of improvement to a 25% catchment load reduction alone. For the three Arrow River flow scenarios (including scenarios Flow 1 and Flow 2; see Table A), the resulting TLI was very similar, in fact, an absence of summer flow yielded slightly favourable water quality compared with scenarios where summer flow was included, suggesting summer diversion may not be required. Model simulations of lake bottom water temperature compared with Arrow River water temperatures showed that diverted water is likely to entrain to the surface of the lake during warmer months and this supply of nutrients to the epilimnion. This may explain the neutral to negative effect of summer flow diversion.

   The modelled scenario of hypolimnetic withdrawal alone gave a slight improvement to overall water quality over the baseline model. When combined with Arrow River diversion, hypolimnetic withdrawal resulted in further water quality improvement over hypolimnetic withdrawal alone. However, due to the small magnitude of change, the cost benefit for this option would need to be carefully considered.

3. **Artificial aeration:** The DYRESM-CAEDYM model allows for the simulation of aeration by a bubbler plume (bottom-up mixing). The two airflow rates assessed (300L/s and 500L/s) yielded broadly similar improvements to water quality to the Arrow River diversion, however, simulations showed that cyanobacteria blooms could be exacerbated by the action of the bubbler–bubbler scenarios showed an increased occurrence of surface algal blooms, presumably due to improving access to light and increasing transport of nutrients from bottom to surface waters, while not sufficiently negating the buoyancy capabilities of cyanobacteria. However, this result could be highly sensitive to the parameterisation of cyanobacteria within the model. Although CAEDYM includes only a simplistic representation

of phytoplankton motility, these results highlight a potential pitfall of aeration and indicate that this option should be thoroughly evaluated. The potential effects of aeration/mixing on aquatic biota (particularly the effects of altered temperature dynamics on the trout population) should also be considered in detail, and were beyond the scope of this study.

4. **Geochemical engineering:** The application of flocculation and/or sediment capping agents such as Phoslock™, Z2G1 (modified zeolite), or aluminium sulphate (alum) is a management approach that has been applied with some success in the Rotorua lakes (Bay of Plenty). Although CAEDYM cannot explicitly simulate the mode of action (i.e., adsorption) of these agents, scenarios were undertaken to approximate their effects by adjusting process rate coefficients to simulate an increase in the settling rate of organic matter (flocculation), and the reduction of internal sediment-water nutrient fluxes (i.e. sediment capping).

   Flocculation and capping scenarios resulted in substantial TLI reductions, although results should be interpreted cautiously due to the conceptual simplifications necessary in these simulations. The efficacy of these agents is highly pH-dependent, and the timing and intensity of their application must be considered in detail, along with the buffering capacity of the waterbody. Further, ecotoxicological and community/cultural factors are important considerations when evaluating geochemical engineering as a lake management option (see Tempero 2015).

Based on scenario simulations, as summarised in Table A, model simulations support catchment nutrient load reduction as central to achieving positive change in the water quality of Lake Hayes. Diversion of Arrow River water, even if only during cooler months, appears to be a promising option to improve water quality and could potentially work synergistically with any catchment nutrient load reductions. Aeration and geoengineering approaches also have potential for water quality improvement, however, these approaches are subject to greater degrees of model uncertainty as well as necessary considerations of direct and indirect consequences, such as effects on lake biota. Further development of the model and scenarios could provide additional guidance for management strategies going forward. Collection of more comprehensive water quality data including lake level, high frequency water quality and climate data, would aid this process as well as enhance general understanding of key processes and trends in Lake Hayes.

Table A. Summary of projected water quality for all Lake Hayes management scenarios. Refer to Table 3 for scenario details. Abbreviations as follows. s: scenario; numbers (50 to 100): percentage multiplier applied to catchment nutrient concentrations. Arr: Arrow diversion; hWQ: Higher water quality for Arrow River; flow 1: low summer flow of Arrow River water to Lake Hayes; Flow2: no summer flow of Arrow River to Lake Hayes; hypWdr: Hypolimnetic withdrawal; bub: Aeration/Bubbler; infDose: Geochemical engineering; sedCap: Sediment capping. Note Trophic Level Index is a three-parameter TLI consisting of total nitrogen total phosphorus and chlorophyll *a*.

Scenario	Trophic Level Index	Total nitrogen (g m^{-3})	Total phosphorus (g m^{-3})	Chlorophyll (mg m^{-3})
s100	4.8	0.37	0.04	16.36
s90	4.65	0.33	0.04	14.81
s75	4.52	0.29	0.03	13.84
s50	4.07	0.2	0.02	9.04
s100_arr	4.64	0.31	0.04	15.23
s90_arr	4.54	0.28	0.03	14.31
s75_arr	4.42	0.25	0.03	13.24
s100_arr_flow1	4.66	0.32	0.04	15.51
s100_arr_flow2	4.62	0.32	0.04	14.91
s100_arr_hWQ	4.6	0.3	0.04	15.02
s100_hypWdr	4.73	0.36	0.04	15.83
s100_arr_hypWdr	4.6	0.31	0.04	14.62
s100_bub_300L	4.67	0.4	0.03	14.12
s100_bub_500L	4.66	0.4	0.03	13.82
s100_infDose	4.76	0.36	0.04	15.99
s100_infDose_sedCap	4.56	0.35	0.03	12.87
s100_sedCap	4.58	0.35	0.03	13.34

Contents

List of Figures

List of Tables

1 Introduction

Lake Hayes is an important ecological, historical and cultural asset to the Otago region. It is a popular recreational destination and is said to be the most photographed lake in New Zealand, due to the spectacular reflection observed from mountains of the Wakatipu Basin. The lake and its catchment have been substantially altered from their natural condition, including conversion of forested catchment to pasture. Degradation of water quality in Lake Hayes is an important issue to Tangata Whenua, local community, and recreational users. Algal blooms associated with eutrophication, as well as declines in the Lake Hayes fishery have been well documented (e.g., Mitchell & Burns 1974, 1980, ORC 1995). The lake was likely degraded relative to reference conditions (i.e., pre-settlement) before limnological studies began (in the 1950s), when bottom water hypoxia was observed along with relatively low clarity (< 6 m Secchi depth), green colour and near-eutrophic conditions. This was attributed in large part to the advent of aerial topdressing within the catchment (Jolly, 1959). Other stressors to lake water quality included wetland drainage, point source discharge from industry (a cheese factory operating from 1912-1955), and land use intensification, including implementation of the Arrow River irrigation scheme.

Ozanne (2014) and Schallenberg & Schallenberg (2017) assessed multiple management strategies to potentially arrest or reverse further declines in water quality. Evaluating the efficacy of various options and prioritising management strategies based on cost-benefit is challenging. To that end, process-based catchment and lake models are the most advanced decision support tool available for evaluating potential management strategies, as well as possible synergistic effects of parallel restoration strategies (Hamilton et al. 2012, Trolle et al. 2012).

1.1 Overview of lake modelling within a management process

The US Environmental Policy Agency defines a numerical model as “a simplification of reality that is constructed to gain insights into select attributes of a particular physical, biological, economic, or social system” (USEPA, 2009). Although there are many reasons for the use of such models in policy making purposes, the present application for Lake Hayes can be considered a scenario analysis. In this type of modelling study, a ‘baseline’ model is developed to reflect the status quo of the environment, and processes of interest are subsequently modified to examine the modelled response relative to the baseline simulation (i.e., to represent various alternative management strategies). Figure 1 summarises how lake modelling can fall within a framework and/or process for lake management.

A comprehensive lake ecological model was first developed in early 1970s (Di Toro et al., 1975), but it is only recently that water quality modelling of freshwater lakes (i.e., more than hydrology) became a major interest of policy makers. A typical lake ecological model is one of the most complex of all aquatic models (Robson, 2014), making it highly specialized and resource hungry. Therefore, to achieve a meaningful outcome it is important to (1) determine an adequate selection of model type and configuration, and (2) generate high quality datasets for model forcing and calibration.

Because of their intricacy, some complex process-based models can suffer from errors and limitations from software malfunctions. The biogeochemical model CAEDYM (Computational Aquatic Ecosystem DYnamics Model) was first developed approximately 20 years ago (Hamilton and

Schladow, 1997; Schladow and Hamilton, 1997), and has since been updated and applied to many lakes and reservoirs globally (e.g. Gal et al., 2009; Özkundakci et al., 2011; Trolle et al., 2011). CAEDYM is an ideal choice for the present project due to its pedigree of global and New Zealand applications, as well as the availability of modules for simulating artificial aeration (within the DYRESM hydrodynamics model). A summary conceptual diagram of a hydrodynamic-biogeochemical lake model is shown in Figure 2, and a more detailed summary is in Appendix figure 1.

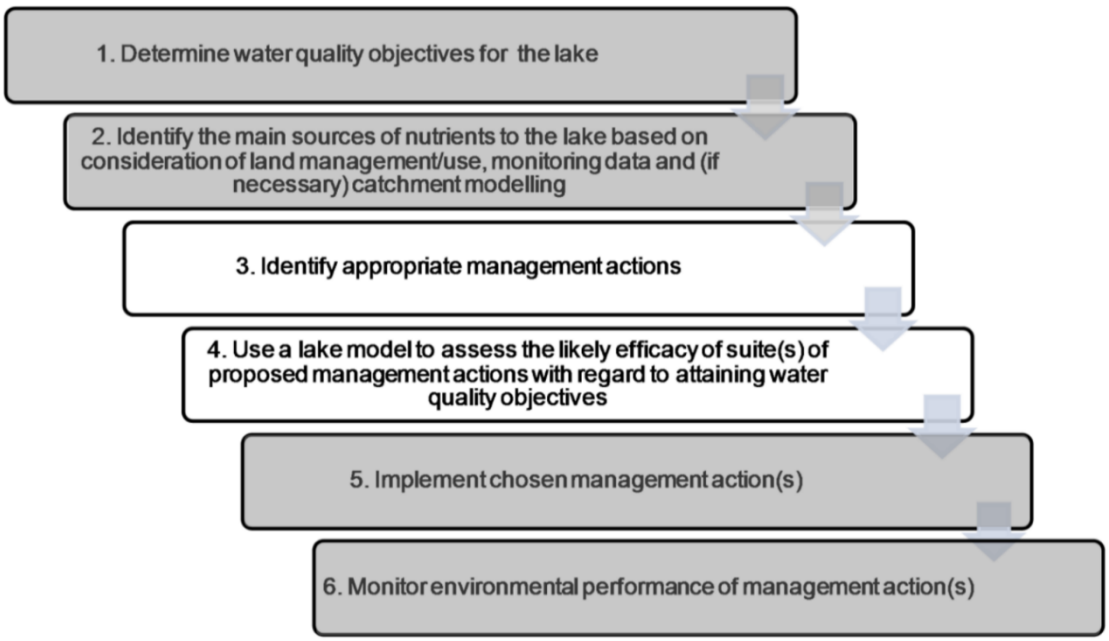

Figure 1. Example of how lake modelling can contribute to the implementation of lake management actions during a consultative process. Adapted from Elliot & Sorrell (2002).

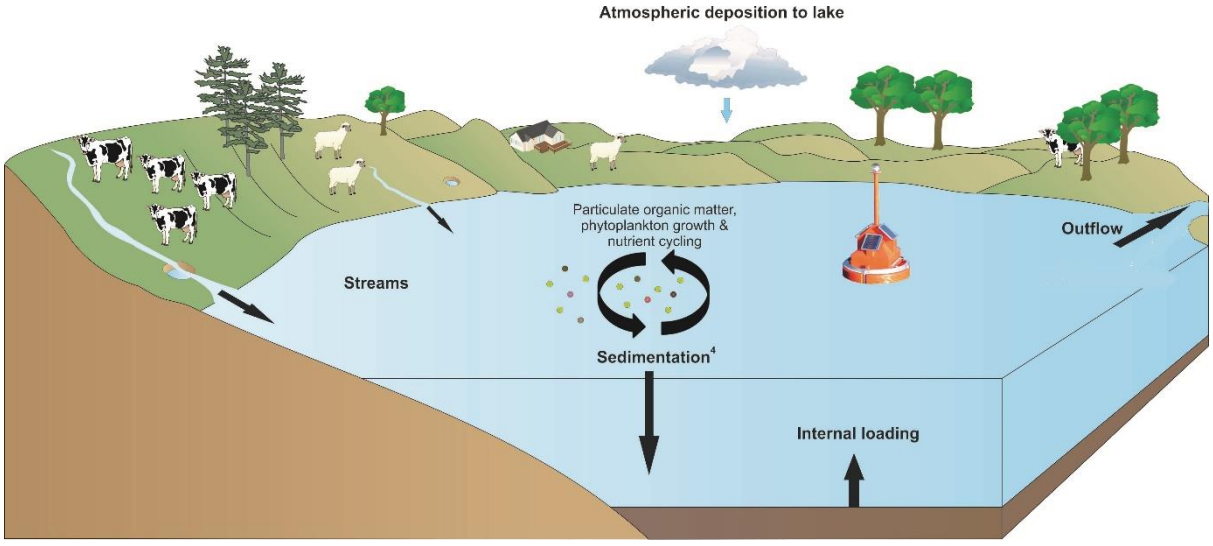

Figure 2. Simplified conceptual diagram of the Lake Hayes water quality model.

For lakes and reservoirs, environmental variability can exist in two primary spatial directions; (a) vertical variability caused by density and light gradients, and (b) horizontal variability, usually caused by morphological complexity (Wetzel 2001). Water quality parameters are heavily influenced by these environmental heterogeneities, and it can be ideal to simulate them in the finest possible resolution. However, a major limitation of any modelling project is the required computational resources and time required to calibrate the model. Modellers are required to carefully examine the best discretization (numerical representation resolution in both time and space) solutions with a good outcome-to-resource balance. Fortunately, the round ('tub-like') morphology of Lake Hayes makes it a near ideal candidate for 1-D modelling. This type of model only considers vertical variability of water parameters over reasonably long time periods (at daily or better time resolution), while assuming negligible spatial variabilities.

Accurate and precise forcing data (environmental fluctuations that externally modify lake conditions) are key to producing an appropriately functional model. Such data include temporally varying *in situ* meteorological conditions, hydrological and water quality characteristics of inflows and outflows, ideally at daily resolution or better. Water level fluctuations are often used to resolve the water mass balance which can be critical to seasonality in lakes. Sediment geochemical composition and sediment diagenesis information is also useful when developing lake models. Unfortunately, such long-term, comprehensive data sets are rarely available, therefore, modelling projects often begin by synthesizing these data using statistical relationships or by assumption and/or expert opinion. Outputs from models simulating water quality in New Zealand lakes are often summarised by transparency, phytoplankton biomass, and nutrient concentrations that comprise the Trophic Lake Index (TLI), or National Objective Framework (NOF) standards.

1.2 Phytoplankton seasonal succession in lakes

Phytoplankton play major roles in regulating lake nutrient concentrations, dictating oxygen fluctuations and other key water quality dynamics. Many New Zealand lakes have undergone nutrient enrichment (eutrophication) resulting in phytoplankton blooms. Blooms may have significant adverse effects including unpleasant odours, reduced water clarity, fish kills from oxygen depletion associated with decomposition or indirectly, benthic macrophyte loss via reduced light availability, and PERHAPS most importantly potential health hazards from cyanobacterial toxin production. These issues are species and condition dependent, making it important to assess and potentially manage which species occur in order to regulate water quality.

Physical and biological factors that favour or suppress certain species (e.g. functional groups) are well described in literature, and several theories have been postulated account for seasonal phytoplankton assembly dynamics in a typical lake. The Plankton Ecology Group (PEG) model is a generalized theory of annual phytoplankton dynamics proposed by Sommer et al. (1986, 1993, 2012). The theory predicts both the timing of the total phytoplankton biomass dynamics and likely functional groups. A simplified schematic of a seasonal phytoplankton biomass dynamics and conditions (dominant pressures) in a typical monomictic eutrophic lake is summarised in Figure 3.

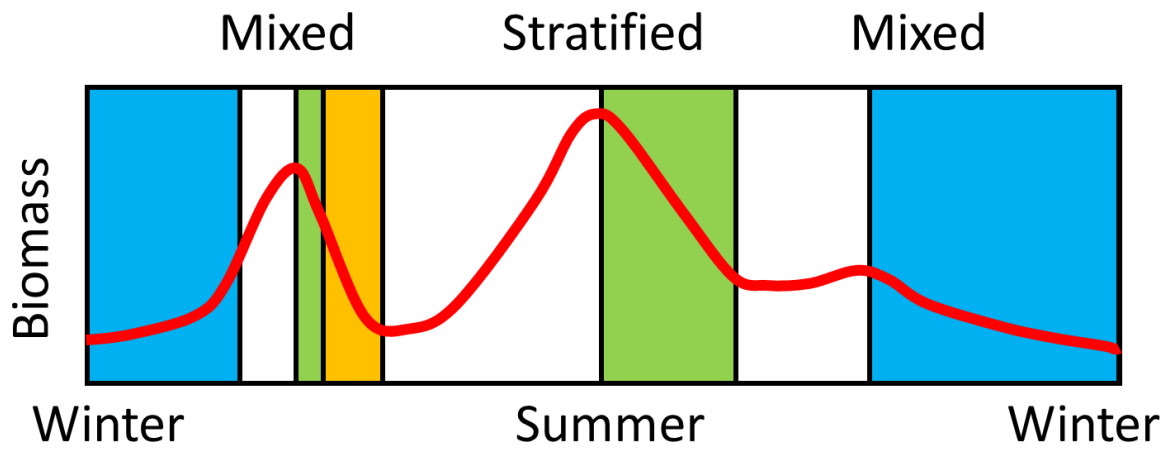

Figure 3. Conceptual seasonal dynamics of phytoplankton biomass (red line) and simplified dominant pressures (colours) that restricts certain types of species of phytoplankton from growing are shown, based on the Plankton Ecology Group (PEG) model (Sommer et al. 1993). Dominant physical pressures colour codes are, blue: light energy and temperature; green: nutrient limitation; and yellow: intense grazing pressure.

Dominant pressures and drivers of phytoplankton succession are summarised in Sommer et al (1993, 2012). In a typical monomictic eutrophic lake, phytoplankton biomass is low during winter due to low light energy and low temperature. Broadly, when physical conditions become sufficient to promote growth in spring, total phytoplankton biomass rapidly increases, reaching a peak otherwise known as the spring bloom. Species likely to dominate during this phase are generally fast growing small unicellular species able to quickly take up nutrients, however other species that benefit from the turbulent environment can also have enhanced survival. When the available resources are fully utilized, this spring increase of biomass reduces due to zooplankton population increase and associated grazing. This leads to an enhanced water clarity condition known as a clear water phase. Zooplankton communities generally cannot sustain their increased population abundance for long periods due to increased fish predation pressures and reduced phytoplankton biomass. Subsequently, grazing pressure is supressed in early summer, allowing phytoplankton biomass to re-grow under non-limiting resources to form summer blooms. The species composition of the algae community during this period reflects the dynamic environment and therefore diversified functional group richness is apparent. For example, re-growth preferentially grazed algal species may occur due to low zooplankton grazing pressure (e.g. cryptophytes), while frequent observations of colony forming algae (less edible to zooplankton) are also reported. Once nutrients are depleted from the epilimnion (likely around mid-summer), the edible fast growing algae have lower survival rates and diatom species begin to establish, however large dinoflagellates or cyanophytes may also dominate depending on the conditions. If nitrogen is depleted, it provides opportunities for nitrogen fixing filamentous cyanobacteria growth due to their ability to convert nitrogen gas into a form suitable for growth. However, summer phytoplankton succession can be disturbed by mixing events in a medium depth lake due to wind drive turbulence and resulting increased epilimnetic nutrient concentrations. This disruption of succession eventually leads to the likely autumn dominance of diatoms, with populations of large unicellular or filamentous algae also occurring, as well as variable occurrences of edible algae species depending on the zooplankton abundance. This phase may promote the total phytoplankton biomass to increase resulting in autumn bloom formation. Once the available light

energy and temperature decreased towards winter, a lake phytoplankton biomass likely reaches winter minimum.

Real-world species assemblages are the result of complex interaction histories between species and the environment, and are often substantially more complex than the theoretically described transitions of species succession models. However, theoretical models provide a basis of understanding for lake- and time-specific conditions which aid in understanding algal community dynamics. From this perspective, any ecological model of algal dynamics needs to achieve a reasonable simulation of environmental conditions and events, in order to drive growth within phytoplankton components of the model.

1.3 Modelling aims and objectives

Through synthesis of available relevant data to Lake Hayes, the present study aims to establish a vertically-resolved, daily resolution model simulation using a robust modelling process, including detailed calibration and validation of both hydrodynamic and biogeochemical (~ecological) components. We then apply a range of 'scenario simulations', whereby forcing data are altered to represent, as best as possible, a suite of potential management strategies for water quality in the lake. In doing so, we aim to provide robust guidance of the appropriateness of the management strategies available. It is not within the scope of the present study to evaluate cost-benefit of the proposed strategies, rather to estimate as thoroughly as possible their likely effects on lake water quality in the medium- to long-term.

2 Methods

2.1 Study site

Lake Hayes (44° 58 51S, 168° 48 27 E; Figure 4) is located 11 km northwest of Queenstown. The lake has a surface area of approximately 2.74 km^2, mean depth of 19.75 m and maximum depth of 33.3 m (Table 1). The lake has a major inflow in Mill Creek to the north (Figure 4), and a watershed of 48.1 km^2. Lake Hayes is situated 327.7 m above sea level. Before Polynesian settlement the catchment was covered with evergreen Kahikatea (*Dacrycarpus dacrydioides*) forest. This was replaced by native tussock in upland areas and swampland in lowland areas. The catchment has been largely transformed into pasture/agriculture since the arrival of European settlers during the early 1900's (Caruso 2000).

Table 1. Lake Hayes morphological and catchment characteristics

Altitude	327.7 m
Area	2.74 km^2
Catchment land area	48.10 km^2
Catchment to lake area ratio (at present)	17.55 : 1
Mean depth	19.75 m
Maximum depth	33.3 m
Shoreline length	7.45 km
Volume	53.1 x 10^6 m^3

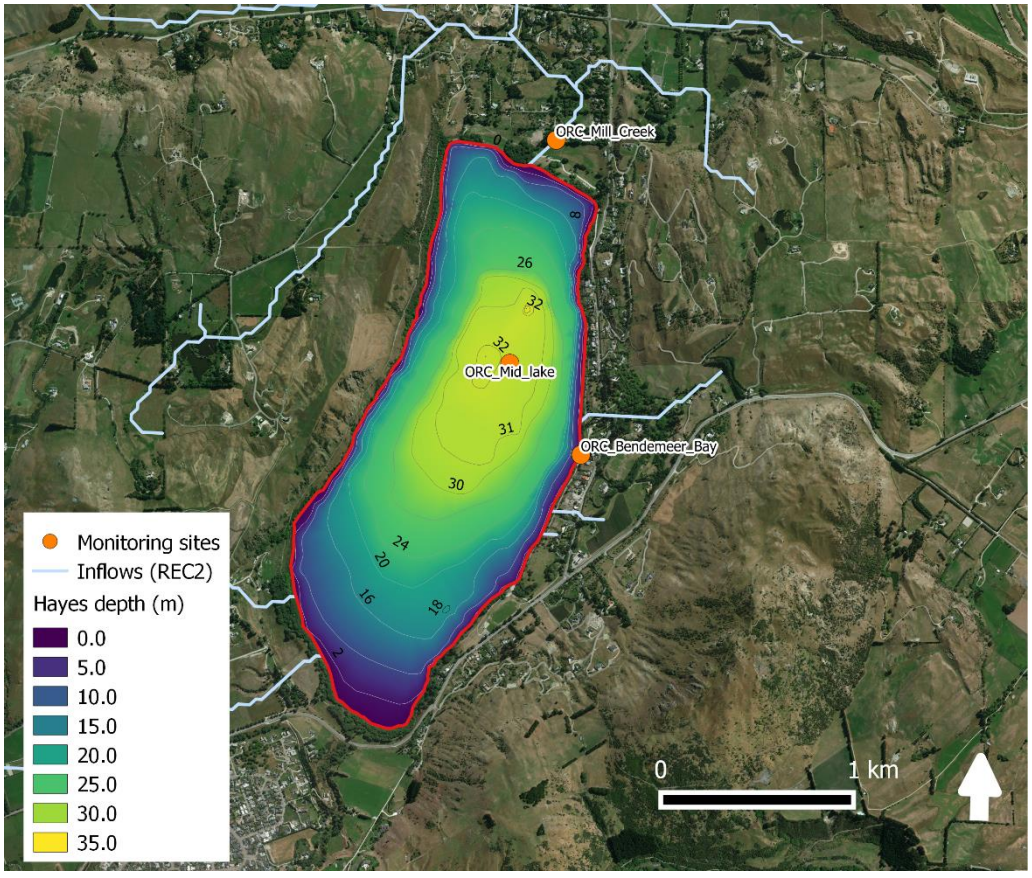

Figure 4. Lake Hayes bathymetry, with ORC monitoring sites (orange point), and REC2 stream network.

2.2 Catchment

2.2.1 Catchment monitoring

In-stream measurements of water temperature, chemistry, and discharge were collected for calibration and validation of catchment models. Otago Regional Council (ORC) has sampled Mill Creek stream inflows from 1983 to present with 15 minute interval flow data and water quality samples bi-monthly or monthly. Sub-daily sampling of water chemistry has been undertaken for certain periods, although not during the past 10 years. The Lake Hayes catchment and monitoring sites are shown in Figure 5. Baseflow for each day was calculated as minimum 10-day flow (Rutherford 2008). Discharge-nutrient concentration relationships were assessed using all available data, and where such relationships were identified, these were used to estimate concentrations for each analyte where flow was greater than baseflow.

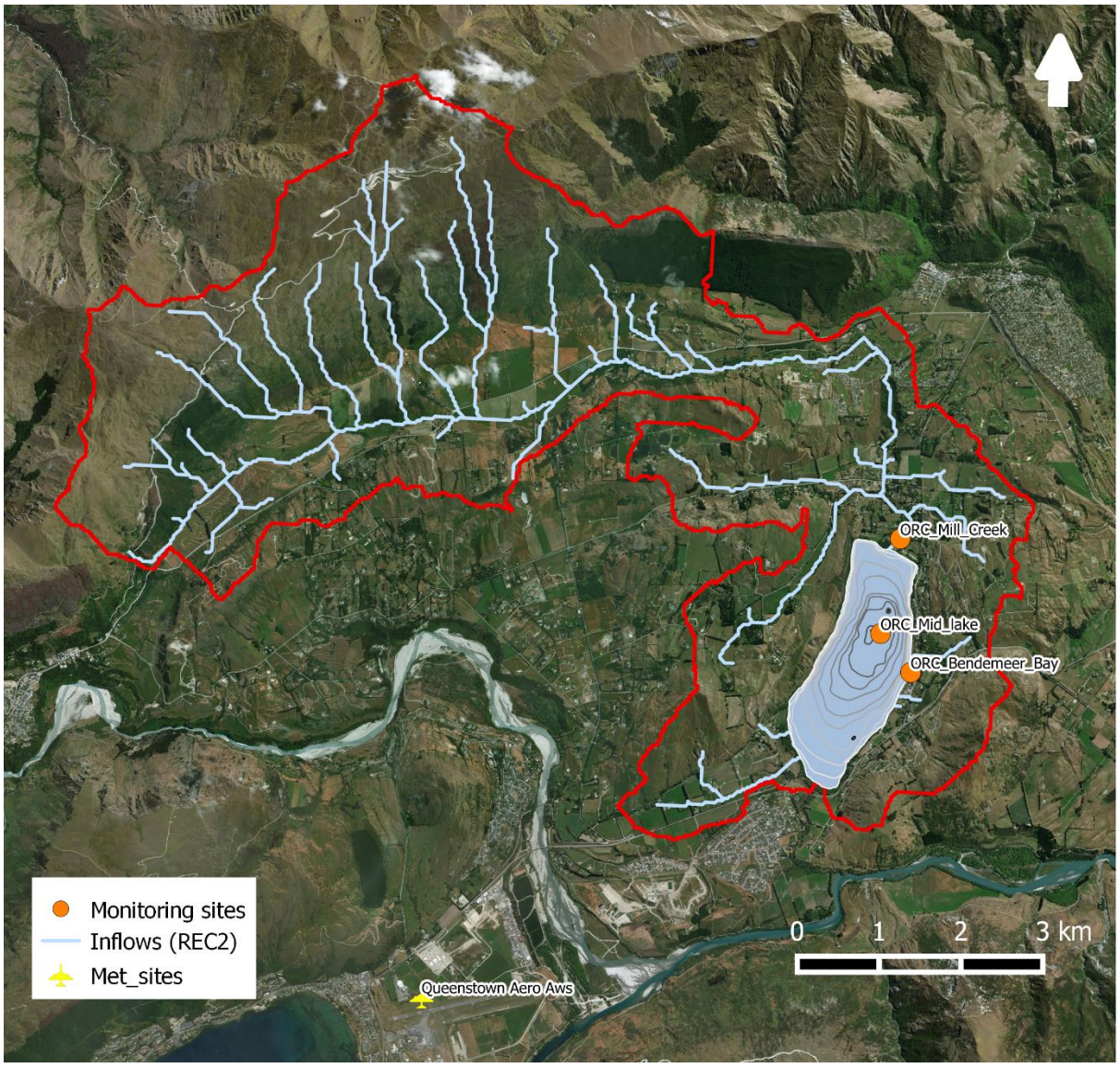

Figure 5. Lake Hayes catchment boundary (red line) in relation to Queenstown Airport (yellow symbol; the meteorological station used for lake modelling forcing data). REC2 = River Environment Classification version 2 (NIWA).

2.3 Lake

2.3.1 Lake monitoring

Otago Regional Council collected samples of physical, chemical, biological properties of water from Lake Hayes approximately monthly commencing January 1983 (however, chlorophyll *a* samples were collected from January 1998 onwards and there are gaps in the monitoring record for certain periods). The Trophic Level Index (TLI; Burns et al. 1999) is calculated from measured water quality variables, and is commonly used in New Zealand to report on lake water quality and assess the performance of restoration initiatives. The TLI is the average of four individual components on standardised (logarithmic) scales, including (annual averages of total nitrogen (TN), total phosphorus (TP), chlorophyll *a*, and transparency (as measured by Secchi depth). TLI equations can be found in Burns (1999). Raw monitoring data from surface waters (ORC) were used to calculate annual TLI for the study period. Because of the sporadic nature of some sampling, sample data were aggregated to a seasonal average, and seasonal means were then averaged to calculated annual (hydrological year) means which were used to estimate TLI for the lake. Not all years had at least one sample point for each season and each TLI variable. Monitoring data sets and monitoring records were assessed for features that could affect the choice of management activities for Lake Hayes (e.g., N:P ratio, evidence of nitrogen-fixation, internal loading). Field measurements were also used for calibration of the lake model and evaluation of its performance.

2.3.2 Lake Hayes seasonal dynamics of phytoplankton functional groups

Phytoplankton cell densities in Lake Hayes were recorded for the period of September 2016 to May 2017 (8 sampling points). Because the model uses elemental ratios such as C:N:P to establish simulation of abundance, cell density can be misleading in terms of resources a species biologically reserves. To overcome this limitation, theoretical cell volumes were estimated using literature values for each species observed, and likely chlorophyll *a* concentrations were calculated using an empirical relationship to cell volumes proposed by Mantagnes and Berges (1994) that:

$$\mathrm{CHLAc} = \mathrm{Vc}^{0.917} \times 0.00429,$$

where CHLAc is the mass of chlorophyll *a* pigment in a cell (pg /cell), and Vc is the volume of a cell (μm3). Individual species' cell density, cell volume and chlorophyll *a* concentration were then aggregated to taxonomical groups.

2.4 Lake modelling

The one-dimensional (1D) hydrodynamic model DYRESM (version 3.1.0-03) was coupled with the aquatic ecological model CAEDYM (version 3.1.0-06), both developed at and used under license from the Centre for Water Research, The University of Western Australia. DYRESM resolves the vertical distribution of temperature, salinity, and density in lakes and reservoirs, while CAEDYM simulates time varying fluxes of biogeochemical variables (e.g., nutrient species, phytoplankton biomass). The model includes comprehensive process representations for carbon (C), nitrogen (N), phosphorus (P), and dissolved oxygen (DO) cycles, and several size classes of inorganic suspended solids. Several applications have been made of DYRESM-CAEDYM (e.g., Bruce et al., 2006; Burger et al., 2008; Trolle

et al., 2008; Gal et al., 2009) and these applications provide detailed descriptions of the model equations.

The interactions between phytoplankton growth and losses, sediment nutrient fluxes, and the mineralisation and decomposition of particulate organic matter influence N and P cycling in the model (Appendix figure 3). Fluxes of dissolved inorganic and organic nutrients from the bottom sediments are dependent on temperature, NO_3-N and DO concentration in the water layer immediately above the sediment surface. In the present application, CAEDYM was configured with three phytoplankton groups (positively buoyant cyanobacteria, neutrally buoyant green algae and negatively buoyant diatoms) and the effects of higher trophic levels are parameterised through loss terms. Secchi depth is not explicitly simulated by CAEDYM but was estimated from simulated optical properties in order to calculate TLI from model output.

2.4.1 Forcing data for lake modelling

2.4.1.a Bathymetry

Lake Hayes bathymetry was sourced from an echo sounding survey completed from the 22 - 23 March, 1977 (Irwin 1981), which was digitised into a shape file, and subsequent digital elevation model (raster – 5 m resolution) shown in Figure 4. The elevation model was then used to calculate hypsometric data describing relationships between lake height (depth), area and volume used as input to 1-D modelling (Figure 6).

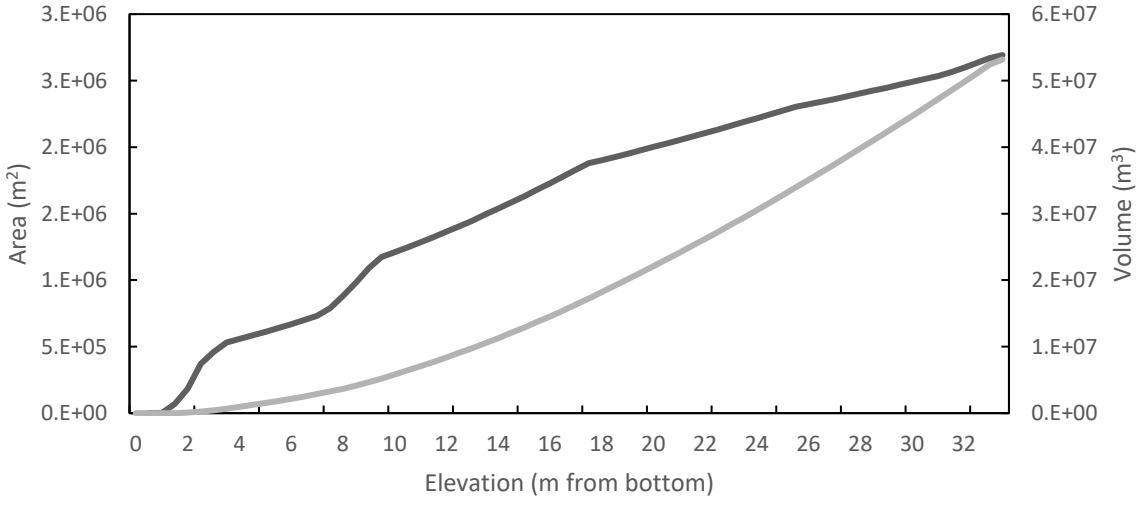

Figure 6. Lake area (dark line) and volume (light line) used as hypsometric data for 1-D modelling (see also, Figure 4).

2.4.1.b Water level

Lake water level data were only available for a short period in the early 1990s (Figure 7). In the absence of further information, we made an assumption of a constant water level of 33.5 m above the lake bottom. This likely introduces substantial error into the model water balance at sub-annual time-scales.

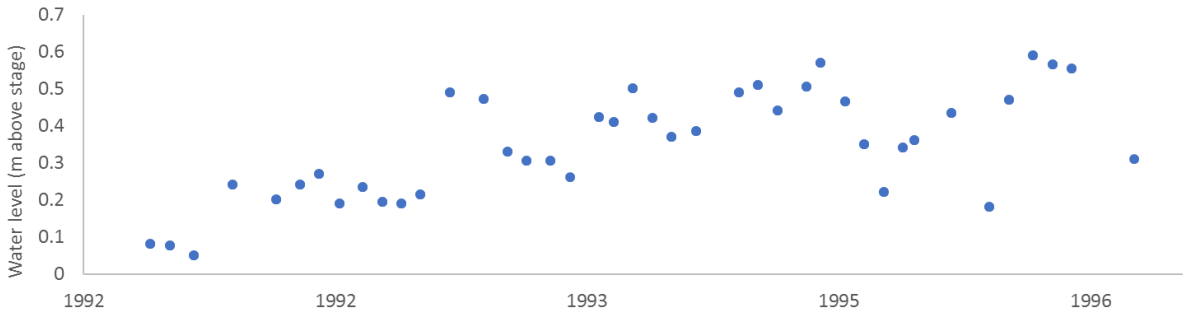

Figure 7. Available water level record for Lake Hayes (data: ORC).

2.4.1.c Meteorology

Meteorological data used as input to 1-D modelling were sourced from a meteorological station at Queenstown airport, which is located approximately 5.5 km from the southern shore of Lake Hayes (Figure 5, 45.0210° S, 168.7399° E).

Most hourly meteorological data for years 1980 - 2013 for the Queenstown airport meteorological station were downloaded from the NIWA Cliflo database (https://cliflo.niwa.co.nz/). Data from this station for the years 2013 - 2018 were acquired through the MetService directly. Data included atmospheric pressure (P, hPa), air temperature (Tair, ˚C), wet bulb temperature (Twet, ˚C), dew point temperature (Tdew, ˚C), relative humidity (RH, %), precipitation (precip, mm), and wind speed (U, m s^{-1}).

Hourly vapor pressure (*Pv,* hPa*)* was estimated as:

$$\mathrm{Vp} = \frac{\mathrm{RH}}{100} \times \mathrm{EXP}(2.303 \times \frac{7.5 \times \mathrm{Tair}}{\mathrm{Tair}+237.3}) + 0.7858. \qquad \text{(TVA, 1972)}$$

The meteorological forcing data (*Tair*, *Pv, U*, *precip*) derived from these observations were generated at daily frequency by averaging or summation, as appropriate. Gaps in the data set were either linearly interpolated or filled with data from nearby stations including Queenstown EWS (-45.03476° S, 168.66364° E; approx. 12 km distance from the lake).

Hourly shortwave radiation (*SW*, W m^{-2}) data for the period of 1991 – 2018 from the same station was downloaded from the NIWA Cliflo database. The cloud cover fraction (*CLOUD*) is required by the model to calculate long wave radiation. CLOUD was derived from the relationship between observed SW and clear-sky shortwave radiation (SW_{clear}) and shortwave radiation under 100% cloud cover (SW_{cloudy}) as follows:

$$CLOUD = 1 - \frac{SW - SW_{cloudy}}{SW_{clear} - SW_{cloudy}},$$

where SW_{clear} was calculated using Bird's clear sky model (Bird and Hulstrom, 1981), and SW_{cloudy} was estimated from historical SW records, where fully cloudy day was assumed as 5% of all the data.

All model input meteorological forcing data are visualised in Figure 18, including daily average air temperature (°C), cloud cover (fraction of whole sky), rainfall (m), shortwave radiation (W m^{-2}), vapour pressure (hPa), and wind speed (m s^{-1}).

2.4.2 Model calibration method

A conceptual diagram summarising the final development process of the Lake Hayes ecological model is shown in Figure 8. In any model, forcing data (inputs such as meteorological data and inflow / outflow data) need to be carefully prepared. Because many forcing data in Lake Hayes have been synthesised due to lack of observations or low sampling resolution (e.g., evaporation form the lake), some of the physically sensitive forcing data were prepared as initial estimates and dynamically adjusted after initial model runs. Once the forcing data were ready to be applied in the model, parameter values for the initial model run was estimated from a typical literature values and from morphologically / ecologically similar lake models, as well as observations if applicable. Initial conditions for temperature, dissolved oxygen, nutrient concentration and phytoplankton biomass were derived from measurements as a representative beginning of hydrological year (July 1st). Model parameters were adjusted manually within a typical range (i.e. from literature and previous model applications) to fit in-lake observations. Manual calibration was operated in stepwise fashion, although feedback and readjustment of calibrated parameters were necessary due to the dynamic nature of the model (e.g., phytoplankton biomass modifies heat budget, whereas this process will influence surface evaporation and eventually water balance and stratification). First, the hydrodynamic component was calibrated, primarily to the water level, and stratification dynamics thereafter. With reasonable stratification dynamics, TN, TP, DO, and suspended sediment (SS) were calibrated to a sustainable level. The model does not explicitly simulate TN, TP or total suspended sediment (TSS), these values were estimated from inorganic and organic nutrients as well as nutrient storage in phytoplankton biomass. Because chlorophyll *a* measurements are composites of phytoplankton species dynamics, chlorophyll *a* dynamics were simulated by modelling five different taxonomical groups' biomass dynamics. This continued until algal and key nutrient species dynamics showed a reasonable match, while adjustment of hydrodynamic components were made simultaneously.

Modelled TLI was compared with observed data and calibration of parameters were undertaken in DYRESM-CAEDYM until an optimal match was achieved between daily simulated variables and available field measurements, and between modelled and measured TLI components. We aimed to calibrate model TLI within ± 0.1 TLI units of measured TLI. During this process, three years of observations from 1 July 2007 to 1 July 2010 were used to calibrate the model. After every few model iterations, the model was extended to 5 years from 1 July 2007 to 1 July 2012 to test if the dynamics of 3 years were naturally extended to 5 years. At the end of calibration, a 5 year validation period of 1 July 2012 to 1 July 2017 was used to determine unbiased model error. Auto-calibration software was developed to assist calibration efforts, and thousands of simulations were run until no further improvement in model performance was achieved. A range of error statistics were used to assess model performance (see Appendix Table 3).

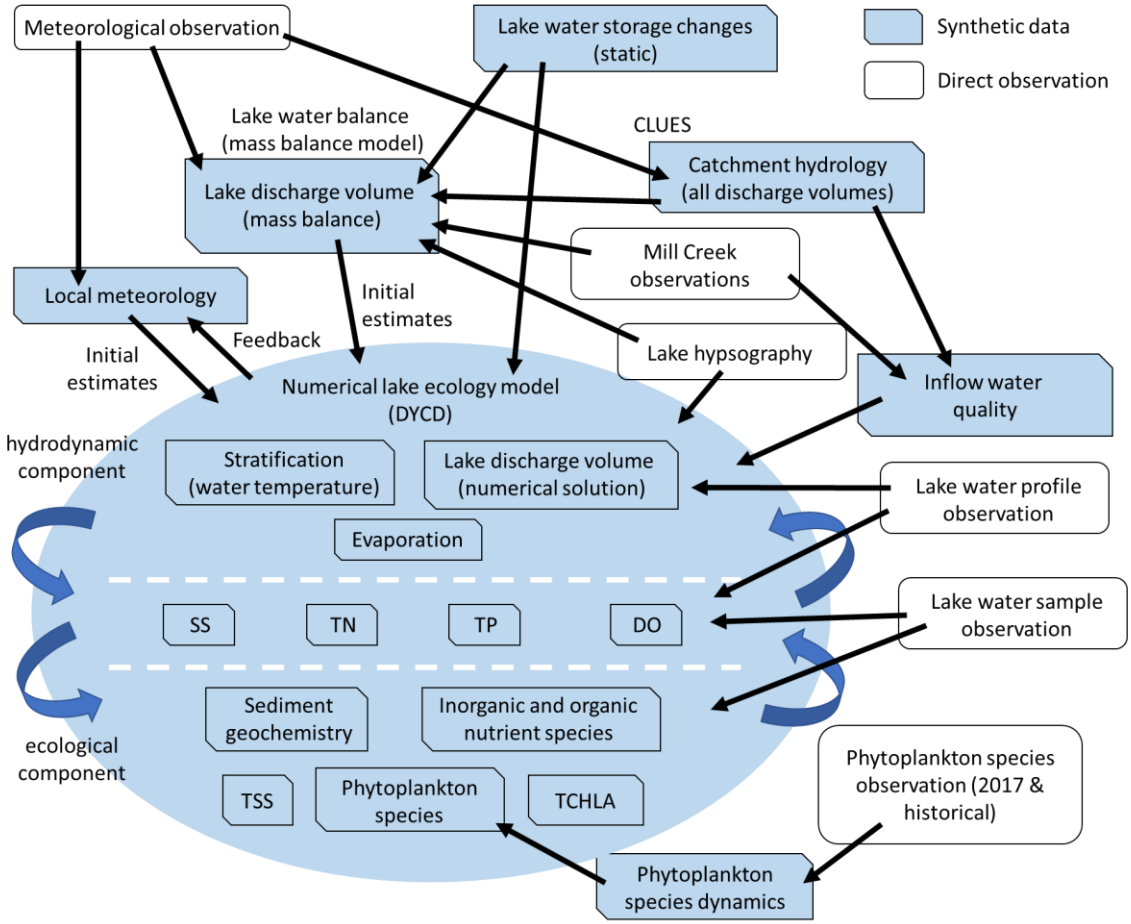

Figure 8. Schematic diagram of data inputs and data processing linkages in development of the Lake Hayes physical-biogeochemical lake model. SS: suspended sediment; TN; Total Nitrogen; TP: Total Phosphorous; DO: Dissolved Oxygen; TCHLA: Total chlorophyll *a*.

2.4.3 Scenario simulations

Multiple lake management 'scenarios' were conceptualised in consultation with ORC, and modelled using DYRESM-CAEDYM for the entire simulation period (2007 – 2017, Table 3). The assessed approaches can be broadly attributed to five categories:

1- **External nutrient load reduction:** associated with land use change or nutrient loss mitigation by improved management practices and/or targeted interventions, e.g. erosion mitigation, denitrification beds. Nutrient reduction scenarios included 10, 25, 50% reductions of N, P and suspended sediment (SS).
2- **Hydrological modifications:** various options to re-route flow from nearby Arrow River Irrigation Scheme to the lake. Options include full or partial diversion, as well as constant or seasonally varying discharge to the lake.
3- **Artificial mixing:** by aeration (bubbler). This included two different air flow rates of 300 and 500 L S^{-1}.
4- **Geochemical engineering:** by sediment capping to reduce internal loading (e.g. Phoslock™) and/or continuous low-dosage alum treatment to reduce dissolved P and increase flocculation in the water column.

5- **Hypolimnetic withdrawal:** Lake water is withdrawn (likely via a pipe) from near the lake bottom, which aims to extract nutrient rich water (due to sediment nutrient release.

The combinations of above management options comprising each simulated management scenario are described in Table 3. TLI values were compared between modelled scenarios to provide an assessment of the predicted effects of each scenario on lake trophic status in the context of water quality objectives.

For scenarios of reduced external loading, maximum modelled fluxes of sediment release and oxygen demand were reduced by a corresponding amount (Table 2). This broad assumption acknowledges that internal loading is likely to change along with external loading, although these processes will likely take a decade or more to equilibrate to one another (Jeppesen et al., 2007; Søndergaard et al., 2007). In this sense the scenarios represent a medium- to long-term outcome for lake water quality, rather than an immediate response to each management strategy.

Table 2. Total nitrogen (TN) and total phosphorus (TP) loads under each management scenario, and corresponding sediment fluxes for oxygen and dissolved nutrients.

Scenario	TN load ($t\ y^{-1}$)	TP load ($t\ y^{-1}$)	PO_4 release ($g\ m^{-2}\ d^{-1}$)	NH_4 release ($g\ m^{-2}\ d^{-1}$)	Oxygen demand ($g\ m^{-2}\ d^{-1}$)
s100	8.68	0.491	0.020	0.025	2.00
s90	7.88	0.449	0.018	0.023	1.82
s75	6.69	0.386	0.016	0.019	1.56
s50	4.69	0.282	0.011	0.013	1.12
s100_arr	9.60	0.604	0.019	0.021	1.90
s90_arr	8.81	0.562	0.018	0.019	1.76
s75_arr	7.61	0.499	0.015	0.016	1.55
s100_arr_flow1	9.41	0.580	0.019	0.021	1.90
s100_arr_flow2	9.22	0.556	0.018	0.021	1.77
s100_arr_hWQ	9.42	0.581	0.018	0.021	1.84
s100_hypWdr	8.68	0.491	0.020	0.025	2.00
S100_arr_hypWdr	9.60	0.604	0.019	0.021	1.90
s100_bub_50L	8.68	0.491	0.020	0.025	2.00
s100_bub_300L	8.68	0.491	0.020	0.025	2.00
s100_infDose	8.68	0.491	0.020	0.025	2.00
s100_infDose_sedCap	8.68	0.491	0.010	0.013	1.00
s100_sedCap	8.68	0.491	0.010	0.013	1.00

Table 3. List of all lake management scenarios simulated using the DYRESM-CAEDYM lake model.

Scenario name	Catchment TN & TP	Flushing flow to Hayes	Aeration/ mixing rate	Inflow flocculant dosing	Sediment capping	Hypolimnetic withdrawal	Description
	(%)	$m^3 s^{-1}$	($L s^{-1}$)	✓	✓	✓	
s100	100	-	-	-	-	-	Baseline ('business-as-usual')
s90	90	-	-	-	-	-	10% reduction in catchment N, P and TSS
s75	75	-	-	-	-	-	25% reduction in catchment N, P and TSS
s50	50	-	-	-	-	-	50% reduction in catchment N, P and TSS
s100_arr	100	0.2	-	-	-	-	Arrow River water added to Mill creek at constant flow of 0.2 $m^3 s^{-1}$, nutrient concentrations set to average of measurements at Morven Ferry Road.
S90_arr	90	0.2	-	-	-	-	25% reduction in catchment N and P, Arrow R. flushing with surface withdrawal.
s75_arr	75	0.2	-	-	-	-	25% reduction in catchment N and P, Arrow R. flushing with surface withdrawal
s100_arr_flow1	100	<0.2	-	-	-	-	Arrow River water added to Mill creek 0.2 $m^3 s^{-1}$ April to October, 0.1 $m^3 s^{-1}$ November to March. Nutrient concentrations set to average of measurements at Morven Ferry Road.
s100_arr_flow2	100	<<0.2	-	-	-	-	Arrow River water added to Mill creek 0.2 $m^3 s^{-1}$, April to October only. Nutrient concentrations set to average of measurements at Morven Ferry Road.
S100_arr_hWQ	100	0.2	-	-	-	-	Arrow River water added to Mill creek 0.2 $m^3 s^{-1}$, nutrient concentrations set to 50% average of measurements at site (to reflect upstream position of offtake relative to monitoring site.
S100_hypWdr	100	-	-	-	-	✓	Hypolimnetic withdrawal of 200 $L s^{-1}$ (replaces some of surface withdrawal)
s100_arr_hypWdr	100	0.2	-	-	-	✓	Arrow River water added to Mill creek 0.2 $m^3 s^{-1}$. Nutrient concentrations as average of measurements at Morven Ferry Road. Hypolimnetic withdrawal of 200 $L s^{-1}$.
s100_bub_300L	100	-	300	-	-	-	Artificial aeration with air flow of 300 $L s^{-1}$
s100_bub_500L	100	-	500	-	-	-	Artificial aeration with air flow of 500 $L s^{-1}$
s100_infDose	100	-	-	✓	-	-	Continuous application of aluminium sulphate (50 % of DRP inflow converted to PIP)
s100_infDose_sedCap	100	-	-	✓	✓	-	Continuous application of high dose of aluminium sulphate (80% of DRP inflow converted to PIP); in-lake PO_4 release rate 50% of s100, oxygen consumption 75%, NH_4 release 75%
s100_sedCap	100	-	-	-	✓	-	Sediment capping dose of aluminium sulphate direct to lake bottom; in-lake PO_4 release rate 50% of s100, oxygen consumption 75%, NH_4 release 75%

3 Results

3.1 Synthesis of Lake Hayes monitoring record

Data from *in situ* sampling provided a background against which to assess more detailed studies of lake processes. Figure 9 summarises all profile sensor observations (Temperature, DO, pH, chlorophyll fluorescence, conductivity and turbidity) from 1980s onwards, Figure 10 focuses on the same data for the period 2005-2017. Figure 11 illustrates nutrient sampling observations (ammonium, nitrate + nitrite, phosphate, total nitrogen, and total phosphorus) from all depths from 1980s onwards, and Figure 12 shows this data plotted in recent years. Figure 13 also summarises nutrient samples in recent years, but only shows hypolimnetic observations which are typically affected by anoxic conditions under stratified environments in summer. Figure 14 displays time-series of Secchi disc depth and chlorophyll *a*.

From temperature and dissolved oxygen profile observations, it is evident that Lake Hayes water column experiences strong yearly stratification (i.e., monomictic). It was also shown that majority of hypolimnetic oxygen is consumed resulting in near anoxia when stratified. An increase in overall turbidity was observed from 2014 onwards, but no clear origin of this increase was present in other water quality indicators. Because the turbidity increase was observed in both the hypolimnion and the epilimnion, it is possible that this change was mainly mechanical in origin, however reduced Secchi disk depths were also indicated from limited recent observations as well as Schallenberg & Schallenberg (2017). Therefore, possibilities of increased TSS due to phytoplankton species shift cannot be eliminated, considering that no TSS increase was present in the *in situ* stream data.

Surface nutrient measurements from the lake, approximately monthly from 2011 to 2018, suggested an average N to P ratio of approximately 10:1. This is lower than the baseline Redfield ratio of 16:1, and may indicate N is a limiting factor for phytoplankton growth. Hypolimnetic P concentration peaks showed signs of gradual decrease since 2011 (Figure 11), and hypolimnetic TP concentration followed a similar trend. However, no major surface TP concentration changes were observed in the data we obtained. No clear trends in N concentration were observed in both surface and deep samples.

Secchi disk depth decreases are apparent since 2005, but there is insufficient data to assess trends over recent years. Chlorophyll *a* concentrations indicate no clear seasonality, but a significant increase from 2007-2009 were observed and attributed to *Ceratium hirundinella*.

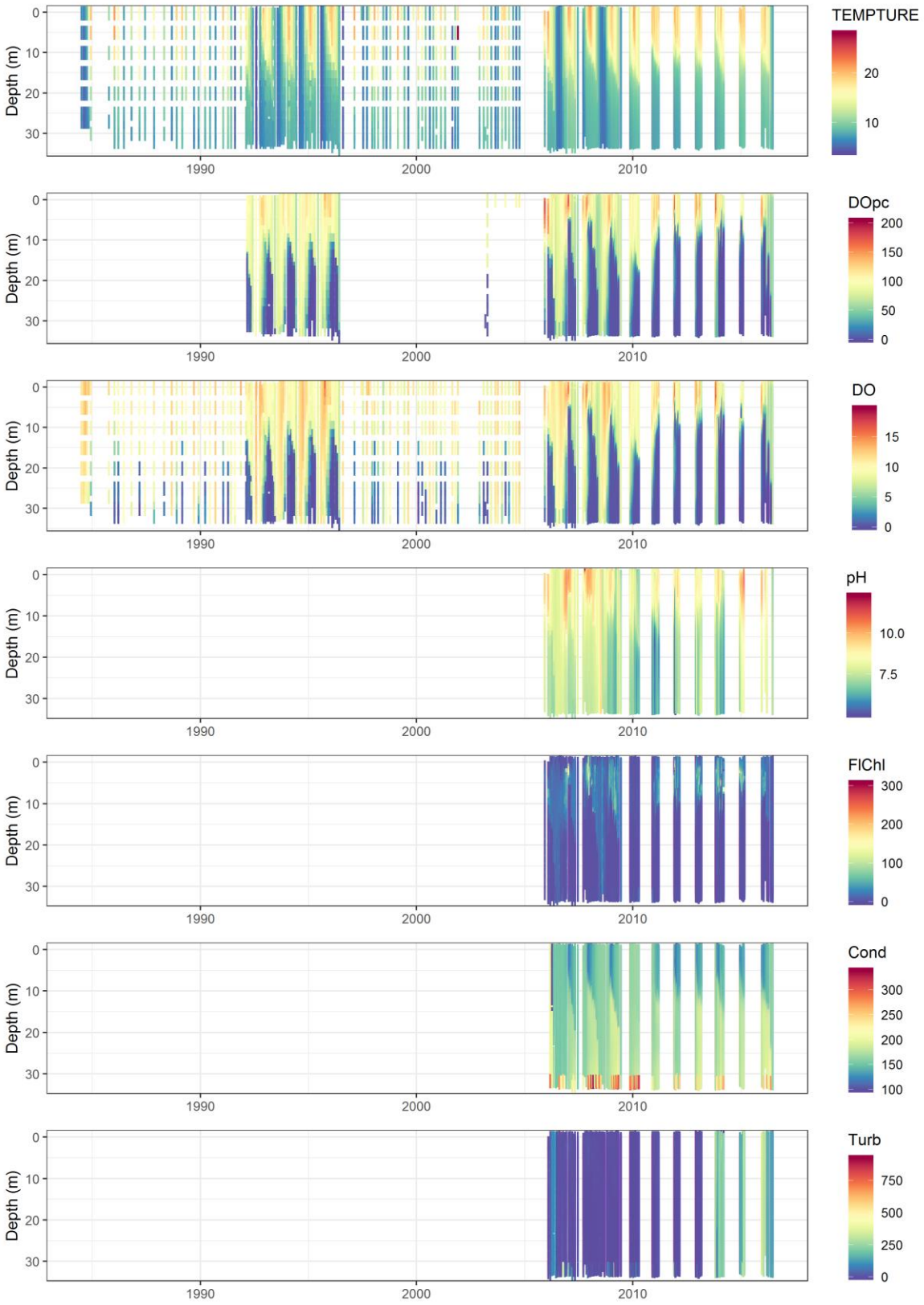

Figure 9. Vertical profiles of water quality in Lake Hayes, 1983 to 2017 for a) water temperature (TEMPTURE), b) dissolved oxygen (% saturation; DOpc), c) dissolved oxygen (mg L^{-1}; DO), d) pH, e) Chlorophyll fluorescence (uncalibrated relative units; FlChl), Conductivity (µS cm^{-1}; Cond), and Turbidity (uncalibrated relative units; Turb). The colour of each point in the plot represents the value of the water quality variable (white space represents no profile taken). Maximum frequency of profiles was approximately monthly, with long periods of discontinuity. Data supplied by Otago Regional Council.

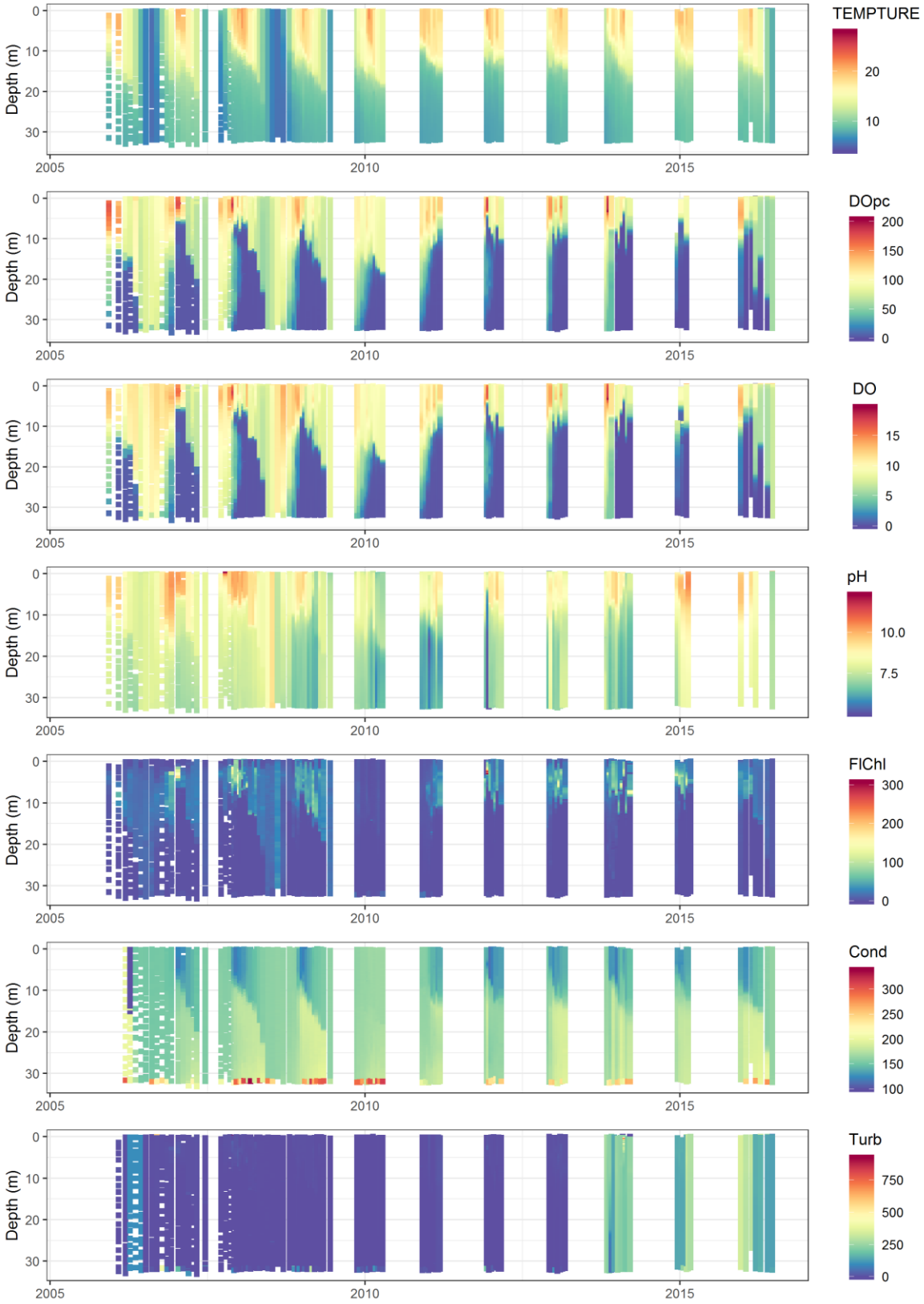

Figure 10. Vertical profiles of water quality in Lake Hayes, 2005 to 2017 for a) water temperature, b) dissolved oxygen (% saturation), c) dissolved oxygen (mg L^{-1}), d) pH, e) Chlorophyll fluorescence (uncalibrated relative units), Conductivity (µS cm^{-1}), and Turbidity (uncalibrated relative units). The colour of each point in the plot represents the value of the water quality variable (white space represents no profile taken). Maximum frequency of profiles was approximately monthly, with long periods of discontinuity. Data supplied by Otago Regional Council.

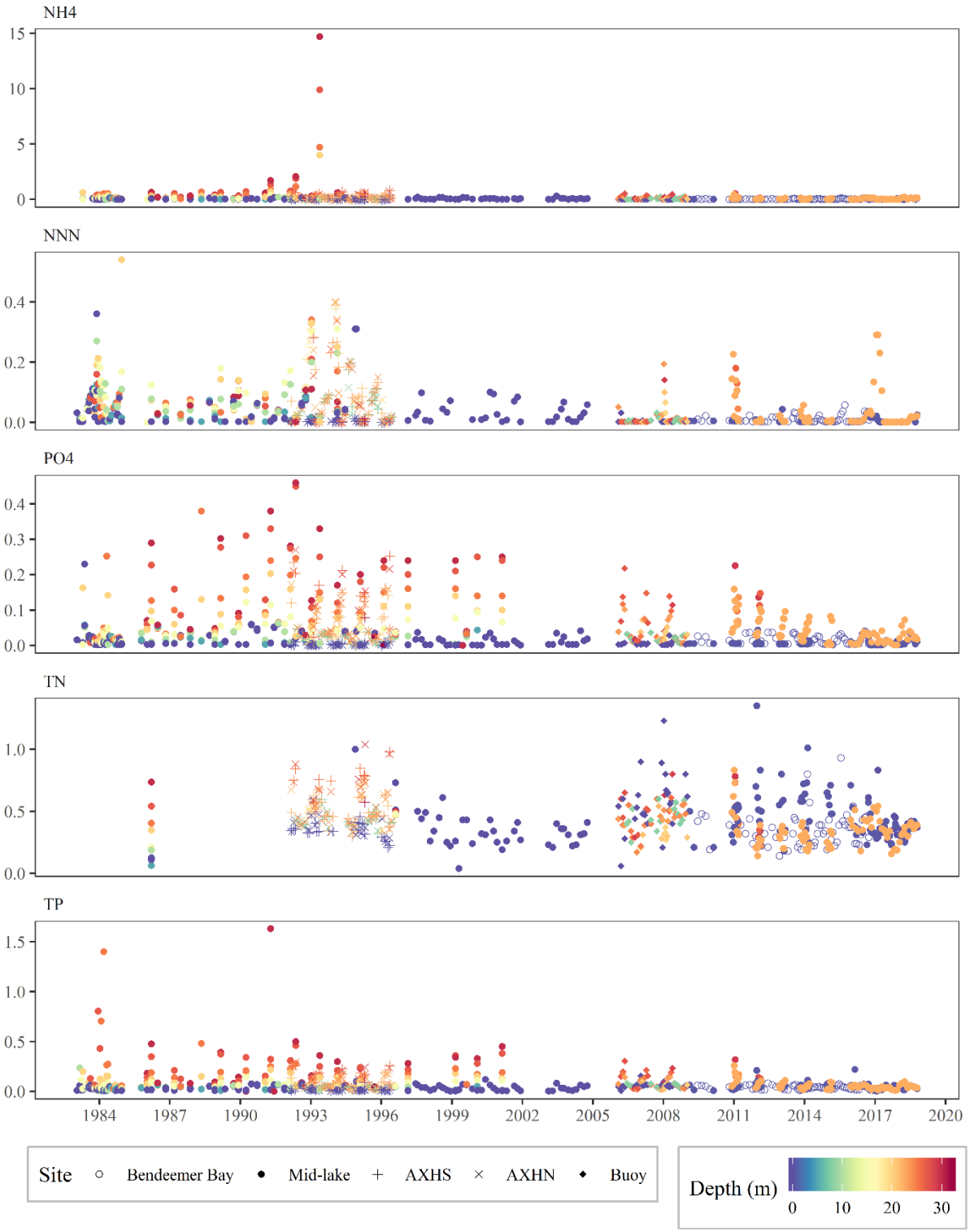

Figure 11. Water quality data from Otago Regional Council sampling of Lake Hayes at multiple sites, 1983 to 2017 for a) ammonium (NH_4, g N m^{-3}), b) nitrate + nitrite (NNN, g N m^{-3}), phosphate (PO_4; g P m^{-3}), total nitrogen (TN; g N m^{-3}), and total phosphorus (TP; g P m^{-3}). Measurement depth is represented by the colour of the dots, ranging from near surface (blue) to nearly 30 m depth (red).

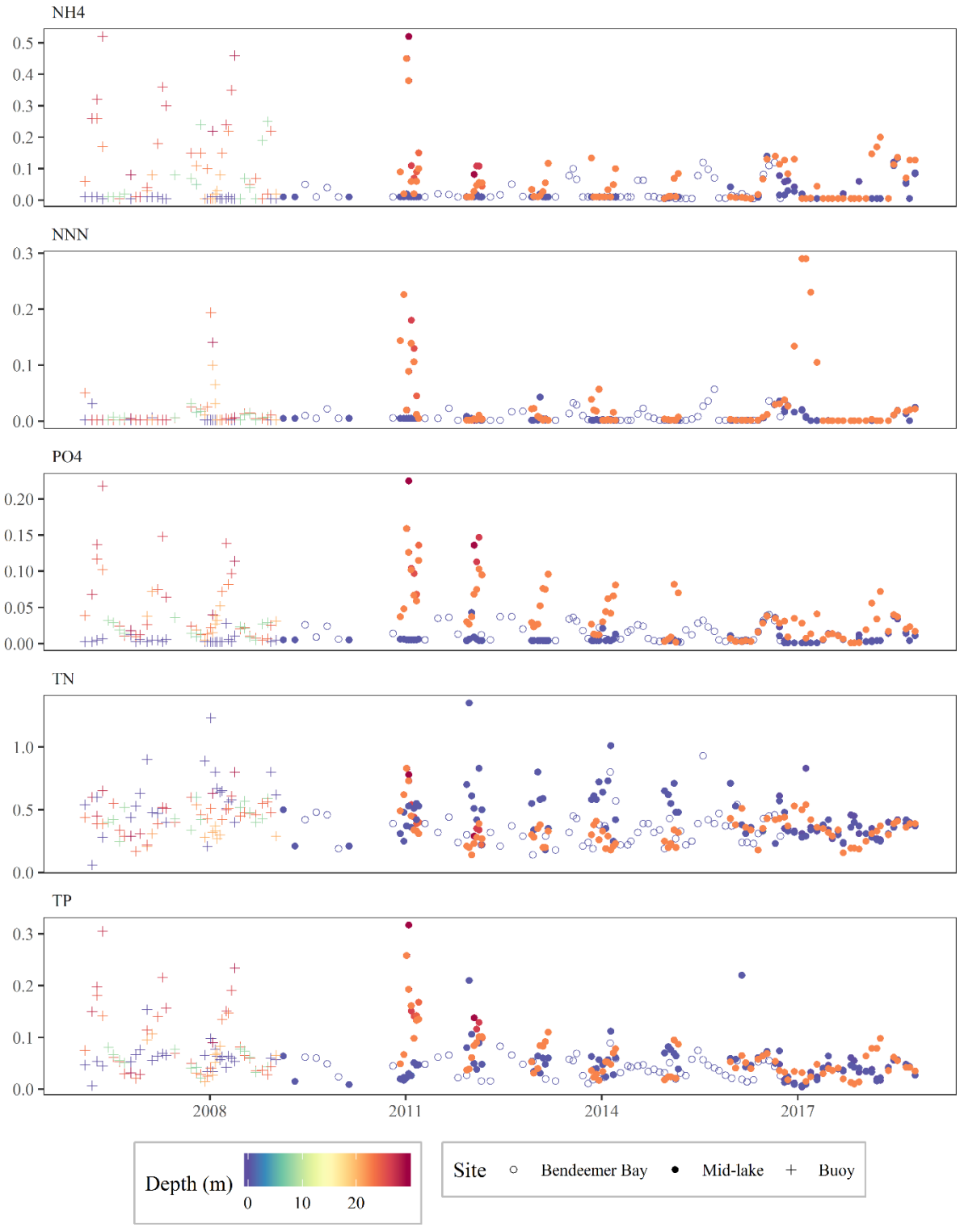

Figure 12. Water quality data from ORC sampling of Lake Hayes at multiple sites, 2005 to 2017 for a) ammonium (NH_4; g N m^{-3}), b) nitrate + nitrite (NNN; g N m^{-3}), phosphate (PO_4; g P m^{-3}), total nitrogen (TN; g N m^{-3}), and total phosphorus (TP; g P m^{-3}). Measurement depth is represented by the colour of the dots, ranging from near surface (blue) to nearly 30 m depth (red).

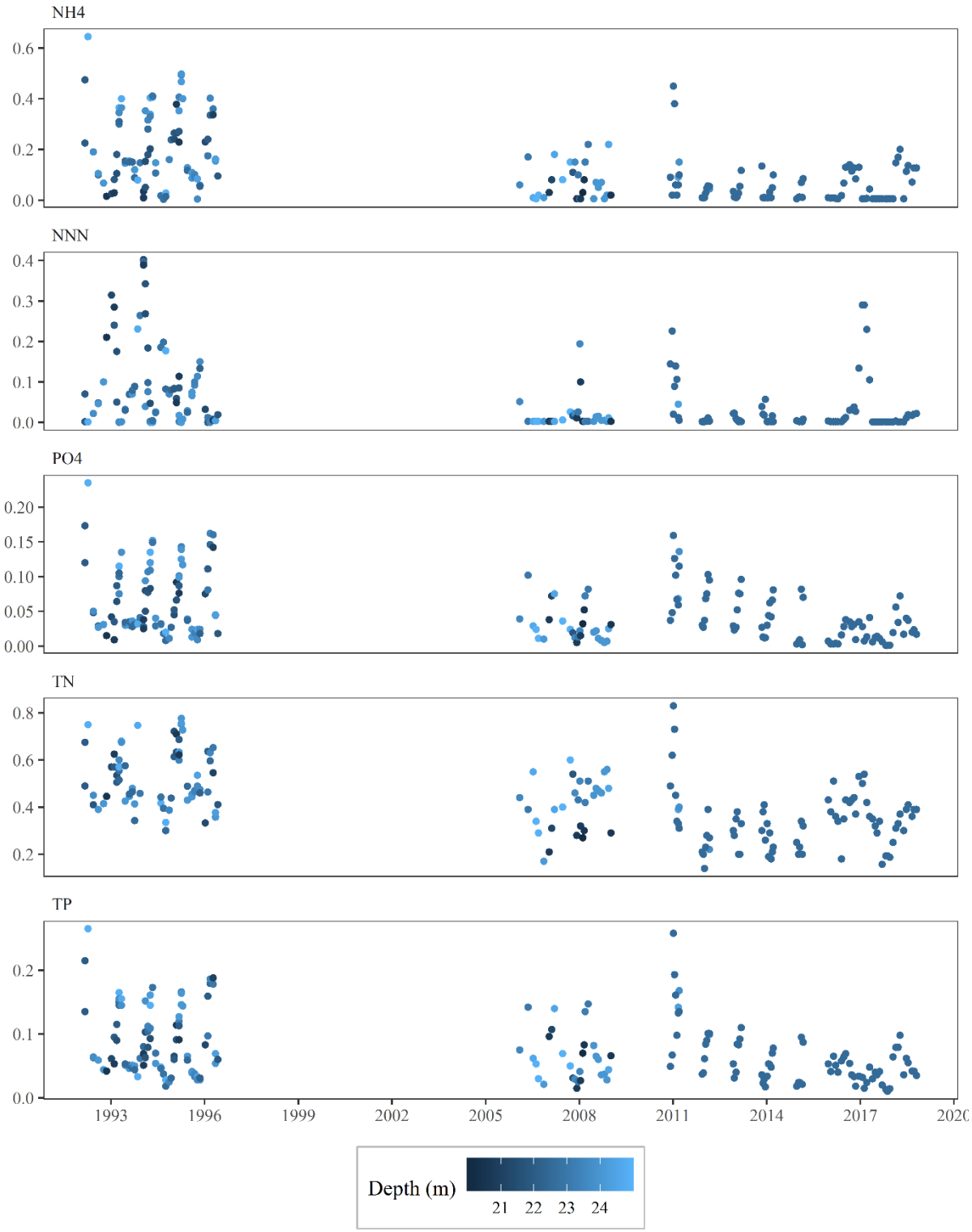

Figure 13. Water quality data derived from Otago Regional Council monitoring on Lake Hayes at multiple sites, 2010 to 2017 and restricted to samples collected between 20 and 25 m depth (with actual depth indicated by the colour of the dot). Values are shown for a) ammonium (NH_4; g N m^{-3}), b) nitrate + nitrite (NNN; g N m^{-3}), phosphate (PO_4; g P m^{-3}), total nitrogen (TN; g N m^{-3}), and total phosphorus (TP; g P m^{-3}). Some evidence of a reduction in internal loading (i.e., reduction in the release of dissolved nutrients from bottom waters during stratification) is indicated by the relatively lower measurements of recent years, however, apparent trends may be due to differences between sampling and analytical methodologies across the three separate monitoring periods evident.

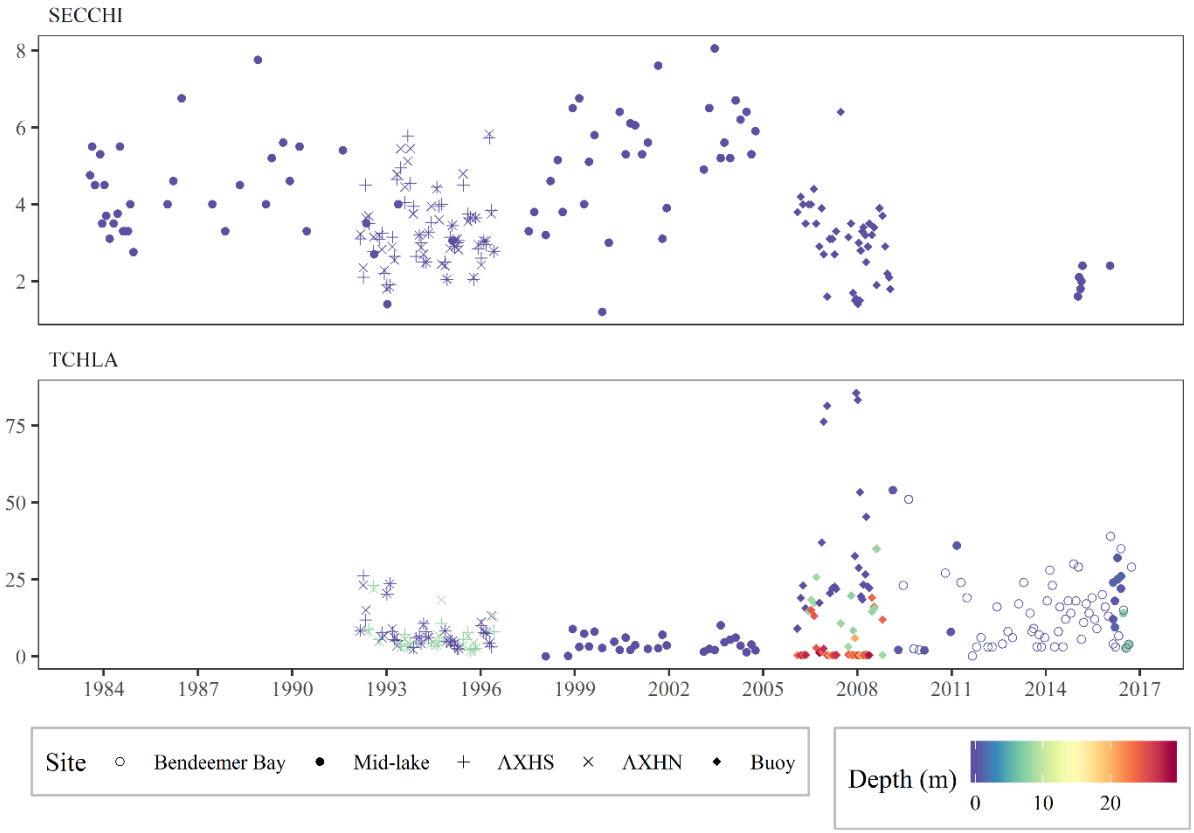

Figure 14. Water quality data from Otago Regional Council sampling of Lake Hayes at multiple sites, 1983 to 2017 for a) Secchi disk depth (m), and b) total chlorophyll *a* (TCHLA; mg m^{-3}). Measurement depth is represented by the colour of the dots, ranging from near surface (blue) to nearly 30 m depth (red). Notable changes in both chlorophyll and clarity are evident over time, although special attention should be paid to differences between sampling and analytical methodologies when interpreting across the various sites and monitoring periods.

A summary of long term yearly time-series of TLI components (in original units) is shown in Figure 15, with seasonal variability for each year were also displayed. Time-series of annual TLI (in TLI scale) with the four TLI components are also summarised in Figure 16.

Steady annual average concentrations of TN, TP and chlorophyll *a* were observed until the mid-2000s. Rapid increases in these variables were observed in the late 2000s, with slow steady reductions thereafter. Seasonal variability of TP has been consistently high since the 1980s. However, while relatively high winter concentrations were found throughout the period, high summer concentrations were only observed since the mid-2000s. Similarly, even though seasonal variability was relatively small for TN and chlorophyll *a* in early years, high summer TN and chlorophyll *a* values were only observed after the mid-2000s. A decline of Secchi disc depth was also observed in the mid-2000s, although observations were infrequent.

Historically Lake Hayes' TLI ranged from 3.5 – 4.0, but clear degradation was observed in the mid-2000s. However, a steady TLI improvement has been observed since 2007, with values between 4.5 and 5.

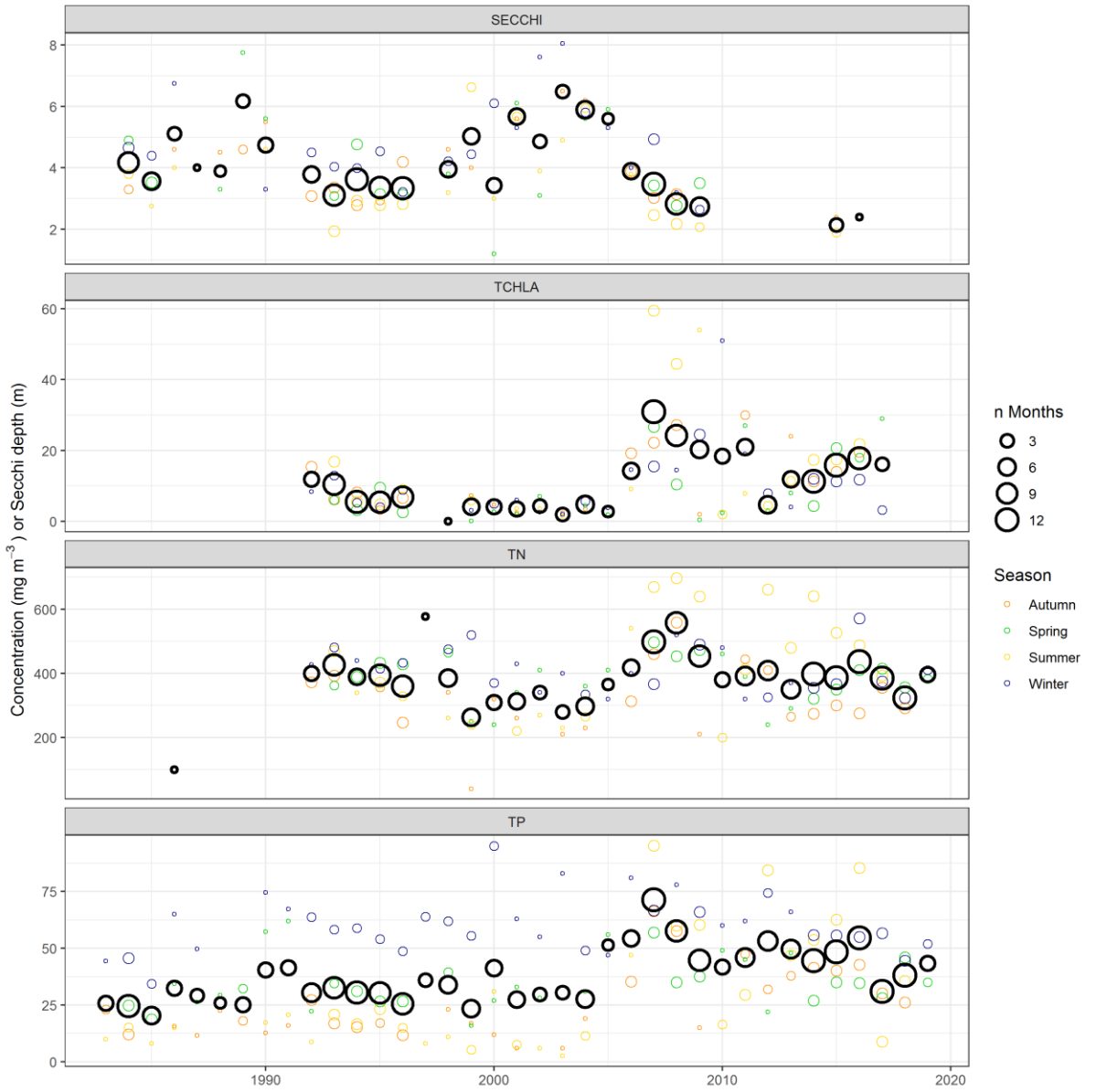

Figure 15. Measurements of TLI variables (Secchi depth, chlorophyll a (TCHLA), total phosphorus (TP) and total nitrogen (TN)) in Lake Hayes, 1983 to 2019. Individual samples were aggregated, retaining only the mean value for each season and variable, shown by the coloured circles. Black circles indicate the mean value of seasonal averages for the four TLI variables. The diameter of all circles is scaled to represent the number of monthly measurements aggregated. Note x axis is hydrological year.

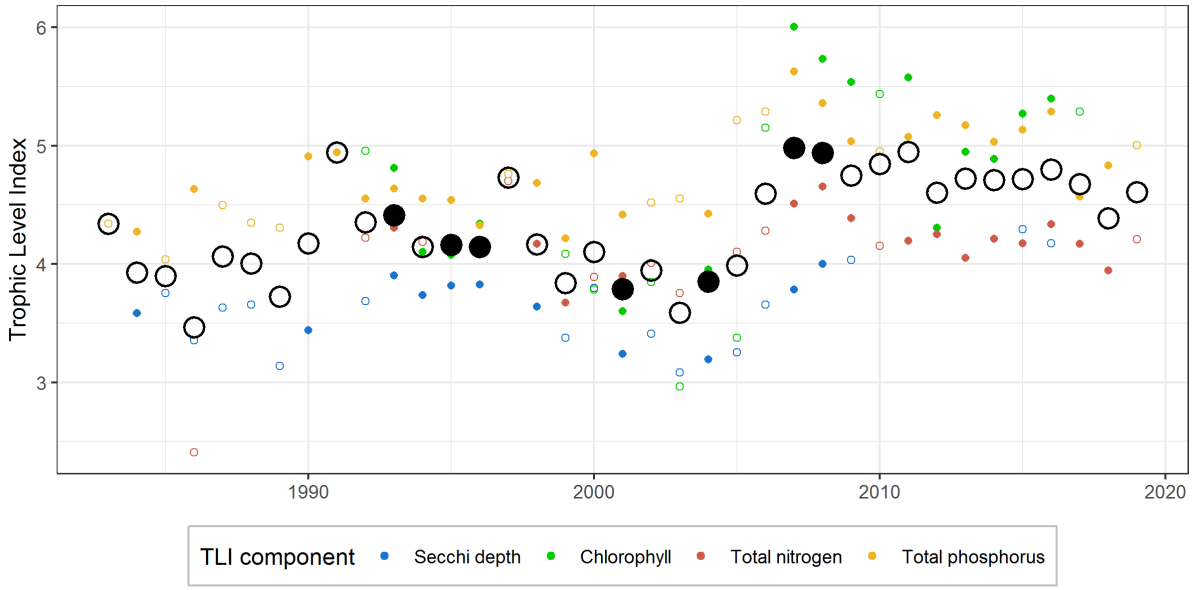

Figure 16. Annual Trophic Level Index (TLI) for Lake Hayes by hydrological year (previous July to present June). Each coloured circle is the mean of seasonal means, for one TLI variable with the relevant TLI equation applied (Burns et al. 1999). Large black circles are the annual TLI (average of four components). Solid circles denote years for which at least one measurement was available for all four seasons (solid black circles denote that all four component variables of the TLI were sampled each season). Open circles denote that measurements were missing for at least one season. Note x axis is hydrological year.

3.2 Meteorological inputs

Rainfall was summed for each hydrological year, with notable high rainfall years being 1989, 1994-1996 and 2000 (Figure 17). Meteorological forcing data (derived from Queenstown Airport) generally showed temporally stable patterns (Figure 18). However, it is notable that rainfall was generally more variable pre-2000.

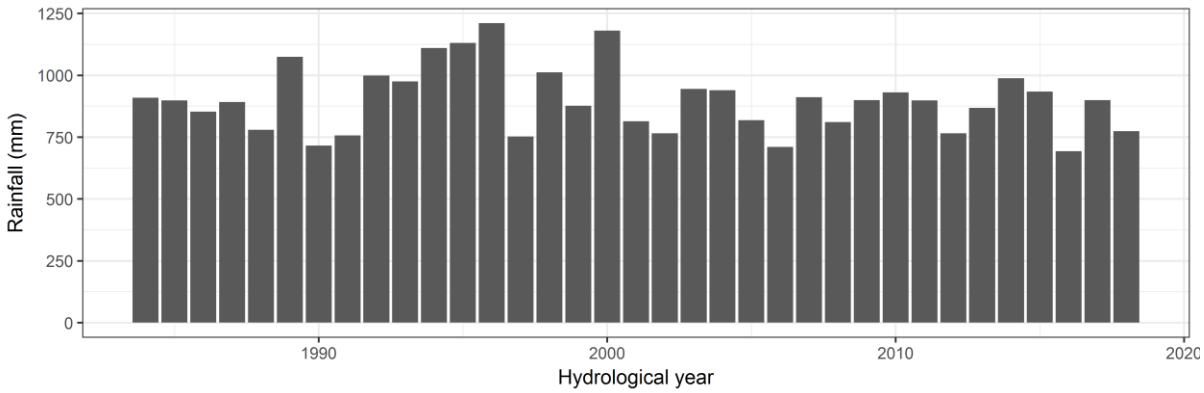

Figure 17. Total annual rainfall from Queenstown Airport, 1984 to 2018.

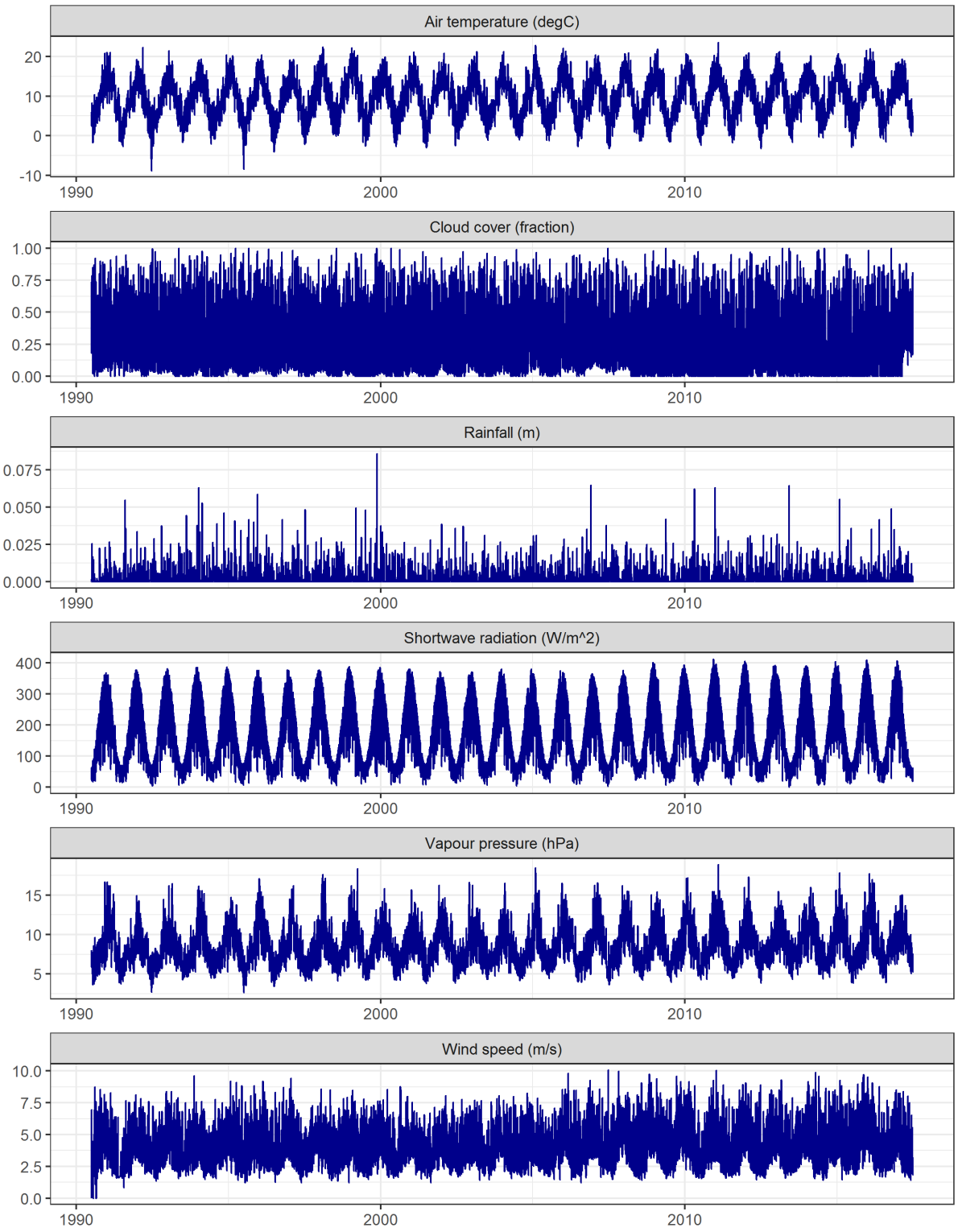

Figure 18. Meteorological data from Queenstown airport (45.0210° S, 168.7399° E) which were used as input to the lake model (2007 to 2017 only).

3.3 Catchment discharge and water quality

3.3.1 Nutrient loads estimated by the 'CLUES' model

Inflows to Lake Hayes were measured at Mill Creek, however this does not account for groundwater and surface water from ephemeral flows directly to the lake edge/bottom. Therefore, an estimate for total inflow (steady state flow) was sourced from the catchment model CLUES (Catchment Land Use for Environmental Sustainability; developed by NIWA) (Table 4). The ratio of CLUES flow and Mill Creek flow were used to derive a west and east catchment flow (representing all streams other than Mill Creek).

Table 4. Hydraulic, nutrient (Total nitrogen (TN); total phosphorus (TP) and sediment (SS) loads predicted by the steady-state catchment model CLUES (Catchment Land Use for Environmental Sustainability model; NIWA NZ). The catchment was divided into three sections; Mill Creek (to the North), and consolidated groups of streams for the eastern and western catchment.

	Type	Discharge ($m^3 s^{-1}$)	TN load ($t y^{-1}$)	TP load ($t y^{-1}$)	SS load ($kt y^{-1}$)
Mill Creek	Major inflow	0.494	14.678	1.487	2.215
East Streams	Multiple small streams	0.024	1.286	0.106	0.077
West Streams	Multiple small streams	0.024	1.249	0.078	0.058
Outflow	Lake outflow	0.547	6.68	0.27	0.072

Total discharge from Mill Creek (Figure 19), West and East, plus rainfall was used to create a water balance (including evaporation loss). From this water balance the lake outflow is calculated as the 30 day rolling average of the water balance residual.

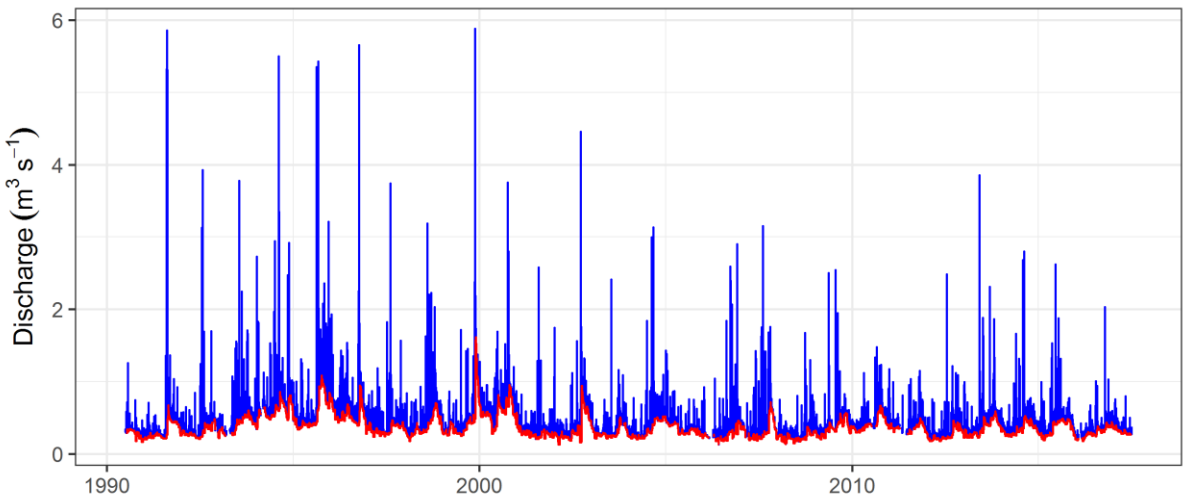

Figure 19. Mill Creek discharge (blue). Baseflow was calculated as a 10 day rolling minimum of Mill Creek discharge (red).

Average discharge per hydrological year was highly variable during the 1990's through 2001, however after this period, average discharge has been generally lower and less variable (Figure 20). The result of this lower average discharge would be longer residence times and lower flushing rates. Lower average discharge post 2000 also corresponds to generally lower nutrient concentrations in Mill Creek (Figure 21).

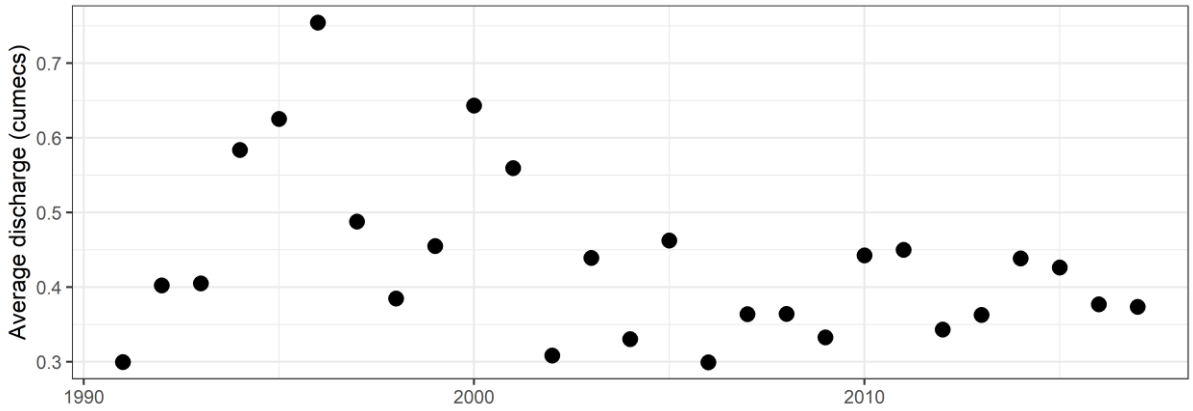

Figure 20. Annual average discharge (cumecs) from Mill Creek into Lake Hayes based on hydrological year.

Linear relationships between monthly measurements of inflowing water quality parameter concentrations and discharge volume at Mill Creek (Figure 21) were applied to estimate daily water quality parameters (Figure 22).

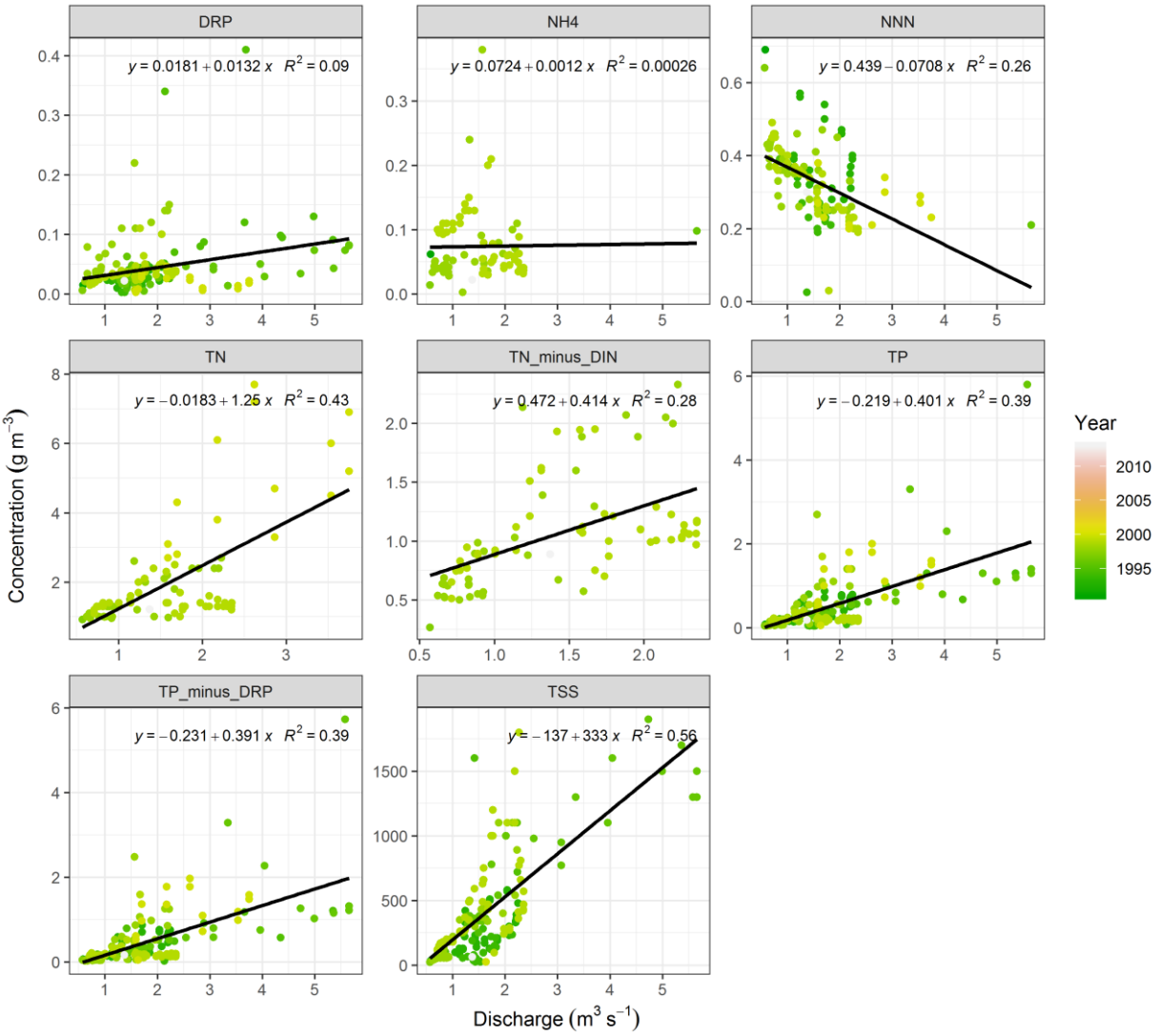

Figure 21. Discharge flow relationships used to estimate daily water quality in Lake Hayes inflows. Ammonium (NH4), Nitrate +Nitrite (NNN), Total nitrogen (TN), Dissolved inorganic nitrogen (DIN), Dissolved reactive phosphate (DRP), Total phosphorus (TP), Total suspended sediment (TSS).

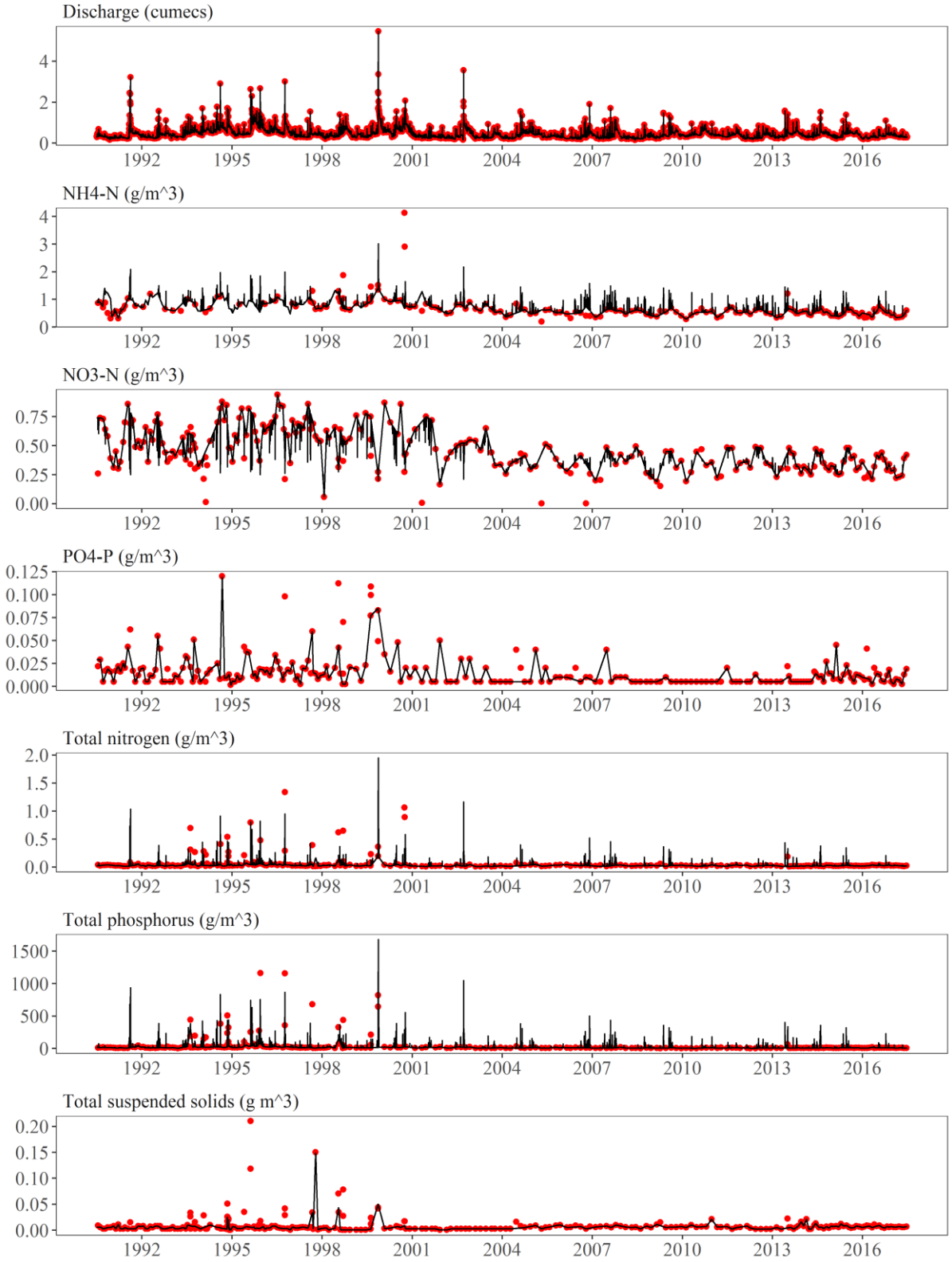

Figure 22. Modelled daily water quality parameters. Ammonium (NH4), Nitrate +Nitrite (NNN), Total nitrogen (TN) Dissolved reactive phosphate (DRP), Total phosphorus (TP), Total suspended sediment (TSS).

3.4 Seasonality in physical drivers

A key factor to consider is the residence time of water, which can be simply determined by dividing the lake water storage by the inflow volume. When the residence time of water is longer, flushing rate reduces and seasonal thermal stratification dynamics become an important influence on water quality.

Figure 23 shows yearly estimates of water retention time. Prior to the mid-2000s, residence time was generally lower than for later years, but more variable. Residence time over recent years was relatively steady at between three and four years.

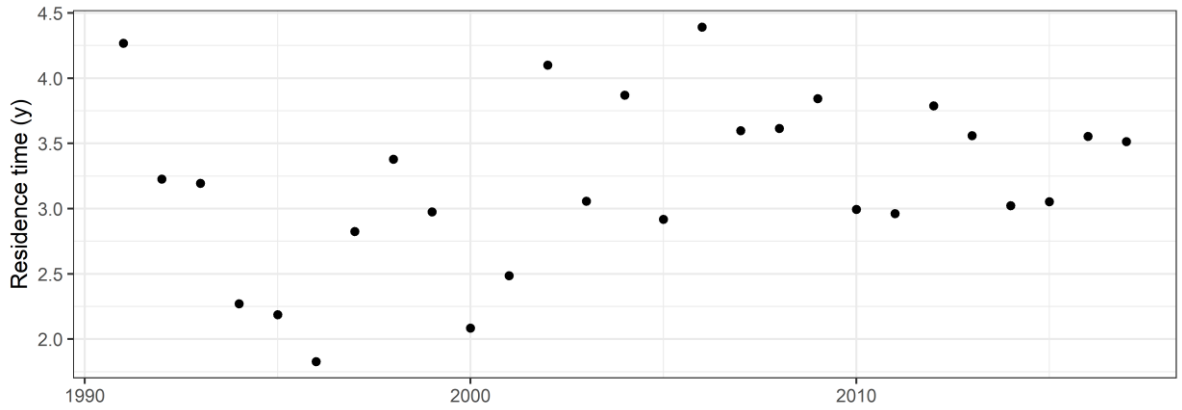

Figure 23. Lake Hayes water residence time based on the annual total inflow volumes. The values were assessed by simply dividing the lake water storage by annual total inflow volumes (hydrological year). Note x axis is hydrological year.

Water movement in lakes are influenced by physical dragging and buoyancy forces. Therefore, inflow, surface wind energy and heat budget are the dominant drivers of physical processes on water transport and stratification. Figure 24, Figure 25, and Figure 26 summarise the seasonality of daily flow volume, daily air temperature and wind speed. In Lake Hayes, inflow volumes generally increase from July, reach peak values around late October, and reduce towards summer (Figure 24). Wind speed also exhibited a strong seasonality with near sinusoidal shape (Figure 25), and daily air temperature also showed a typical sinusoidal pattern with the peak in February (Figure 26).

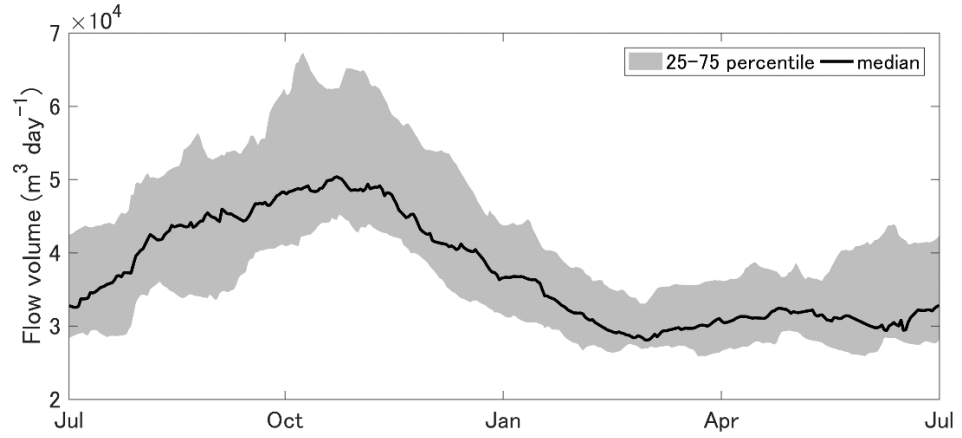

Figure 24. Seasonal patterns of daily total inflow volumes in Lake Hayes. The data from 1990 - 2017 were first smoothed (30 days zero phase moving average) and 25, 50 (median) and 75 percentile values of every day of year were obtained.

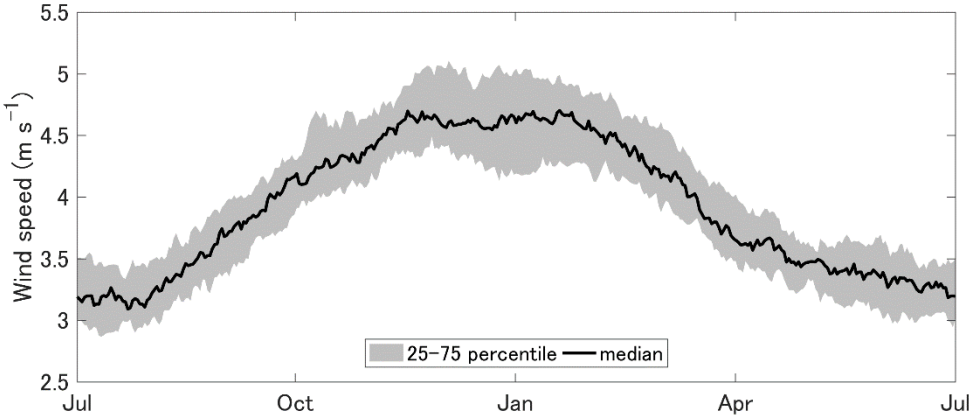

Figure 25. Seasonal patterns of daily average wind speed at Queenstown Airport meteorological station. The data from 1980 - 2018 were first smoothed (30 days zero phase moving average) and 25, 50 (median) and 75 percentile values of every day of year were obtained.

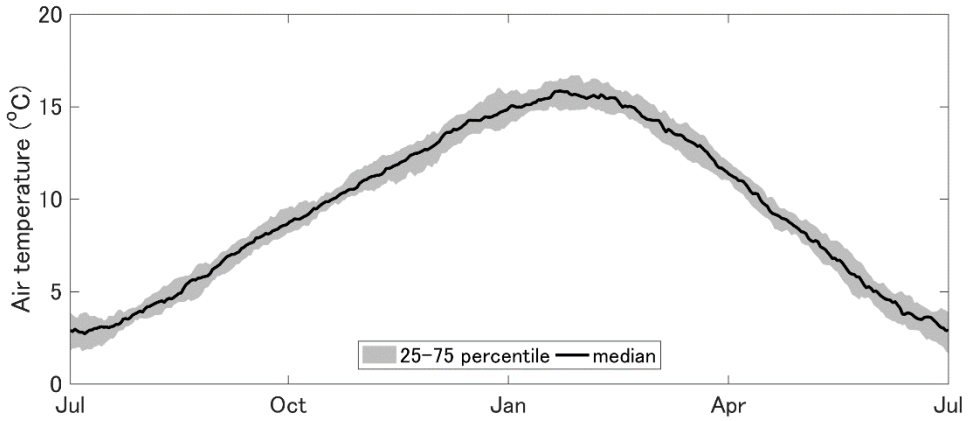

Figure 26. Seasonal patterns of daily average temperature at Queenstown Airport meteorological station. The data from 1980 - 2018 were first smoothed (30 days zero phase moving average) and 25, 50 (median) and 75 percentile values of every day of year were obtained.

3.5 Reconstructed phytoplankton dynamics in Lake Hayes

Observations of 2016-2017 phytoplankton dynamics (Figure 27) highlights the differences in characteristics between cell biovolume and cell density. The figure also suggests that grouped cell biovolumes is an adequate indicator of grouped chlorophyll *a* concentration. The results also indicate a spring bloom which was predominantly composed of Chlorophytes. The bloom collapsed soon after the beginning of October, presumably as a result of increased zooplankton grazing pressure. A reduced Chlorophyte reduction rate and increase of *Cryptomonas* sp. biovolume were observed before January, most likely due to reduced grazing pressure. The reduction of total biovolume around February is likely the result of the reduced nutrient availability in the epilimnion, whereas the increase of Chlorophytes and large Dinoflagellates biovolumes in autumn can be associated with a post stratification autumn bloom. This succession was in alignment with our knowledge of theoretical phytoplankton succession. However, this series of observation highlighted no signs of Cyanophyte blooms, and winter dynamics were not included.

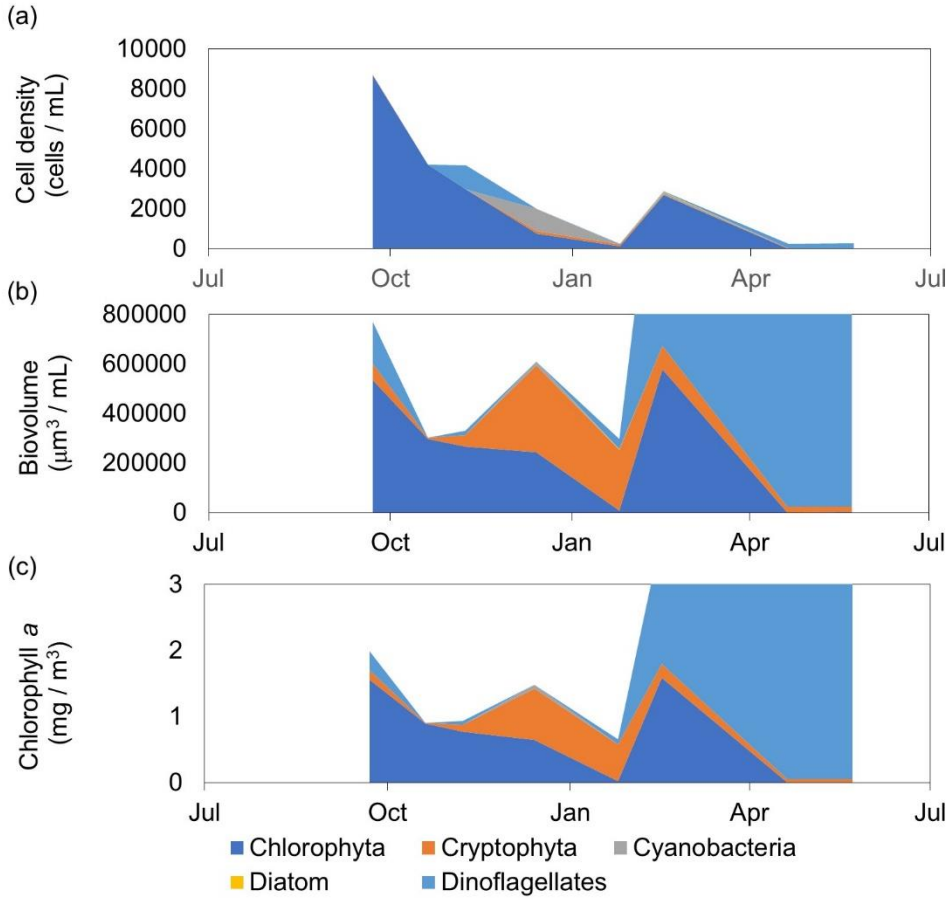

Figure 27. Phytoplankton taxonomic group dynamics in Lake Hayes for the period of 2016 to 2017 based on samples collected by Otago Regional Council. The dynamics are described in (a) cell density, (b) biovolume, and (c) chlorophyll *a* concentration.

Studies by Burns and Mitchell (1974) and Burns and Stockner (1991) were reviewed, and dominant taxa of each four seasons were extracted (

Table 5). Consistent dominant groups were observed when cell density is considered, whereas dominant functional groups in terms of biovolume were variable. Cyanophytes were only dominant in terms of biovolume from spring 1972.

Table 5. Summary of historical and recent dominant phytoplankton taxa by season for Lake Hayes. Data obtained from Otago Regional Council (recent measurements) and literature review (historical data). Abbreviations are BACI: Bacillariophytes (diatoms); Chlor: Chlorophytes; CRYP: Cryptophytes; DINO: Dinoflagellates and CYAN: Cyanobacteria. Abbreviations for sources are B&M: Burns and Mitchell (1974); B&S: Burns and Stockner (1991); and ORC: Otago Regional Council (2016). Colour is added to provide visual representation of the different groups.

	Source	Year	Spring	Summer	Autumn	Winter
			Oct, Nov, Dec	Jan, Feb, Mar	Apr, May, Jun	Jul, Aug, Sep
Density	B&M	1970	CYAN	CHLO	BACI	BACI
	B&M	1971	BACI / CYAN	CHLO	CHLO / BACI	BACI / CYAN
	B&M	1972	CYAN	-	-	-
	B&S	1990	CHLO	CHLO	CHLO / CRYP	BACI
	ORC	2017	CHLO / CYAN	CYAN / CHLO	CHLO / DINO	-
Biovolume	B&M	1970	DINO	DINO	DINO / BACI	BACI
	B&M	1971	CRYP / CHLO	CHLO	CHLO / BACI	BACI / CRYP
	B&M	1972	CYAN	-	-	-
	ORC	2017	CHLO / CRYP	CRYP / CHLO / DINO	DINO	-

The low level of data available meant that no consistent seasonal dynamic patterns could be discerned, therefore we attempted to create synthetic seasonal dynamics using both available data and expert knowledge. We adopted the philosophy of theory guided data science, which is an emerging work flow concept for scientific research (Karpatne et al., 2016). Instead of relying heavily on either theoretical knowledge or observation, information was harvested from both theory and observation. The aim of the concept is to reduce the variance of model results without significantly biasing them. To achieve this, we extracted approximate monthly biovolume proportions of functional groups from Burns and Mitchell (1974) and ORC observations (Figure 28). All information was merged to determine the probability of dominant functional groups in every month of a year (Figure 28-a). Based on the knowledge of phytoplankton community development, as well as notable events described in Schallenberg and Schallenberg (2017), synthetic seasonal dominance of phytoplankton groups was generated in monthly resolution (Figure 28b).

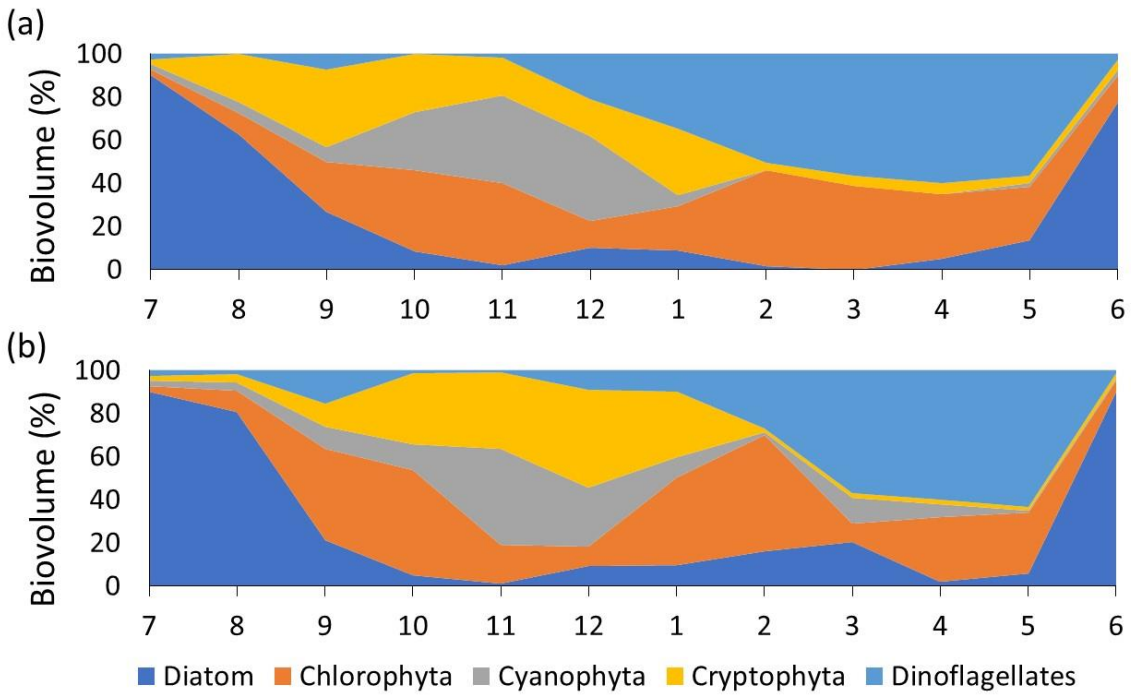

Figure 28. Synthetic (estimated) average monthly phytoplankton biovolume proportion of phytoplankton for Lake Hayes, a) statistical likelihood based on values obtained from literature, and b) adjusted dynamics considering recent event-based information as well as phytoplankton seasonal succession theory. Note x axis is month number.

3.6 Model calibration

Temperature and oxygen model results (both calibration and validation) are shown in Figure 29 and Figure 30. Temperature and oxygen dynamics were well simulated by the calibrated model, including hypolimnetic oxygen demand (slope of oxygen decline over time in bottom waters during stratification) and metalimnion depths (the zone of temperature and density change). The timing of stratification onset and mixing was also acceptably simulated, as evidenced by comparison of modelled temperature and oxygen with measurements from the profile monitoring (

Figure 31).

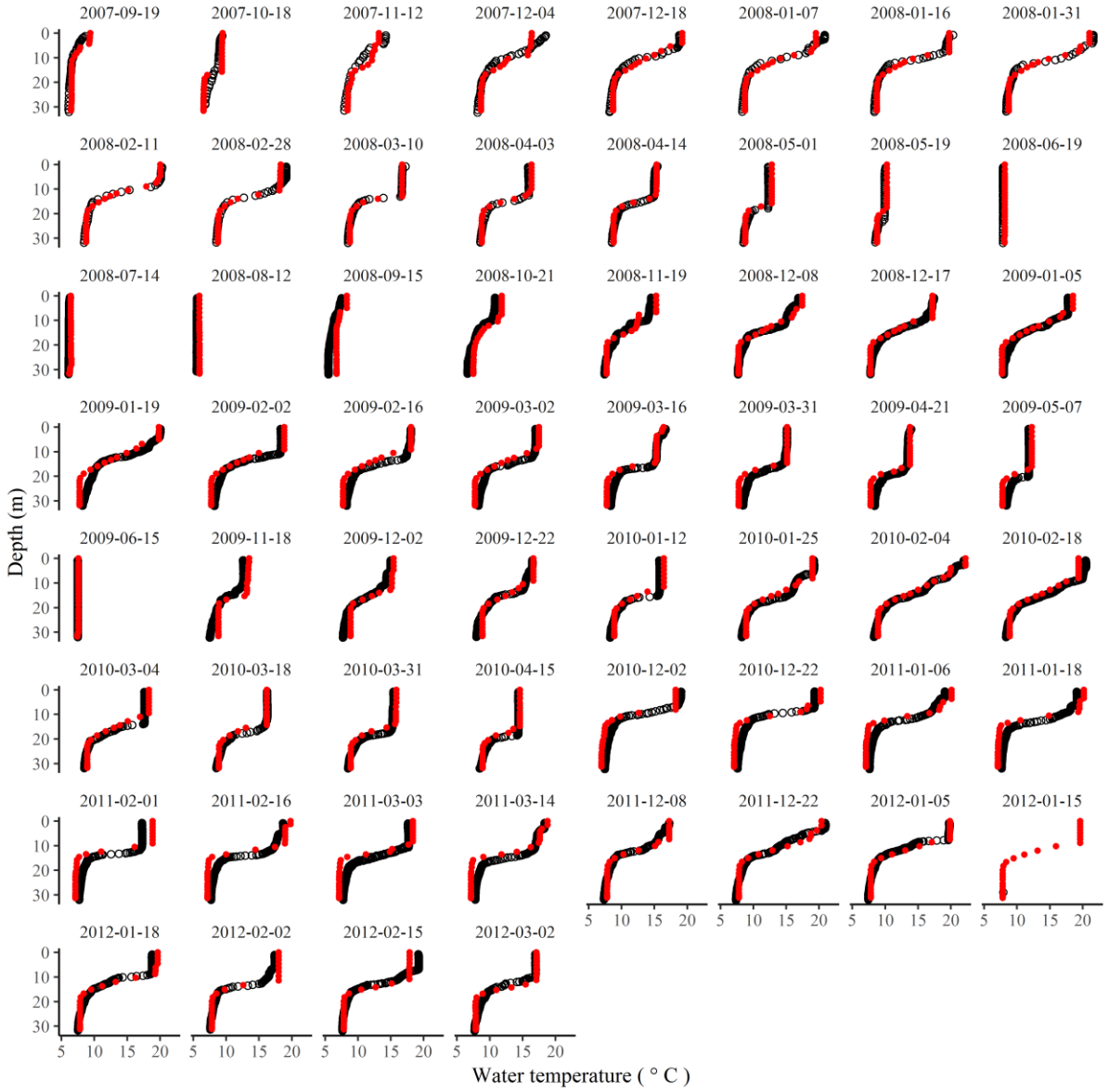

Figure 29. Model simulations (red dots) and field observations (black dots) for water column profiles of temperature, 2007 to 2012. A close match between black and red dots represents an ideal calibration.

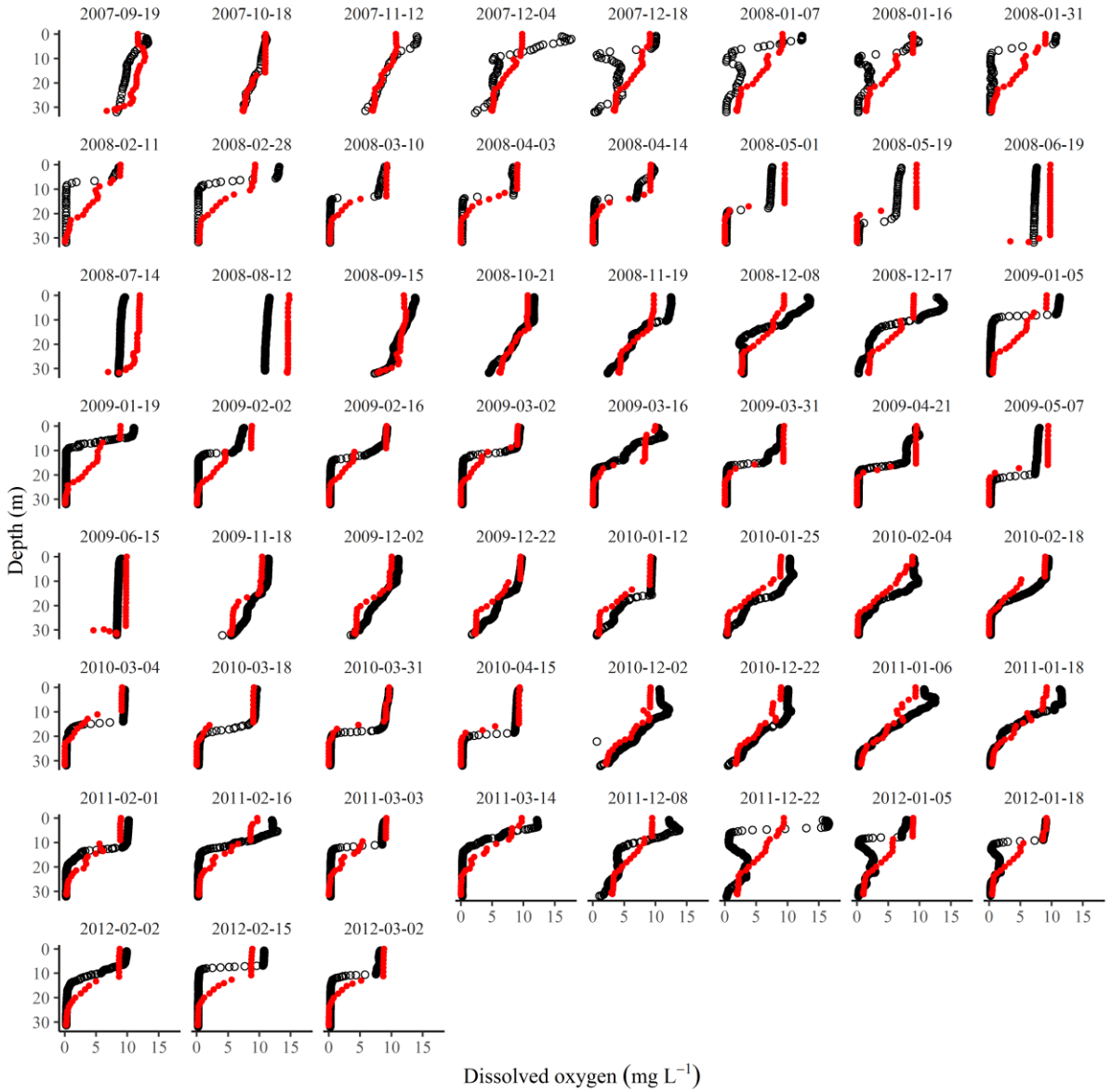

Figure 30. Model simulations (red dots) and field observations (black dots) for water column profiles of dissolved oxygen (mg L^{-1}), 2007 to 2012. A close match between black and red dots represents an ideal calibration.

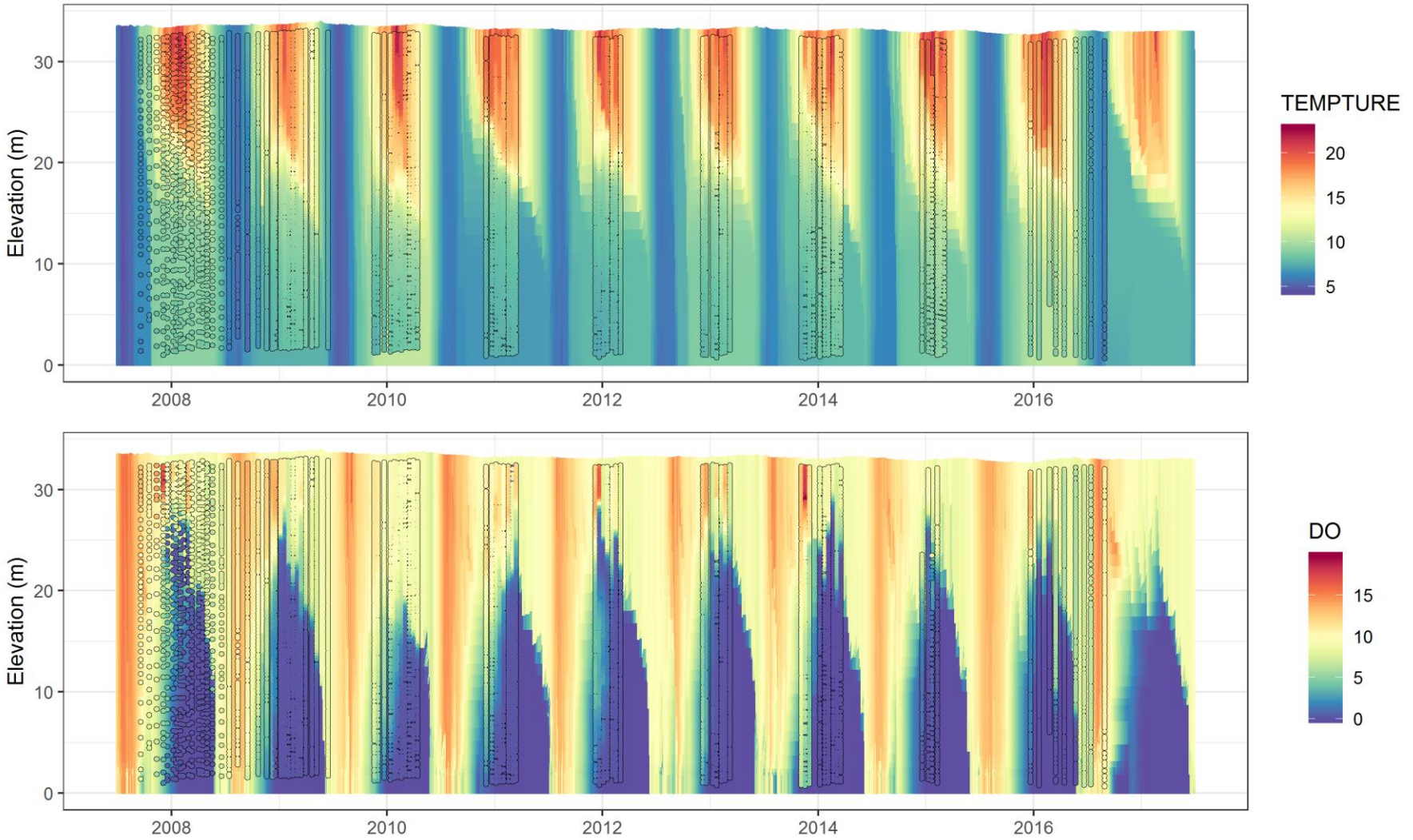

Figure 31. Model simulations (coloured background) and field observations (coloured dots with black outline) for water column profiles of water temperature (°C; TEMPTURE) and dissolved oxygen (mg L^{-1}; DO), 2007 to 2017. Note where observations are of a similar magnitude to simulations the coloured dots become less obvious.

Detailed comparison of simulated and observed nutrient dynamics in surface waters in both the calibration period and validation period is given in Figure 32. Good baseline concentrations were established in all variables, and reasonable seasonal dynamics were simulated in the majority of cases. However, some extreme values of NH_4, TN and TSS were not observed in the model outputs.

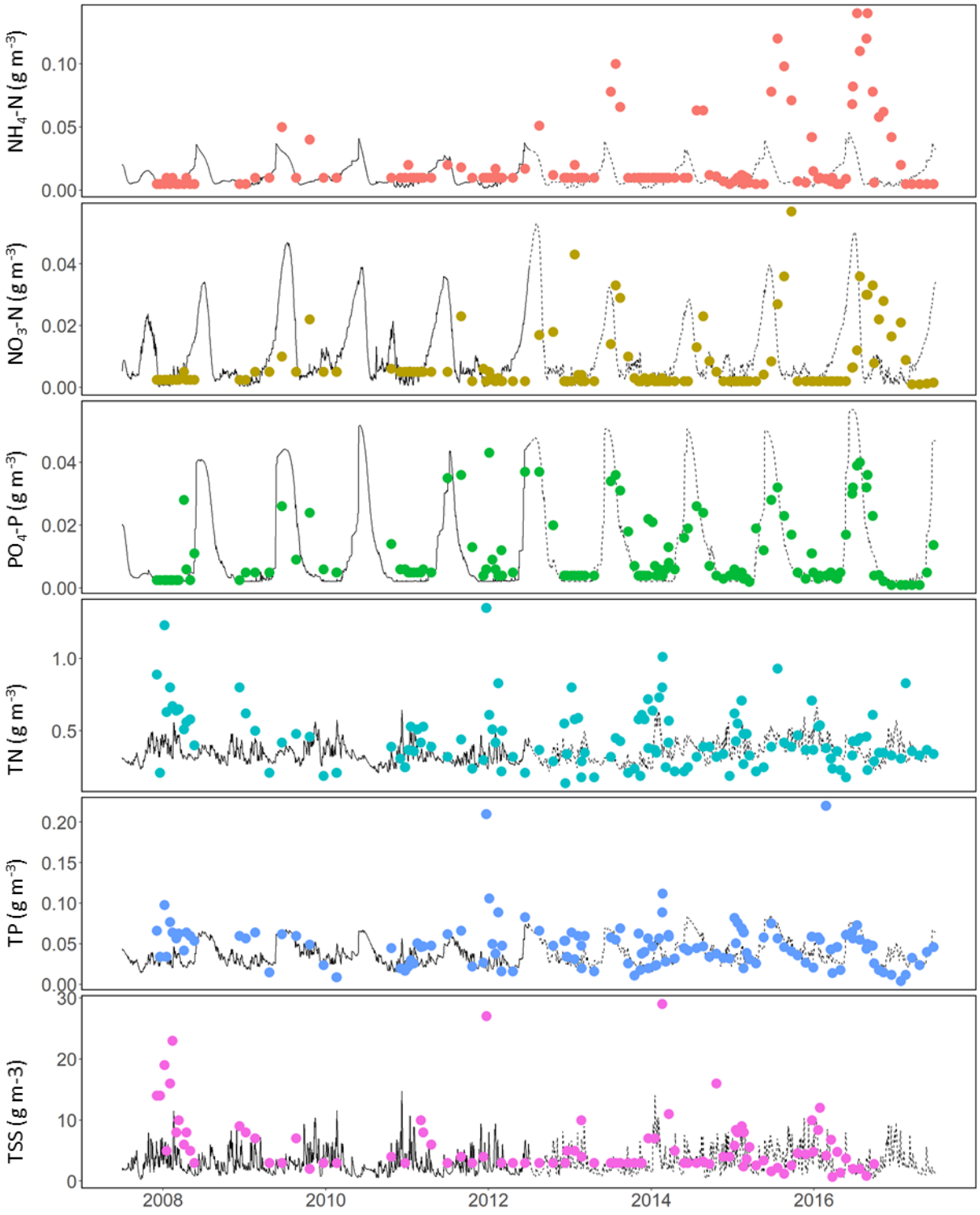

Figure 32. Model simulations (black line) and field observations (coloured dots) for near-surface water quality in Lake Hayes, 2007 to 2017. The calibration period (2007 to 2012) is shown by the solid line, and the independent validation period (2012 to 2017) is shown by the dashed line. Ammonium (NH4), Nitrate (NO3), Total nitrogen (TN) Dissolved phosphate (PO4), Total phosphorus (TP), Total suspended sediment (TSS).

Calibration and validation results of nutrient concentration profiles are shown in Figure 33. Under estimation of hypolimnetic NO_3 was found in 2011 and 2017, while seasonal hypolimnetic dynamics in PO4, TP, TN and TSS were reasonably well established.

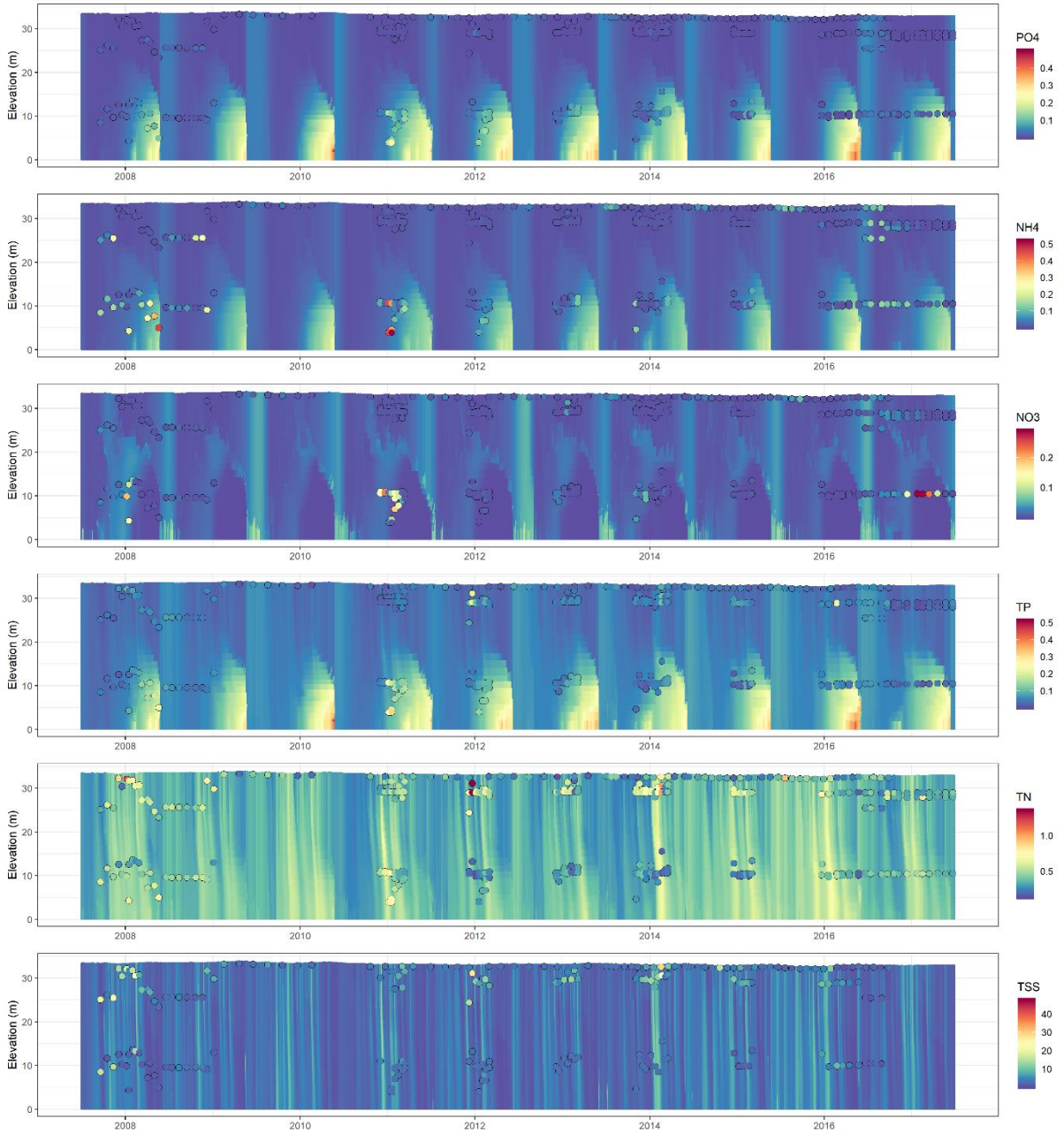

Figure 33. Model simulations (coloured background) and field observations (coloured dots with black borders) for water quality in Lake Hayes, 2007 to 2017. All colour scale units are g m^{-3}. Lake elevation (y-axis) is elevation above the lake bed at the deepest point of the lake. Note where observations are of a similar magnitude to simulations the coloured dots become less obvious.

Surface total chlorophyll *a* concentrations showed little to no seasonal patterns. This suggests that the dynamics were driven by complex phytoplankton community development. We calibrated the model using five different groups to synthesise the overall chlorophyll *a* concentration. Figure 34 shows surface phytoplankton chlorophyll *a* concentration for five simulated phytoplankton groups as well as total chlorophyll *a* along with synthetic observations. All five groups successfully sustained

their populations for ten years, while some years where taxa were absent from the lake were also simulated well in the model results (for example, the observed absence of Cryptophytes in the summer of 2010). The extreme measured concentrations of chlorophyll in 2007 and 2008 was not seen in the model, but general peak values as well as timing of all five functional groups were well simulated (Figure 35).

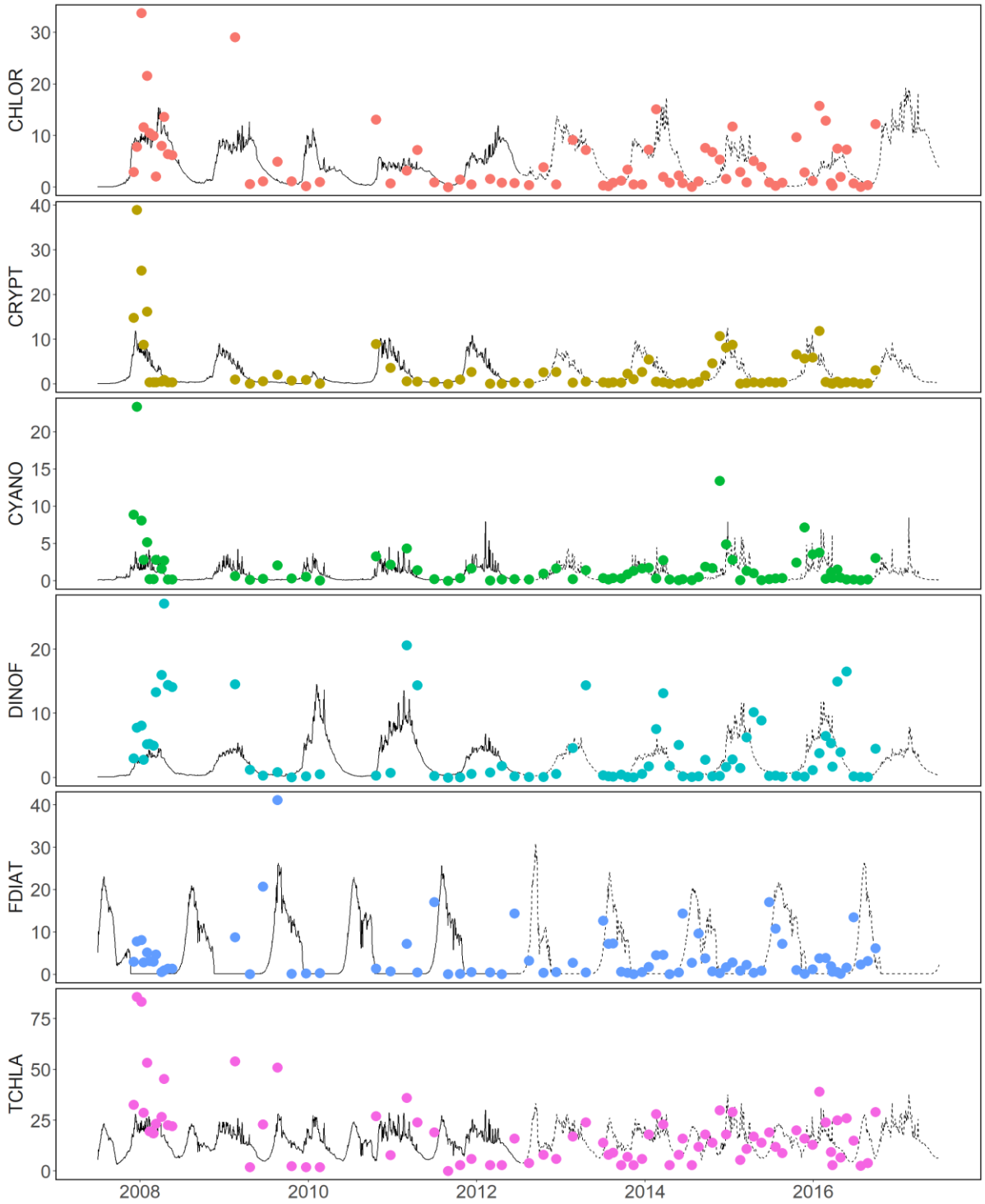

Figure 34. Model simulations (black line) and field observations (coloured dots) for chlorophyll *a* in Lake Hayes, 2007 to 2017, for a) chlorophytes (CHLOR), b) cryptophytes (CRYPT), c) cyanobacteria (CYANO), d) dinoflagellates (DINOF), e) diatoms (FDIAT) and f) total chlorophyll *a* (TCHLA). The calibration period (2007 to 2012) is shown by the solid line,

and the independent validation period (2012 to 2017) is shown by the dashed line. Field observations for phytoplankton taxa are estimates based on the synthesis presented in Figure 28. All units are µg chl L^{-1}.

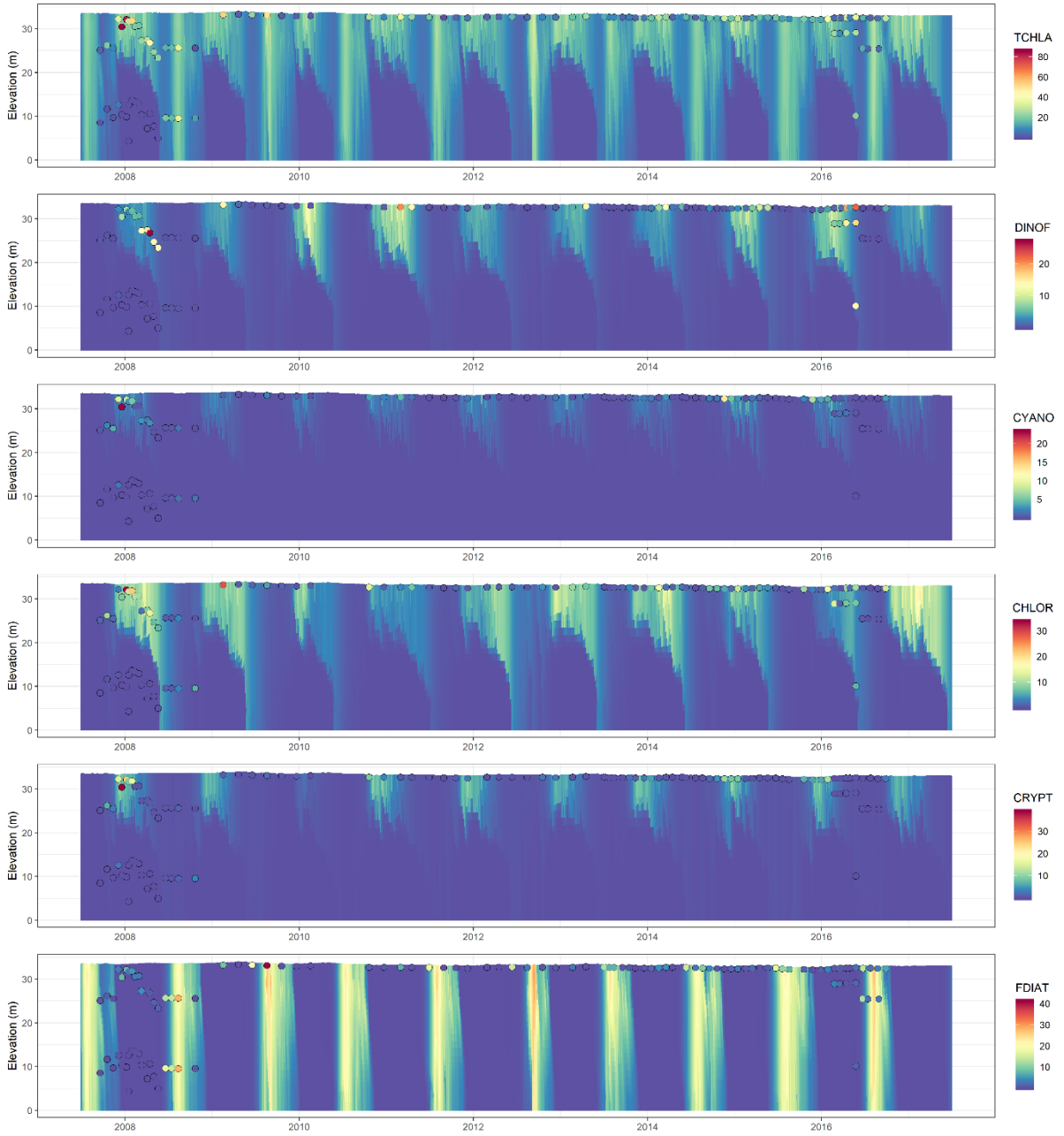

Figure 35. Model simulations (coloured background) and field observations (coloured dots with black borders) for phytoplankton in Lake Hayes, 2007 to 2017. All colour scale units are ug chl a L^{-1}. Lake elevation (y-axis) is elevation above the lake bed at the deepest point of the lake. Note where observations are of a similar magnitude to simulations the coloured dots become less obvious.

Annual TLI was somewhat well simulated by the lake model (Figure 36). Although interannual variability was not always well characterised, it should be noted that field observations were collected among variable sites and temporal coverage was not always adequate to calculate a robust TLI value (see Figure 16).

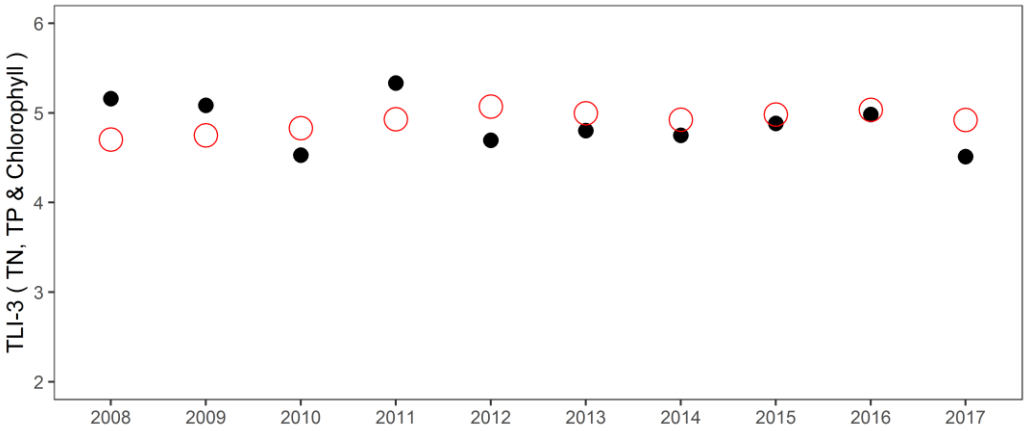

Figure 36. Lake Hayes three-parameter Trophic Level Index (TN, TP and chlorophyll *a*) from observations (black dots), and model simulations (red circles). Note x-axis is hydrological year (July of previous calendar year until June).

A statistical summary of the model results is provided in Table 6. Pearson correlation coefficient (R) indicates the linear correlation between the model results and the observation, which can be easily biased by the number of baseline observations and extreme values. Root mean square error (RMSE) illustrates errors in actual observation units. Coefficient of variation (CV) provides normalised RMSE that can be used to inter-compare error in different variables. Model performance for both temperature and dissolved oxygen was very good for both calibration and validation. Phosphorus dynamics were reasonably well simulated in PO_4, while TP linear correlation was lower for the validation period. All phytoplankton dynamics were well established in calibration, but the correlation coefficients were lower in the validation period.

Table 6. Model statistical performances for state variables in both calibration period (2007-2012) and validation period (2012-2017). Performances were measured using Pearson's correlation coefficient (R), mean average error (MAE), root mean square error (RMSE), and coefficient of variation (CV). Units are applied only in MAE and RMSE.

		R		MAE		RMSE		CV	
Variables	**Units**	**CAL**	**VAL**	**CAL**	**VAL**	**CAL**	**VAL**	**CAL**	**VAL**
Temperature	°C	0.97	0.95	0.85	1.18	1.08	1.41	0.07	0.09
Dissolved oxygen	mg L^{-1}	0.88	0.79	1.55	2.09	2.18	2.85	0.14	0.18
PO_4-P	g m^{-3}	0.81	0.40	0.01	0.02	0.03	0.04	0.00	0.00
TP	g m^{-3}	0.65	0.06	0.03	0.03	0.05	0.05	0.00	0.00
NH_4-N	g m^{-3}	0.49	0.02	0.04	0.03	0.10	0.05	0.01	0.00
NO_3-N	g m^{-3}	0.24	-0.04	0.02	0.02	0.05	0.04	0.00	0.00
TN	g m^{-3}	-0.08	-0.10	0.18	0.15	0.24	0.20	0.02	0.02
Chlorophytes	mg m^{-3}	0.56	0.12	3.20	3.73	5.65	4.99	0.50	2.87
Cryptophytes	mg m^{-3}	0.68	0.54	2.30	1.64	5.21	2.55	0.46	1.46
Cyanobacteria	mg m^{-3}	0.43	0.06	1.32	1.28	3.26	2.67	0.29	1.53
Dinoflagellates	mg m^{-3}	0.43	0.19	2.79	3.63	5.59	5.92	0.49	3.40
Diatoms	mg m^{-3}	0.59	0.21	4.66	4.80	7.07	6.94	0.62	3.99
Total chlorophyll	mg m^{-3}	0.64	-0.23	11.22	10.58	16.74	12.50	1.47	7.18

3.7 Scenario results

Overall the chosen management scenarios simulated a large change in water quality ranging from TLI 4.72 in s100 (base case or current lake state) to 4.04 under s50 (50% reduction in internal and external nutrient loading). It should be noted that when interpreting TLI values, the TLI components are log transformed. For example, from s100 to s50 mean chlorophyll *a* reduced by ca. 40%. Such large reductions may be unachievable from a practical standpoint, however combinations of external nutrient load reduction and Arrow River flow diversion (e.g. s75_arr) showed considerable promise.

Table 7. Summary of projected water quality for all management scenarios. Note Trophic Level Index is a three-parameter TLI consisting of total nitrogen total phosphorus and chlorophyll *a*.

Scenario	Trophic Level Index	Total nitrogen (g m^{-3})	Total phosphorus (g m^{-3})	Chlorophyll (mg m^{-3})
s100	4.8	0.37	0.04	16.36
s90	4.65	0.33	0.04	14.81
s75	4.52	0.29	0.03	13.84
s50	4.07	0.2	0.02	9.04
s100_arr	4.64	0.31	0.04	15.23
s90_arr	4.54	0.28	0.03	14.31
s75_arr	4.42	0.25	0.03	13.24
s100_arr_flow1	4.66	0.32	0.04	15.51
s100_arr_flow2	4.62	0.32	0.04	14.91
s100_arr_hWQ	4.6	0.3	0.04	15.02
s100_hypWdr	4.73	0.36	0.04	15.83
s100_arr_hypWdr	4.6	0.31	0.04	14.62
s100_bub_300L	4.67	0.4	0.03	14.12
s100_bub_500L	4.66	0.4	0.03	13.82
s100_infDose	4.76	0.36	0.04	15.99
s100_infDose_sedCap	4.56	0.35	0.03	12.87
s100_sedCap	4.58	0.35	0.03	13.34

Nutrient load reduction: Reducing nutrient loading to Lake Hayes showed an improvement in the overall water quality, resulting from load reductions targets of 10% and 25% (Figure 43 and Figure 44, Table 7) reducing TLI to 4.59 and 4.48 respectively**.** A further scenario of 50% reduction, which can more appropriately considered a sensitivity test rather than a realistic management option showed a dramatic water quality improvement (TLI reduced to 4.04), reducing TLI to near mesotrophic from the current upper eutrophic state.

Arrow River diversion: Where scenarios simulated addition of the Arrow irrigation scheme water to Mill Creek, a linear relationship was applied to transform previously estimated Mill Creek water temperature to estimated Arrow river temperature (equation shown in Figure 37). Arrow River water temperature was generally 2° C colder than the Mill Creek water temperature. Note that model simulations for Arrow River diversions were applied at the lake edge. In practice, if Arrow River water has either long transit times, or travels through exposed pipework, or is mixed into Mill

Creek substantially upstream of the point of entry into the lake, then the actual temperature may differ substantially from that simulated here.

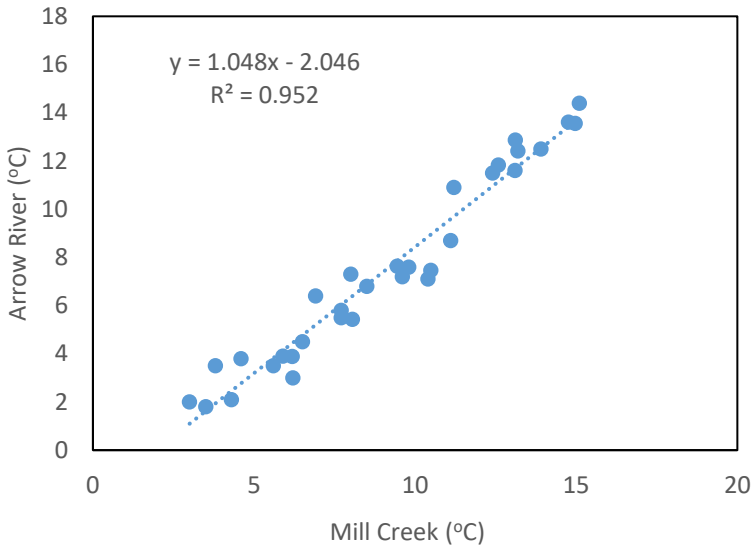

Figure 37. Comparison of water temperature in Arrow River and Mill Creek for samples collected on the same day at each site.

A comparison of the lake model versus observed Arrow River and Mill Creek water temperature alongside lake surface and lake hypolimnion water temperature indicates that during stratified periods Arrow/Mill inflow water temperature is usually warmer than the lake hypolimnion temperatures, and during winter (unstratified) periods these inflows are usually cooler than lake surface/bottom temperatures (Figure 38). Broadly, between September and April the inflows would not plunge below the thermocline, but be entrained into surface waters. This supply of nutrients to the epilimnion may be the reason for the neutral to negative to negative effect of summer flow diversion. In summary, any effect of bottom water oxygenation by plunging inflow of Arrow River is likely to be minor, and restricted to either very early or very late in the stratified period.

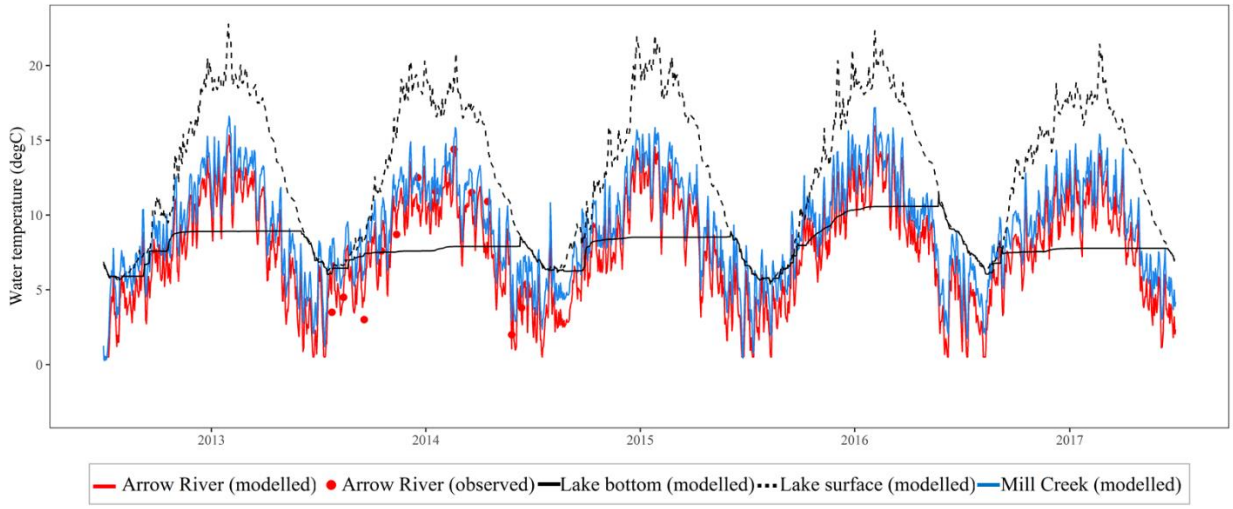

Figure 38. Comparison of water temperature in Arrow River (red line for modelled temperature and red dots for observations) and Mill Creek (blue line for modelled water temperature) against simulated lake surface (dashed line)

and bottom (solid line) waters. When Arrow River falls below the lake bottom water temperature, deep insertion of the Arrow River water is possible –this typically occurs between approximately April and October.

Diversion of Arrow River water into Lake Hayes had a positive effect on overall water quality. Synergistic effects were observed such that diversion of Arrow River water in combination with a 10% catchment load reduction produced a similar magnitude of improvement in water quality to a 25% catchment load reduction without Arrow River water diversion. Of the three Arrow River flow scenarios (including scenarios Flow 1 and Flow 2) resulting TLI was very similar, in fact the absence of summer flow yielded slightly favourable water quality compared with scenarios where summer flow was included, suggesting summer diversion may not be required.

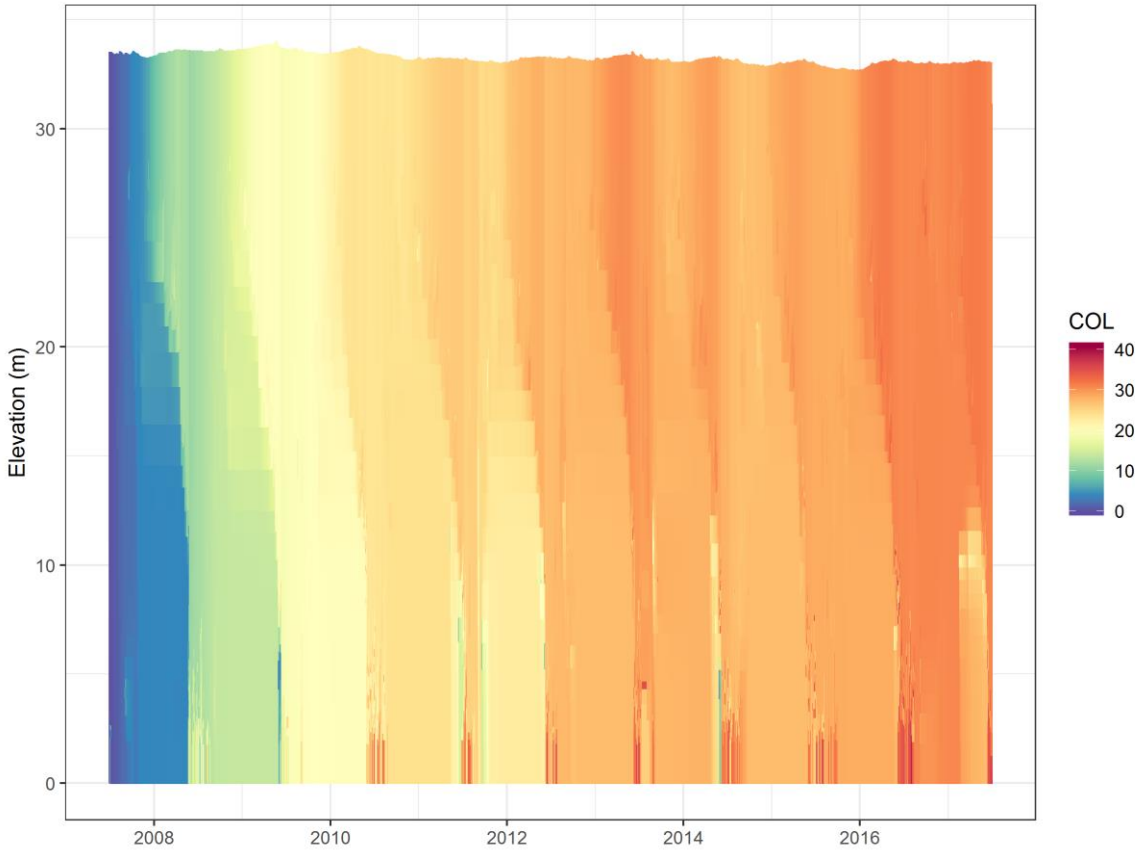

Figure 39. Model simulations showing tracer concentration for intrusion of arrow river irrigation scheme water (200 L s^{-1}) for the scenario s100_arrow_hWQ. The colour ramp (COL) refers to tracer concentration (0-100) where the tracer in applied to Arrow diversion flows. Therefore, based on this tracer, Lake Hayes contains up to 40% by volume of Arrow flow after 10 years of diversion. Intrusions of Arrow water have higher tracer concentration (see red areas near the lake bottom). Blue colours represent Mill Creek (and other inflows).

Artificial aeration: The two airflow rates assessed (300L s^{-1} and 500L s^{-1}) yielded similar improvements to water quality results as the Arrow River diversion, however, simulations showed that cyanobacteria blooms could be exacerbated by the action of the bubbler. Bubbler scenarios showed an increased modelled occurrence of surface blooms, presumably due to improving access to light and increasing transport of nutrients from bottom to surface waters, while not sufficiently negating the buoyancy capabilities of cyanobacteria. The 500L s^{-1} airflow rate significantly increased lake bottom and surface water mixing (compare baseline simulation in Figure 40 to s100_bub_500L simulation in Figure 41 showing water column simulated dissolved oxygen and temperature)

resulting in generally fully mixed water column during summer where stratification is present in baseline.

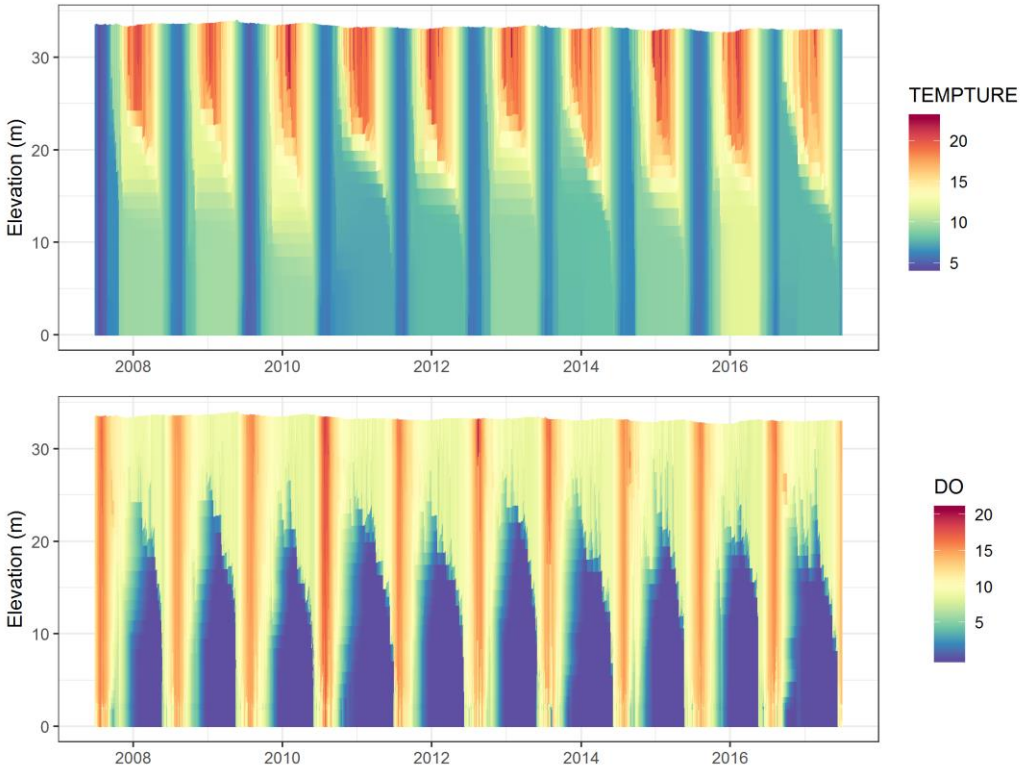

Figure 40. Model simulations showing water temperature (top) and dissolved oxygen concentration for simulation of the baseline lake model (s100). Dissolved oxygen is described in the key as DO (mg L^{-1}) and TEMPTURE is temperature in ^{o}C.

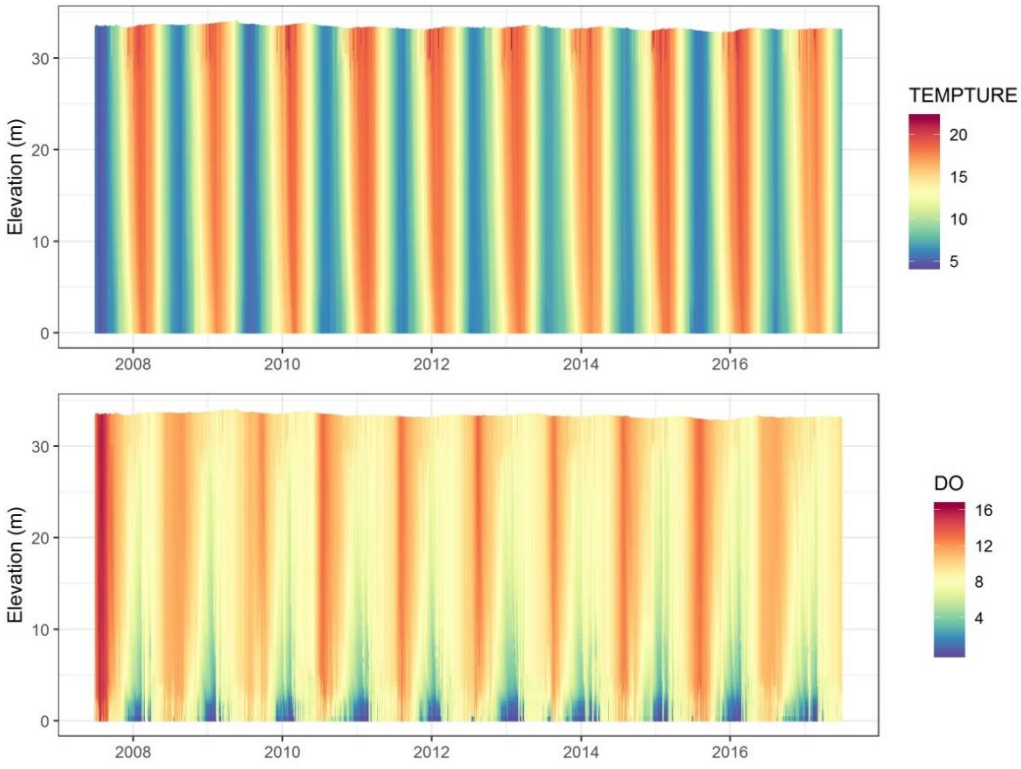

Figure 41. Model simulations showing water temperature (top) and dissolved oxygen concentration for simulation of an aeration bubbler with an air flow rate of (500 L s-) for the scenario s100_bub_500L. Dissolved oxygen is described in the key as DO (mg L^{-1}) and TEMPTURE is temperature in ^{o}C.

3.7.1 Frequency and intensity of algal abundance under model scenarios

The frequency and intensity of algal abundance under model scenarios varied substantially ranging large reductions in maximum bloom concentrations under inflow dosing and sediment capping scenarios to increases in abundance over current calibration within bubbler scenarios (ca. 17 ug/L under s100_bub_500L) (Figure 42). Note, the calibration is based on a synthetic phytoplankton seasonality due to lack of field data.

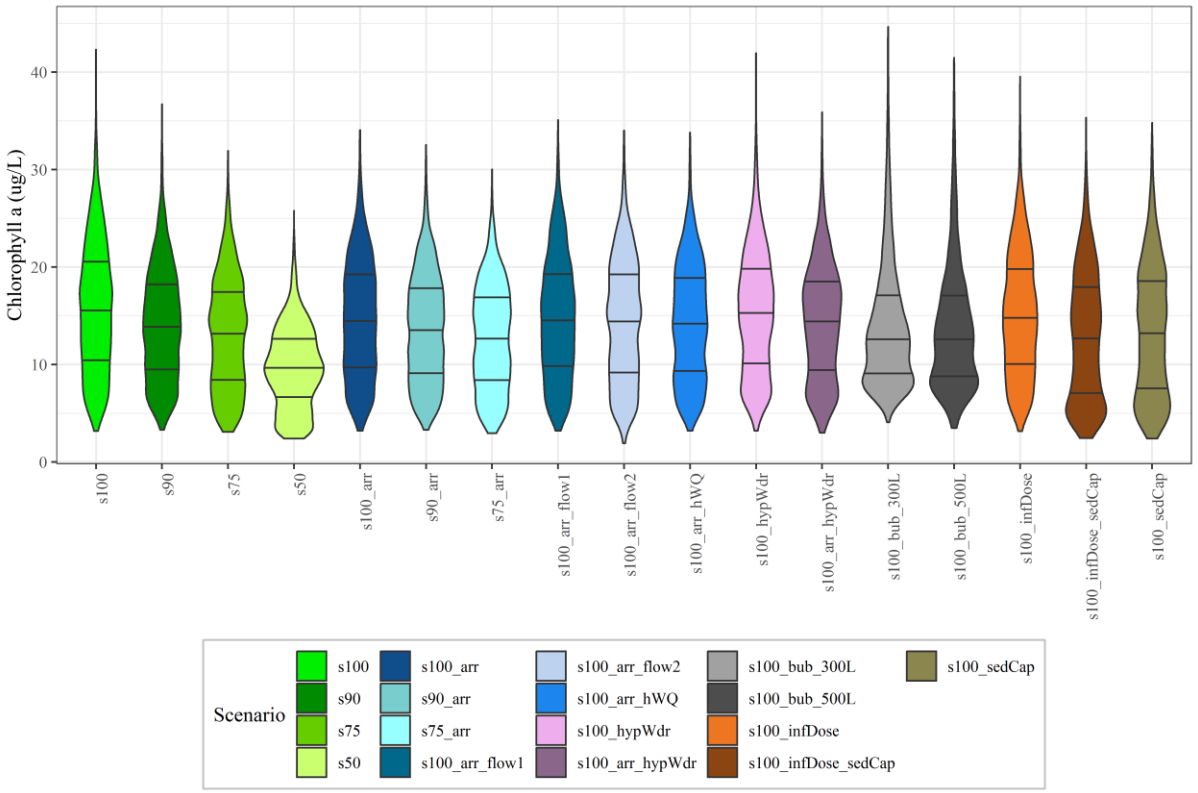

Figure 42. 'Violin' plot, showing the relative distribution of cyanobacteria concentrations over a simulation period of 2007 to 2017 for all scenario simulations. Not that the width of each violin represents relative frequency ditribution.

3.7.1 Response of overall water quality to management scenarios

Total chlorophyll *a* reduced under all scenarios. Observing overall water quality under various scenarios presented through time (Figure 43) and temporally averaged (Figure 44), s50 (50% nutrient reduction) stands out as an end member, and as stated above is unlikely to be achievable. However, s75_arr generally represents the next best performing scenario in terms of lake restoration, with the largest increase in Secchi depth, and greatest reduction in TLI and TN concentrations (Figure 43).

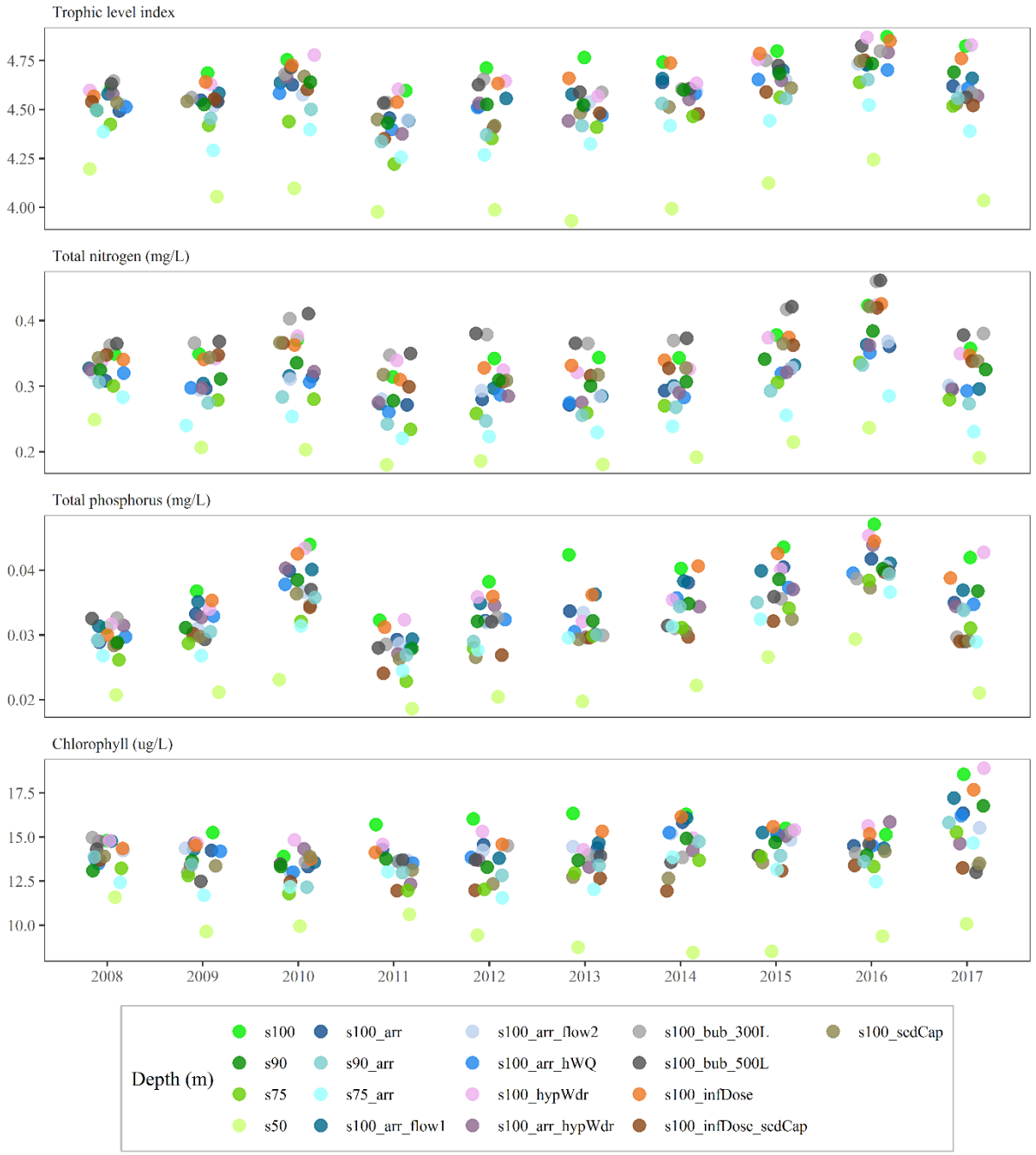

Figure 43. Annual average water quality for all simulation scenarios (surface). Note x axis is hydrological year. Different scenarios are represented by different colours, with each point on the plot showing the average annual value for one scenario. Note; 'Trophic Level Index' is a three-parameter TLI calculated from total nitrogen, total phosphorus and chlorophyll *a*, because DYRESM-CAEDYM does not explicitly simulate Secchi disk depth.

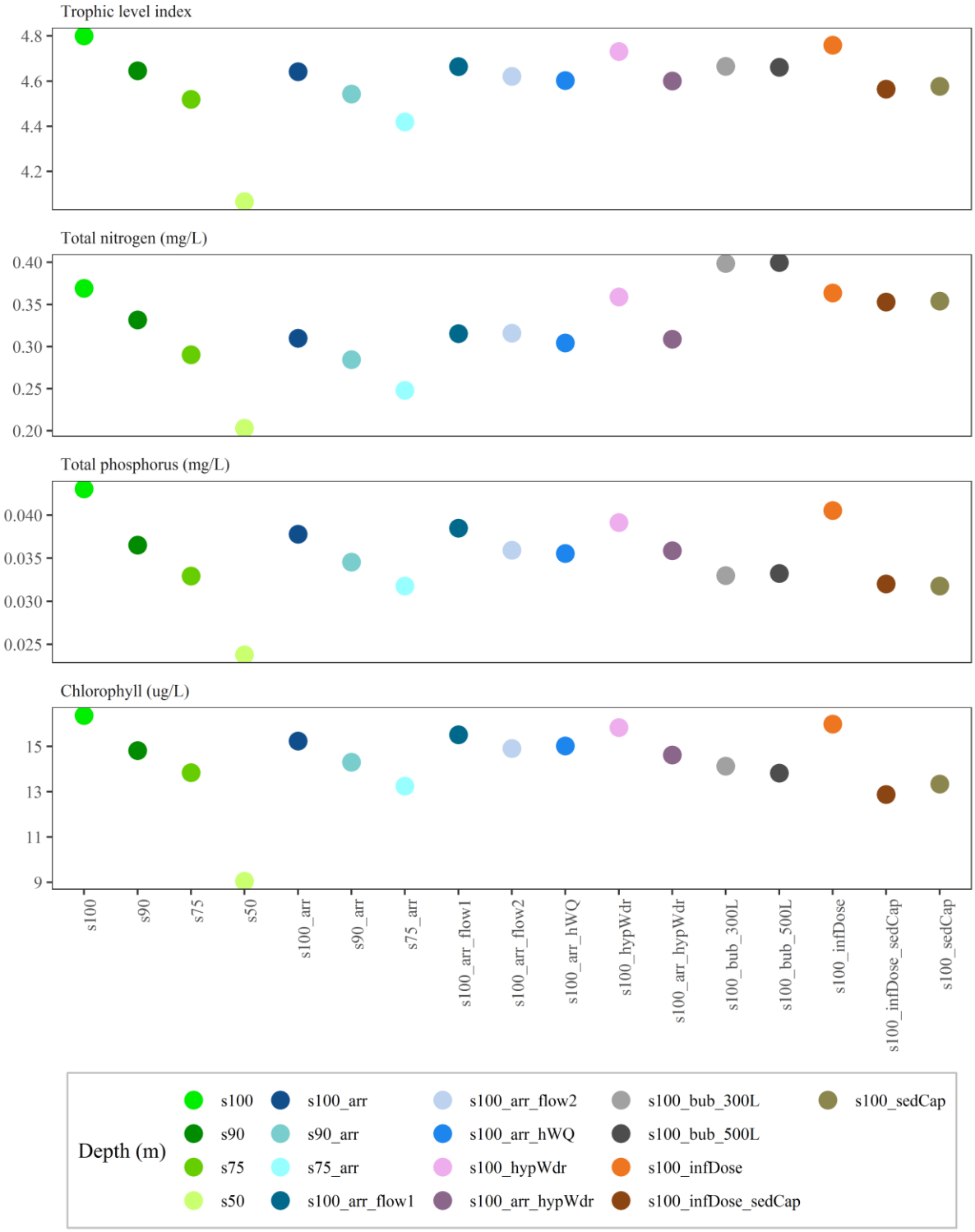

Figure 44. Summary of average water quality for all simulation scenarios over the simulation period (surface). Different scenarios are represented by different colours, with each point on the plot showing the average value (2007 – 2017) for one scenario simulation. Note; 'Trophic Level Index' is a three-parameter TLI calculated from total nitrogen, total phosphorus and chlorophyll *a*, because DYRESM-CAEDYM does not explicitly simulate Secchi disk depth.

4 Discussion

This study considered the drivers of poor water quality and associated algal blooms in Lake Hayes, and used a complex process-based hydrodynamic-biogeochemical model to assesses various management options that have been either specifically proposed for Hayes, or have proven effective for other lakes in New Zealand and globally. The primary objective was to use the configuration of the chosen modelling platform (DYRESM-CAEDYM) as both motivation for collating all relevant data available to important processes in the waterbody, and for the objective comparison of these management options under the same simulation framework. In summary, the model was applied as a decision support tool for management options for Lake Hayes water quality.

4.1 Water quality monitoring in Lake Hayes

Catchment and lake monitoring data were synthesised for the period 1983 to 2017. Long-term monitoring data showed strong evidence for substantial internal nutrient loading to the lake (i.e., recycling of nitrogen (N) and phosphorus (P) from bottom sediments during lake stratification over warmer months). Also evident were changes in the magnitude of internal loading (evidenced by deep water concentrations of dissolved N and P) over the c. 35 years of monitoring data. However, the variable timing and sampling depth of measurements made interpreting any trends difficult. Similarly, calculation of long-term changes in lake Trophic Level Index (TLI) was confounded somewhat by intermittent sampling, but nonetheless showed a sharp increase in the mid-2000s with a steady decline in TLI since, indicating degraded but slowly improving water quality. Through compilation and investigation of the water chemistry dataset for Lake Hayes, we described further evidence for the suggestion in Schallenberg and Schallenberg (2016) that internal loading may have been reducing, particularly over recent years (see Figure 13). Estimation of emerging trends in this regard were confounded somewhat by the irregularity of sample collection, although recent years have consistent monthly intervals. We recommend continuing to monitor the deep waters of Hayes (> 28 m) for concentrations of dissolved N and P, particularly during thermal stratification periods. One of the pathways to lake restoration is effective lake monitoring, which should be an essential component of lake restoration and rigorous statistical design should be woven into the restoration plan (Hamilton et al. 2019).

4.2 Lake model performance

The present application of the DYRESM-CAEDYM (DY-CD) lake model aims to simulate ecological and physical processes that influence water quality in Lake Hayes, including projection of likely effects on water quality of various management scenarios. The calibrated model incorporates best-estimates of daily hydraulic and catchment loading derived from a synthesis of *in situ* monitoring of inflows. Error statistics for key state variables in DY-CD calibration/validation were comparable and in many cases superior to, previously published applications of the model to other lakes (e.g., Burger, 2008; Gal et al., 2009; Özkundakci et al., 2010; Trolle et al., 2012). Simulation of water temperature and stratification dynamics matched *in situ* data well (r = 0.97, RMSE = 1.08 ^{o}C), such as dissolved oxygen (r = 0.88, RMSE = 2.18 mg L^{-1}). Capturing the dynamics of these variables is critical to the estimation of internal loading due to the dependence of key sediment nutrient fluxes on concentrations of dissolved oxygen and other oxidised compounds such as nitrate (Burger et al 2008). Nutrient dynamics in surface and bottom waters were generally well-simulated, particularly pulses of N and P

associated with releases from bottom sediments during stratification. Nevertheless, inter-annual variability in the field measurements meant that for some years the model performed better than others in this regard (Figure 33). Internal loading must be considered in any restoration efforts within Lake Hayes, and the length of recovery period following external phosphorus load reduction will be determined by the loading history and the amount of phosphorus bound within sediment (Burger et al. 2008).

4.3 Model limitations

"All models are wrong, but some models are useful" (Box, 1979). Contributors to model uncertainty include observational error (or spatially/temporally limited datasets), model structural uncertainty, and model parameter uncertainty. The application of models to scenarios encountering physiochemical conditions not within ranges of conditions to which the model was calibrated can lead to greater uncertainty. However, the process-based representation of equations within lake models generally represent the current scientific consensus, based on the best empirical and analytical algorithms available. The Lake Hayes DY-CD model was able to reproduce physical and chemical in-lake dynamics with a good degree of accuracy relative to previous published applications of DYRESM-CAEDYM. The established model can therefore be considered the most advanced tool available with which to assess potential management options for Lake Hayes.

4.3.1.a Limiting assumptions

- The current model water balance was not informed by measured lake level, however water level changes can be an important factor for heat budgets (stratification) and physical mixing, as well as resuspension.
- The rating curve-based estimation of storm nutrient and sediment contents may be over/underestimated.
- On-lake meteorology including wind speed, air temperature and humidity were not available, and likely differ from the data derived from Queenstown airport.
- Long wave radiation was estimated from cloud cover, which was calculated using short wave radiation using a clear-sky model. Completely clouded sky was assumed to be 5 % of total observation (days).
- Sediment dynamics and content for Lake Hayes are not well described. This includes sediment nutrient storage, sediment nutrient exchange and resuspension.
- Suspended sediment particle sizes were estimated iteratively via model calibration.
- The magnitude of sediment capping nutrient reductions is dose-dependent and unknown.
- Zooplankton grazing pressure can be an important factor especially in oligotrophic to mesotrophic lakes. The model did not include processes relating to zooplankton grazing. Instead, an increased rate of phytoplankton respiration was used to account for losses due to grazing pressure (Trolle et al. 2010).
- The model did not simulate fish or macrophyte ecosystem components.
- Total chlorophyll *a* seasonality was not well observed in Lake Hayes. The approach adopted was to estimate dynamics of different functional groups as described in chapter 2.3.2.
- Species cell counts can be useful, but chlorophyll *a* is relative to biomass/biovolume, because of differing ratios to carbon, nitrogen and phosphorus. It is useful to know the biovolume of each species, especially as species were not taxonomically identified to species level. We

assumed likely species and estimated biovolumes and chlorophyll *a* concentration per cell unit, but this is subject to uncertainty.

- The 1-D modelling approach does not simulate spatial heterogeneity in the horizontal dimension. Therefore, no horizontal transport or seiche effects were included.
- Some *in situ* samples for calibration/validation were collected at the lake shore and may not be representative of horizontally averaged water quality simulated.

4.3.2 Model performance and scenario outputs

Four broad categories of model scenarios were undertaken using model simulations, with results as follows:

1. **Nutrient load reduction:** Reduction of nutrient loads from the immediate catchment of Lake Hayes resulted in improved overall water quality, with reductions in lake TLI resulting from catchment reductions of just 10 and 25%**.** A further scenario of 50% reduction, which can be perhaps considered as a sensitivity test rather than an achievable management option, showed a significant water quality improvement.

2. **Arrow River diversion**: Diversion of Arrow River irrigation water into Lake Hayes had a positive effect on overall water quality. Synergistic effects were observed such that diversion of Arrow River water in combination with a 10% catchment load reduction gave a similar magnitude of improvement to a 25% catchment load reduction without Arrow River water diversion. Of the three Arrow River flow scenarios (including scenarios Flow 1 and Flow 2), resulting TLI was very similar, in fact, an absence of summer flow yielded slightly favourable water quality compared with scenarios where summer flow was included, suggesting summer diversion may not be required. Model simulations of bottom water temperature when compared with Arrow River water temperatures showed that diverted water is likely to entrain to the surface of the lake during warmer months and this supply of nutrients to the epilimnion may be the reason for the neutral to negative effect of summer flow diversion. Therefore, the water quality gains are likely the result of flushing with relatively lower concentrations of nutrients for Arrow River. Nevertheless, because we have not considered here possible responses of biodiversity to various flow regimes, flexibility in the engineering design of the diversion could be desirable, so that real-world testing of summer diversion could be carried out.

   Hypolimnetic withdrawal alone gave a slight improvement to overall water quality over the baseline model. When combined with Arrow River diversion, hypolimnetic withdrawal resulted in further water quality improvement than hypolimnetic withdrawal alone. However, due to the small magnitude of change, cost benefit for this option would need to be carefully considered.

3. **Artificial aeration:** DYRESM-CAEDYM allows for the simulation of aeration by a bubbler plume (bottom-up mixing). Simulation of aeration within DYRESM is by definition limited to one dimension only (i.e., vertical). In practice, aeration is likely to be via one or more horizontal bubble lines, and in this sense the model represents a conceptual simplification of the aeration engineering design. Nevertheless, the DYRESM aeration module has been calibrated and

applied successfully for many real-world lakes and reservoirs with artificial aeration (Moshfeghi et al. 2005). The two airflow rates assessed here (300L s^{-1} and 500L s^{-1}) yielded similar improvements to water quality results as the Arrow River diversion, however, simulations showed that cyanobacteria blooms could be exacerbated by the action of the bubbler. Bubbler scenarios showed an increased modelled occurrence of surface blooms, presumably due to improving access to light and increasing transport of nutrients from bottom to surface waters, while not sufficiently negating the buoyancy capabilities of cyanobacteria. Although CAEDYM includes only a simplistic representation of phytoplankton motility, these results highlight potential pitfalls of aeration, and suggest that this option should be treated with caution. The potential effects of aeration/mixing on aquatic biota (particularly the effects of altered temperature dynamics on the trout population) should also be considered in detail and are beyond the scope of the present study.

4. **Geochemical engineering:** The application of flocculation and/or sediment capping agents such as Phoslock™, Z2G1 (modified zeolite), or aluminium sulphate (alum) is a management approach that has been applied with some success in the Rotorua lakes (Bay of Plenty). Although CAEDYM cannot explicitly simulate the mode of action (adsorption) of these agents, scenarios were undertaken to approximate their effects by adjusting process rate coefficients to simulate an increase in the settling rate of organic matter (flocculation), and the reduction of internal sediment-water nutrient fluxes (sediment capping).

   Flocculation and capping resulted in substantial reductions in TLI in the Lake Hayes model (as has also been the real-world experience in Lake Rotorua), although results should be interpreted cautiously due to conceptual simplifications necessary in these scenario simulations. The efficacy of these agents is highly pH-dependent, and the timing and intensity of their application must be considered in detail. Further, ecotoxicological and community/cultural considerations are important considerations when evaluating geochemical engineering as a lake management option. A summary of potential geochemical and ecological consequences of these geochemical engineering approach can be fouond in Tempero (2015).

5 Conclusions and recommendations

In a synthesis of lake restoration success and failures for more than 70 lake restoration projects in the Netherlands and Denmark, the main cause for restoration failure was attributed to insufficient external loading reduction, internal phosphorus loading and absence of stable submerged macrophyte community (Søndergaard et al. 2007). Reviews of lake restoration efforts globally and in New Zealand suggest a holistic approach to restoration is required that acknowledges interdependence of aquatic ecosystems and includes consideration of hydrology (in the case of Lake Hayes, groundwater may be important), water quality and flora and fauna (Hamilton et al. 2018).

Additional data collection could support further development of the configured model and refinement of the modelled scenarios presented here, in order to provide additional guidance for management strategies going forward. Collection of more comprehensive water quality data including lake level, high frequency water quality and climate data from on the lake, and continuation of the present programme of minimum monthly water quality samples would aid this process as well as enhance general understanding of key processes and trends in Lake Hayes. A more complete record of water chemistry and temperature in Arrow River (preferably at the proposed site of diversion, and encompassing water quality during higher flow events) would enable more accurate estimations of the Arrow River diversion scenarios. Data from a continuous lake monitoring platform would enable superior calibration of temperature and oxygen dynamics in the lake, as well as providing valuable insight into the lake's phytoplankton dynamics in time and space.

All simulations presented within this report assume that lake response to mitigations takes effect almost immediately. For example, reductions in external nutrient loading are immediately reflected in nutrient release rates within the sediments. In reality, this response can potentially take decades, depending on the residence time (Søndergaard et al. 2003) and sediment nutrient status.

Based on the modelled scenarios presented above, simulations support catchment nutrient load reduction as important to achieving positive change in the water quality of Lake Hayes. Diversion of Arrow River water, even during cooler months only, appears also to be a promising option to improve water quality and possibly enhance the response of the lake to any catchment nutrient load reductions. Aeration and geoengineering approaches also show potential for water quality improvement, however, these options are subject to greater degrees of model uncertainty as well as necessary considerations of direct and indirect consequences of these approaches, such as effects on lake biota.

6 References

Bird, R. E., & Hulstrom, R. L. (1981). Simplified clear sky model for direct and diffuse insolation on horizontal surfaces (No. SERI/TR-642-761). Solar Energy Research Inst., Golden, CO (USA).

Box, G. E. (1979). Robustness in the strategy of scientific model building. In Robustness in statistics. Academic Press.

Bruce, L. C., Hamilton, D., Imberger, J., Gal, G., Gophen, M., Zohary, T., & Hambright, K. D. (2006). A numerical simulation of the role of zooplankton in C, N and P cycling in Lake Kinneret, Israel. Ecological Modelling, 193(3-4), 412-436.

Burger, D. F., Hamilton, D. P., & Pilditch, C. A. (2008). Modelling the relative importance of internal and external nutrient loads on water column nutrient concentrations and phytoplankton biomass in a shallow polymictic lake. Ecological Modelling, 211(3-4), 411-423.

Burns, C. W., and S. F. Mitchell. (1974). Seasonal succession and vertical distribution of phytoplankton in Lake Hayes and Lake Johnson, South Island, New Zealand. New Zealand Journal of Marine and Freshwater Research. 8: 167–209. doi:10.1080/00288330.1974.9515496

Burns, C. W., and S. F. Mitchell. (1980). Seasonal succession and vertical distribution of zooplankton in Lake Hayes and Lake Johnson. New Zealand Journal of Marine and Freshwater Research . 14: 189–204. doi:10.1080/00288330.1980.9515860

Burns, C. W., and J. G. Stockner. (1991). Picoplankton in Six New Zealand Lakes: Abundance in Relation to Season and Trophic State. International Reviews der gesamten Hydrobiology und Hydrography. 76: 523–536. doi:10.1002/iroh.19910760405

Burns, N. M., Rutherford, J. C., & Clayton, J. S. (1999). A monitoring and classification system for New Zealand lakes and reservoirs. Lake and Reservoir Management, 15(4), 255-271.

Caruso, B. S. (2000). Integrated assessment of phosphorus in the lake hayes catchment, south island, new zealand. *Journal of Hydrology*, *229*(3-4), 168-189.

Di Toro, D.; O'Connor, D.; Thomann, R. & Mancini, J. (1975). Phytoplankton-zooplankton-nutrient interaction model for western Lake Erie Systems analysis and simulation in ecology, Academic Press, New York, 423-474

Elliott, S., & Sorrell, B. (2002). Land-water Interactions. Ministry for the Environment.

Gal, G., Hipsey, M. R., Parparov, A., Wagner, U., Makler, V., & Zohary, T. (2009). Implementation of ecological modeling as an effective management and investigation tool: Lake Kinneret as a case study. Ecological Modelling, 220(13), 1697-1718.

Hamilton, D., Özkundakci, D., McBride, C. G., Ye, W., Luo, L., Silvester, W. B., & White, P. A. (2012). Predicting the effects of nutrient loads, management regimes and climate change on water quality of Lake Rotorua (p. 71). Bay of Plenty Regional Council.

Hamilton, D. P., and S. G. Schladow. (1997). Prediction of water quality in lakes and reservoirs. Part I - Model description. Ecological Modelling. 96: 91–110. doi:10.1016/S0304-3800(96)00062-2

Hamilton, D. P., Collier, K. J., Quinn, J. M., & Howard-Williams, C. (Eds.). (2018). *Lake Restoration Handbook: A New Zealand Perspective*. Springer.

Irwin, J. (1981). Lake Hayes Scale 1: 5000 Bathymetry. Lake Chart Series. New Zealand Oceanographic Institute

Jeppesen, E., Søndergaard, M., Meerhoff, M., Lauridsen, T. L., & Jensen, J. P. (2007). Shallow lake restoration by nutrient loading reduction—some recent findings and challenges ahead. In Shallow Lakes in a Changing World (pp. 239-252). Springer, Dordrecht.

Jolly, V.H. (1959). A limnological study of some New Zealand lakes. Dissertation. University of Otago

Karpatne, A., G. Atluri, J. H. Faghmous, and others. (2017). Theory-guided data science: A new paradigm for scientific discovery from data. IEEE Transactions on Knowledge and Data Engineering. 29: 2318–2331. doi:10.1109/TKDE.2017.2720168

Winslow, L., Read, J., Woolway, J., Brentrup, J., Leach, T., Zwart, J., Albers, S., & Collinge D., (2018). rLakeAnalyzer: Lake Physics Tools. R package version 1.11.4. https://CRAN.R-project.org/package=rLakeAnalyzer

Makler-Pick, V., Gal, G.,Gorfine, M., Hipsey, M., & Carmel, Y., (2011). Sensitivity analysis for complex ecological models – A new approach. Environmental Modelling Software. 26: 124–134. doi:10.1016/j.envsoft.2010.06.010

Moshfeghi, H., Etemad-Shahidi, A., & Imberger, J. (2005). Modelling of bubble plume destratification using DYRESM. *Journal of Water Supply: Research and Technology-Aqua*, *54*(1), 37-46.

Otago Regional Council, and Queenstown Lakes District Council (1995). Lake Hayes Management Strategy. Dunedin, Otago.

Ozanne R. (2014). Lake Hayes Restoration Options. Otago Regional Council File Note A652726, Dunedin, Otago.

Özkundakci, D., Hamilton, D.P. & Scholes, P. (2010) Effect of intensive catchment and in–lake restoration procedures on phosphorus concentrations in a eutrophic lake. Ecological Engineering 36: 396–405.

Read, J. S., Hamilton, D. P., Jones, I. D., Muraoka, K., Winslow, L. A., Kroiss, R., Wu, C. H., & Gaiser, E. (2011). Derivation of lake mixing and stratification indices from high-resolution lake buoy data. Environmental Modelling Software. 26: 1325–1336. doi:10.1016/j.envsoft.2011.05.006

Robson, B. J. (2014). State of the art in modelling of phosphorus in aquatic systems: Review, criticisms and commentary. Environmental Modelling Software. 61: 339–359. doi:10.1016/j.envsoft.2014.01.012

Rutherford, K. (2008). Nutrient load targets for Lake Rotorua – a revisit. NIWA client report: HAM2008-080 prepared for the Bay of Plenty Regional Council., Hamilton., Waikato.

Schallenberg & Schallenberg (2017) provided a review of known phytoplankton dominance information in Lake Hayes., Dunedin, Otago.

Schladow, S. G., & Hamilton, D. P. (1997). Prediction of water quality in lakes and reservoirs: Part II - Model calibration, sensitivity analysis and application. Ecological Modelling. 96: 111–123. doi:10.1016/S0304-3800(96)00063-4

Sommer, U., Padisák, J., Reynolds, C. S., & Juhász-Nagy, P. (1993). Hutchinson's heritage: the diversity-disturbance relationship in phytoplankton. Hydrobiologia 249: 1–7. doi:10.1007/BF00008837

Sommer, U., Adrian R., De Senerpont Domis L., and others. (2012). Beyond the Plankton Ecology Group (PEG) Model: Mechanisms driving plankton succession. Annual Review of Ecology, Evolution, and Systematics. 43: 429–448. doi:10.1146/annurev-ecolsys-110411-160251

Søndergaard, M., Jensen, J. P., & Jeppesen, E. (2003). Role of sediment and internal loading of phosphorus in shallow lakes. Hydrobiologia, 506–509(1–3), 135–145. http://doi.org/10.1023/B:HYDR.0000008611.12704.dd

Søndergaard, M., Jeppesen, E., Lauridsen, T. L., Skov, C., Van Nes, E. H., Roijackers, R., ... & Portielje, R. O. B. (2007). Lake restoration: successes, failures and long-term effects. Journal of Applied Ecology, 44(6), 1095-1105.

Tennessee Valley Authority. (1972). Heat and mass transfer between a water surface and the atmosphere. Tennessee Valley Authority, Division of Water Control Planning, Engineering Laboratory.

Tempero, G. (2015). Ecotoxicological review of alum applications to the Rotorua Lakes. *Environmental Research Institute Report*, *52*.

Trolle, D., Hamilton, D. P., Pilditch, C. A., Duggan, I. C., & Jeppesen, E. (2011). Predicting the effects of climate change on trophic status of three morphologically varying lakes: Implications for lake restoration and management. Environmental Modelling & Software, 26(4), 354-370.

Trolle, D., Hamilton, D. P., Hipsey, M. R., Bolding, K., Bruggeman, J., Mooij, W. M., ... & Makler-Pick, V. (2012). A community-based framework for aquatic ecosystem models. Hydrobiologia, 683(1), 25-34.

Trolle, D., Skovgaard, H., & Jeppesen, E. (2008). The Water Framework Directive: setting the phosphorus loading target for a deep lake in Denmark using the 1D lake ecosystem model DYRESM–CAEDYM. Ecological Modelling, 219(1), 138-152.

U.S. Environmental Protection Agency. (2009). Guidance on the Development, Evaluation, and Application of Environmental Models. USEPA Publ. EPA/100/K-: 90.

Wetzel, R. G. (2001). *Limnology: lake and river ecosystems*. Gulf professional publishing.

7 Appendices

Methods

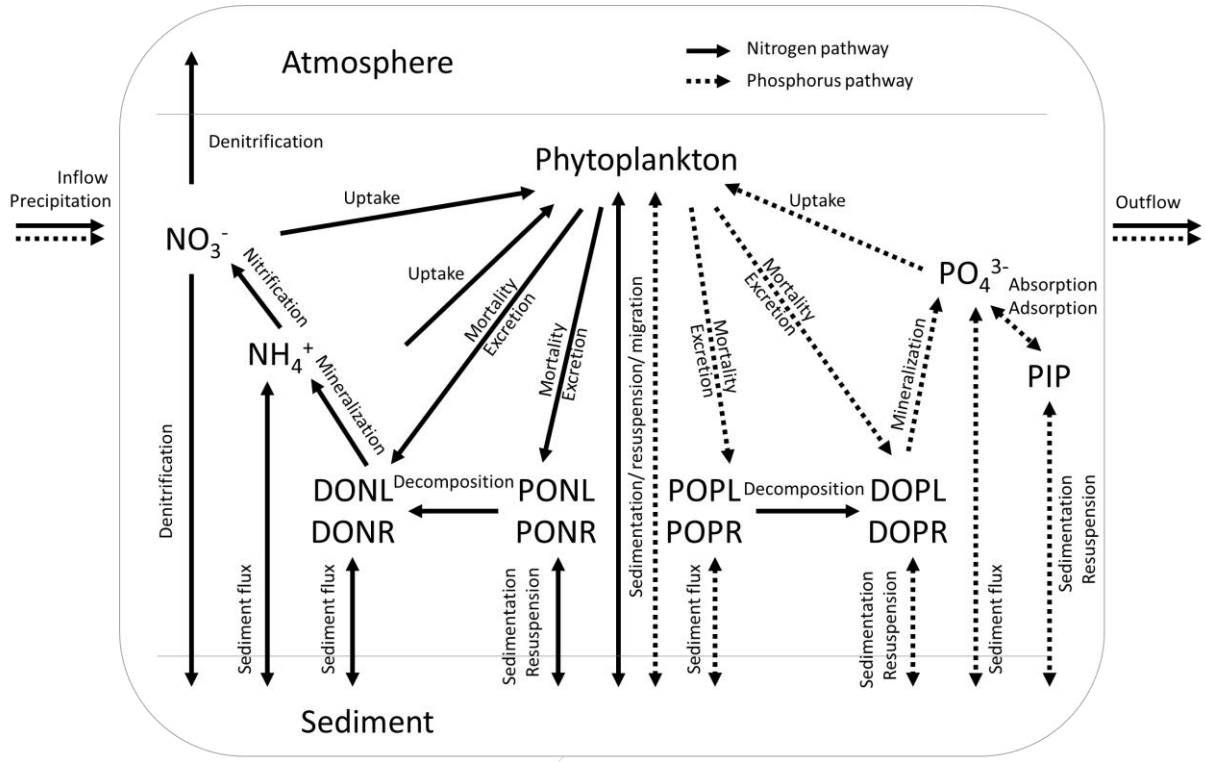

Appendix figure 1. Conceptual diagram of nitrogen and phosphorus cycle in Lake Hayes model. PONL, PONR, DONL, and DONR represent labile particulate organic nitrogen, refractory particulate organic nitrogen, labile dissolved organic nitrogen, and refractory dissolved organic nitrogen respectively. POPL, POPR, DOPL, and DOPR represent labile particulate organic phosphorus, refractory particulate organic phosphorus, labile dissolved organic phosphorus, and refractory dissolved organic phosphorus respectively, and PIP stands for particulate inorganic phosphorus.

Field observations

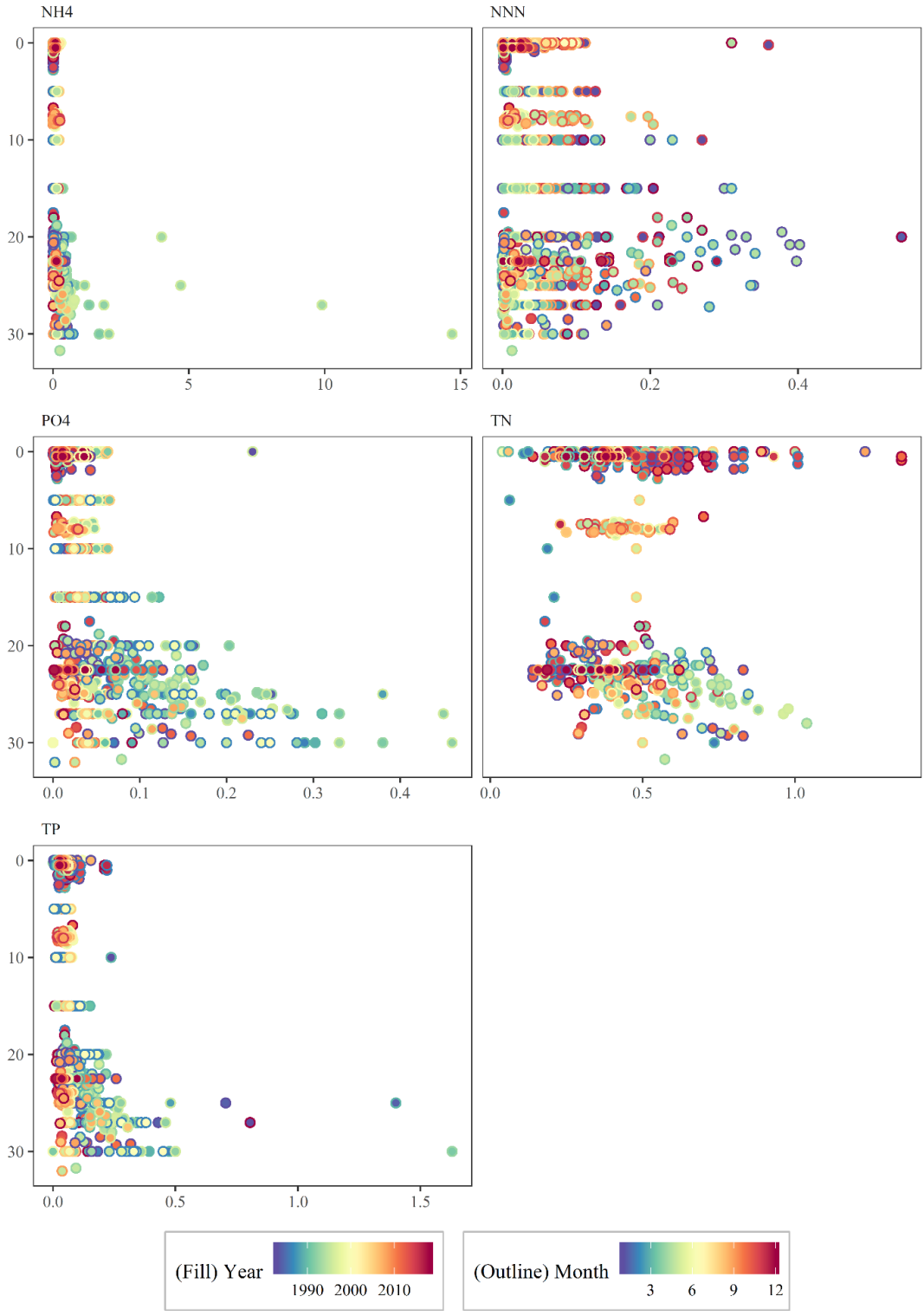

Appendix figure 2. Water quality data derived from ORC monitoring on Lake Hayes at multiple sites, 2010 to 2017 for a) ammonium (g N m^{-3}), b) nitrate + nitrite (g N m^{-3}), phosphate (g P m^{-3}), total nitrogen (g N m^{-3}), and total phosphorus (g P m^{-3}). The y-axis represents depth below water surface (m), the colour of the outline of each dot represents the month of collection and the fill of each dot represents the year of collection.

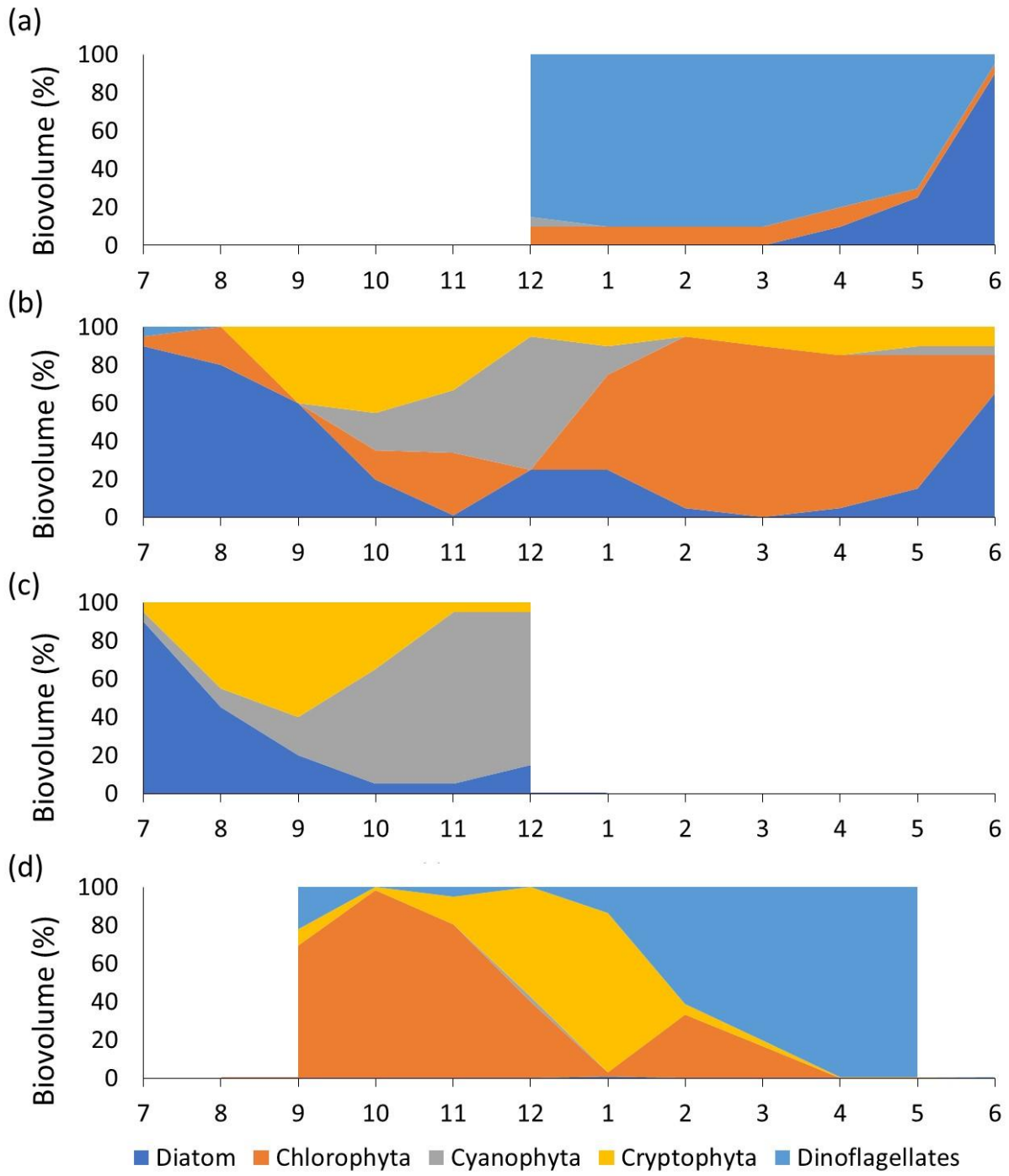

Appendix figure 3. Approximate monthly estimates of proportional phytoplankton group biovolume dynamics in Lake Hayes. The data are approximated based on the published results described in Burns and Mitchell (1974) (a 1969-1970; b 1970-1971; c 1971-1972) as well as data provided by ORC (d 2016-2017).

Model calibration

Appendix Table 1. Assigned values for parameters used in DYRESM.

Parameter	Unit	Calibrated value	Reference
Critical wind speed	m s^{-1}	3.0	Best fit to data
Emissivity of water surface	-	0.96	Imberger & Patterson (1981)
Mean albedo of water	-	0.07	Patten et al. (1975)
Potential energy mixing efficiency	-	0.18	Best fit to data
Shear production efficiency	-	0.06	Best fit to data
Wind stirring efficiency	-	0.4	Best fit to data
Vertical mixing coefficient	-	200	Yeates (2002)
Effective surface area coefficient	m^2	7.2×10^6	Best fit to data

Appendix Table 2. Assigned values used in CAEDYM for Lake Hayes; DOPL and DONL are dissolved organic phosphorus and nitrogen, respectively.

Parameter	Unit	Calibrated value	Reference source
Sediment parameters			
Sediment oxygen demand	$g\ m^{-2}\ d^{-1}$	2	Best fit to data
Half-saturation coefficient for sediment oxygen demand	$mg\ L^{-1}$	2	Best fit to data
Maximum potential PO_4 release rate	$g\ m^{-2}\ d^{-1}$	0.02	Best fit to data
Oxygen and nitrate half-saturation for release of phosphate from bottom sediments	$g\ m^{-3}$	1	Best fit to data
Maximum potential NH_4 release rate	$g\ m^{-2}\ d^{-1}$	0.01	Best fit to data
Oxygen half-saturation constant for release of ammonium from bottom sediments	$g\ m^{-3}$	1	Best fit to data
Maximum potential NO_3 release rate	$g\ m^{-2}\ d^{-1}$	0	Best fit to data
Oxygen half-saturation constant for release of nitrate from bottom sediments	$g\ m^{-3}$	1	Best fit to data
Temperature multiplier for nutrient release	-	1.08	Best fit to data
Nutrient parameters			
Decomposition rate of POPL to DOPL	d^{-1}	0.015	Makler-Pick et al. (2011)
Mineralisation rate of DOPL to PO_4	d^{-1}	0.06	Makler-Pick et al. (2011)
Decomposition rate of PONL to DONL	d^{-1}	0.0075	Makler-Pick et al. (2011)
Mineralisation rate of DONL to NH_4	d^{-1}	0.01	Makler-Pick et al. (2011)
Denitrification rate coefficient	d^{-1}	0.35	Makler-Pick et al. (2011)
Oxygen half-saturation constant for denitrification	$mg\ L^{-1}$	0.75	Makler-Pick et al. (2011)
Temperature multiplier for denitrification	-	1.08	Best fit to data
Nitrification rate coefficient	d^{-1}	0.07	Makler-Pick et al. (2011)
Nitrification half-saturation constant for oxygen	$mg\ L^{-1}$	0.5	Best fit to data
Temperature multiplier for nitrification	-	1.083	Best fit to data
Phytoplankton parameters		**Dino, Cyano, Chloro, Crypto, Diatom**	
Maximum potential growth rate at 20°C	d^{-1}	1, 1, 1.225, 1.65, 6	Best fit to data
Parameter for initial slope of P_I curve	$\mu Em^{-2}\ s^{-1}$	140, 250, 40, 40, 20	Best fit to data
Half saturation constant for phosphorus uptake	$mg\ L^{-1}$	0.0008, 0.0025, 0.001, 0.001, 0.004	Best fit to data
Half saturation constant for nitrogen uptake	$mg\ L^{-1}$	0.075, 0.05, 0.05, 0.005, 0.05	Best fit to data
Minimum internal nitrogen concentration	mg N $(mg\ chl\ a)^{-1}$	0.25, 0.375, 0.4, 1, 0.75	Best fit to data
Maximum internal nitrogen concentration	mg N $(mg\ chl\ a)^{-1}$	5, 4, 3, 9, 11	Best fit to data
Maximum rate of nitrogen uptake	mg N $(mg\ chl\ a)^{-1}\ d^{-1}$	0.525, 0.5, 0.71, 0.7175, 1.2	Best fit to data
Minimum internal phosphorus concentration	mg P $(mg\ chl\ a)^{-1}$	0.15, 0.13, 0.195, 0.07, 0.24	Best fit to data
Maximum internal phosphorus concentration	mg P $(mg\ chl\ a)^{-1}$	0.9, 0.4, 0.65, 0.6, 0.9	Best fit to data
Maximum rate of phosphorus uptake	mg P $(mg\ chl\ a)^{-1}\ d^{-1}$	0.65, 0.3, 0.4, 0.4, 0.2	Best fit to data
Temperature multiplier for growth limitation	-	1.08, 1.1, 1.08, 1.08, 1.04	Best fit to data
Standard temperature for growth	°C	20, 22, 18, 20, 15	Best fit to data
Optimum temperature for growth	°C	25, 28, 25, 23, 23	Best fit to data
Maximum temperature for growth	°C	35, 35, 40, 35, 38	Best fit to data
Respiration rate coefficient	d^{-1}	0.07, 0.07, 0.09, 0.12, 0.12	Best fit to data
Temperature multiplier for respiration	-	1.04, 1.04, 1.05, 1.08, 1.07	Best fit to data
Fraction of respiration relative to total metabolic loss rate	-	0.5, 0.5, 0.5, 0.7, 0.5	Best fit to data
Fraction of metabolic loss rate that goes to DOM	-	0.55, 0.55, 0.6, 0.6, 0.7	Best fit to data
Constant settling velocity	$m\ s^{-1}$	-1×10^{-7}, 2×10^{-5}, -3×10^{-7}, -5×10^{-7}, -1.4×10^{-5}	Best fit to data

Appendix Table 3. Model performance statistics

Abbreviation	Statistic	Details	Equation
r	Pearson product moment correlation	Measures the strength of the correlation between modelled and measured data, i.e. how 'in phase' the two signals are. Vales range from -1 (perfect negative correlation) to 1 (perfect positive correlation).	$\frac{\sum_{i=1}^{n}(o_i - \bar{o}) \times (m_i - \bar{m})}{\sqrt{\sum_{i=1}^{n}(o_i - \bar{o})} \times \sqrt{\sum_{i=1}^{n}(m_i - \bar{m})}}$
RMSE	Root mean square error	A measure of the magnitude of the error between modelled and measured data which is disproportionately affected by large errors.	$\sqrt{\frac{\sum_{i=1}^{n}(m_i - o_i)^2}{n}}$
MAE	Mean absolute error	Measures the average error, irrespective of whether the model under– or over–predicts measurements.	$\frac{\sum_{i=1}^{n}\lvert(m_i - o_i)\rvert}{n}$